On the Spanning and Routing Properties of Grade-1 Emanation Graphs

Nader El-Ghotmi

Thesis submitted to the University of Ottawa in partial fulfillment of the requirements for the degree of Master of Science, Computer Science

School of Electrical Engineering and Computer Science
Faculty of Engineering
University of Ottawa

Supervisor: Jean-Lou De Carufel

Abstract

Families of geometric spanners are sets of graphs $G = (V, E)$ defined by construction rules such that for any two vertices $p, q \in V$, there exists a path whose length is at most $\sigma|pq|$, where σ is a constant. In this work, we study a family of graphs called *grade-1 emanation graphs*, obtained by taking a point set P, shooting rays from each point in four equidistant directions, introducing Steiner vertices at ray intersections, and interrupting rays upon intersection.

We first show that grade-1 emanation graphs form a subclass of motorcycle graphs. We then investigate their spanning properties. In particular, we strengthen existing results by showing that grade-1 emanation graphs are $\sqrt{10}$-spanners even when one of the vertices is a Steiner vertex, while no constant stretch factor exists when both vertices are Steiner vertices.

We next study local routing on grade-1 emanation graphs. We demonstrate that several classical routing strategies, including greedy, compass, and greedy-compass routing, all fail in this setting, and that face routing can incur arbitrarily large routing ratios. To address this, we introduce a new routing algorithm, the Marking Algorithm, and show that it guarantees delivery on grade-1 emanation graphs in general position. Our analysis further establishes a routing ratio of $2+24\sqrt{2}$ for all paths that do not contain a subpath belonging to a group of subpaths, which we identify as pattern $G10$.

These results provide new insight into the structure and limitations of emanation graphs and contribute to the broader understanding of geometric spanners and local routing algorithms.

Acknowledgements

While writing this thesis I learned that work in the field of theoretical computer science can feel like getting lost in a maze of words I came up with. I would like to thank my thesis supervisor, as well as my family and friends, for directly and indirectly helping me find my way.

Contents

List of Figures

List of Tables

1

Introduction

In computational geometry, the *complete Euclidean graph* on a point set $P \subset \mathbb{R}^d$ is the graph in which every pair of distinct points $p, q \in P$ is connected by an edge pq whose weight is the Euclidean distance $|pq|$. This graph contains $O(n^2)$ edges, where $n = |P|$. We prefer graphs that have strictly less than a quadratic number of edges relative to the number of nodes. As a result, a central problem in the field is to construct sparse graphs that approximate the complete Euclidean graph while using significantly fewer edges [1], [2].

Such sparse approximations are known as *geometric spanners* [1], [3]. A *good* geometric spanner is typically one that optimizes certain desirable properties, such as low spanning ratio, sparsity, or efficiency of construction; a comprehensive discussion of these properties can be found in Chapter 1 of [1]. In this thesis, we are interested in studying graphs with small spanning ratio while maintaining sparsity. In particular, we discuss graphs in which the shortest path between any two vertices is within a constant factor of their Euclidean distance, and the total number of edges is sub-quadratic in the number of vertices.

This trade-off is especially important in practical applications, where edges may represent costly connections. For example, in transportation or communication networks, constructing a direct connection between two nodes can be expensive. Therefore, we aim to design graphs that use relatively few edges while still providing paths that closely approximate true geometric distances.

While every connected geometric graph is trivially a spanner for some (possibly large) constant, the goal is to identify *families* of geometric graphs for which the spanning ratio can be bounded by a small constant [1]. A family of geometric graphs $\mathcal{F}$ is a collection of graphs often defined over point sets according to a common construction rule or algorithm. Thus, we aim to define families where, among other attributes, we can guarantee a constant σ such that all graphs in $\mathcal{F}$ have a path between any two points p and q that is at most $\sigma|pq|$ in length.

One problem that is often applied to spanners is the problem of path-finding with two constraints. Namely, we are concerned with studying *online* path-finding algorithms which use sublinear memory. An online algorithm is an algorithm where the input space is not known at the beginning of the algorithm, and thus decision making needs to be done with limited information. Observe that if we allow memory that is proportional to the size of the graph, then the problem of path-finding is as trivial as exploring the graph and then using one's choice of path-finding algorithm, such as Dijkstra's algorithm. Thus we aim to design algorithms which use the information available to make educated or advantageous decisions to reach the target vertex. We call these algorithms *local routing algorithms*.

In this thesis, we study a family of geometric graphs known as *grade*-1 *emanation graphs* [4]. This graph family is of particular interest due to several distinctive features: it is constructed using a ray-shooting process [5], all of its edges are axis-aligned, and it incorporates Steiner vertices [1]. We investigate the spanning ratio of this graph, as well as properties of a routing algorithm defined on it, drawing on ideas from prior work on routing in geometric graphs [6], [7], [8].

1.1 Definitions

A *geometric graph* $G = (V, E)$ is an undirected and weighted graph embedded in $\mathbb{R}^d$, where the set V of vertices (or nodes) is a finite subset of $\mathbb{R}^d$ and edges in E are line segments between vertices. Given two points $p, q \in \mathbb{R}^d$, we denote the line segment between p and q by pq. Moreover, if there is an edge in G between p and q, we also denote this edge by pq. Let us denote the Euclidean length of a line segment pq by $|pq|$. If pq is an edge in G, then its weight is $|pq|$. The length of a path in G is equal to the sum of the lengths of the edges along that path. The distance between two vertices p and q in G is then the length of a shortest path between p and q in G. We denote the distance between p and q in G by $|pq|_G$.

A geometric graph $G = (V, E)$ is called a σ*-spanner* if, for every pair of points $p, q \in V$,

$$\frac{|pq|_G}{|pq|} \leq \sigma,$$

where $\sigma \geq 1$ is a real number known as the *spanning ratio* [1], [2]. We say that the spanning ratio of G is the smallest such σ such that this inequality holds. We say that the spanning ratio of a family of graphs $\mathcal{F}$ is *at most* σ if every graph in $\mathcal{F}$ has a spanning ratio of at most σ. When the spanning ratio of a family of graphs $\mathcal{F}$ is at most σ, we say this spanning ratio is *tight* if for all $\epsilon > 0$ there exists a graph in $\mathcal{F}$ whose spanning ratio is at least $\sigma - \epsilon$.

Local routing algorithms are path-finding algorithms in which knowledge of the graph is restricted to a local neighbourhood. To build intuition, it is helpful to consider the analogy of a robot navigating a city. The graph represents the city and each vertex corresponds to an intersection. The target vertex is a prominent landmark (e.g., the CN Tower in Toronto) that is visible from anywhere in the city. At each intersection, the robot can observe its neighbouring intersections and has access to a limited amount of memory. Based on this information, it applies a local routing algorithm to decide its next move.

An agent operating on a geometric graph G constructs a walk from a source vertex s to a target vertex t. We assume that the agent always knows the coordinates of its current vertex, as well as the coordinates of the target vertex t. For a vertex u, let $\mathcal{N}(u)$ denote the set of neighbours of u in G. When located at u, the agent knows the coordinates of all vertices in $\mathcal{N}(u) \cup \{u\}$. A local routing algorithm specifies which vertex in $\mathcal{N}(u)$ the agent visits next.

An algorithm $\mathcal{A}$ is said to *succeed* on a graph $G = (V, E)$ if, for every pair of vertices $s, t \in V$ with $s \neq t$, it produces a path from s to t in a finite number of steps. If there exists a graph G for which $\mathcal{A}$ fails to terminate or does not reach t, we say that G *defeats* $\mathcal{A}$. If $\mathcal{A}$ succeeds for every graph in a family $\mathcal{F}$ of graphs, then $\mathcal{A}$ *succeeds for* $\mathcal{F}$.

A local routing algorithm $\mathcal{A}$ is *c-competitive* for a family $\mathcal{F}$ of graphs if, for every graph $G \in \mathcal{F}$ and all distinct vertices $s, t \in V$, the length of the path produced by $\mathcal{A}$ is at most c times the length of a shortest path between s and t. The *routing ratio* of $\mathcal{A}$ for $\mathcal{F}$ is defined as

$$\sup_{G \in \mathcal{F}} \sup_{\substack{s,t \in V(G) \\ s \neq t}} \frac{|\mathcal{A}(G, s, t)|}{|st|},$$

where $|\mathcal{A}(G, s, t)|$ denotes the length of the path produced by $\mathcal{A}$, and $|st|$ is the Euclidean distance between s and t [8].

1.2 Geometric Spanners

In this section, we discuss geometric spanners that are relevant in the literature.

1.2.1 Theta-Graphs

Let P be a set of points in the plane. For each point $p \in P$, we partition the plane around p into k cones of equal angle $\frac{2\pi}{k}$, defined with respect to a fixed reference direction (e.g., the negative y-axis). We denote these cones by $C_0(p), C_1(p), \ldots, C_{k-1}(p)$.

For each cone $C_i(p)$ and each point $q \in C_i(p)$, let q' denote the orthogonal projection of q onto the bisector of $C_i(p)$. We add an edge between p and the point $q \in C_i(p)$ whose projection q' is closest to p along the bisector. The resulting graph is called the *θ_k-graph*.

The spanner status of θ_k-graphs depends heavily on k. For $k \leq 2$, the graph may be disconnected. For $k = 3$, the graph is connected [9] but is *not* a spanner; there is no constant σ for which a θ_3 graph on a point set P is guaranteed to be a σ-spanner [10]. For $k \geq 4$, θ_k-graphs are known to be geometric spanners, though the spanning ratio is tight only for certain values of k. The known upper and lower bounds are summarized in Table 1.1.

k	Upper bound	Lower bound	References
≤ 2	Not connected	—	[11]
3	Connected, not a spanner	—	[9], [10]
4	≈ 17	7	[11], [12]
5	< 5.70	≈ 3.78	[13], [14]
6	2 (tight)	2	[15]
7	≈ 3.51	—	[13]
8	$1 + 2\sin(\pi/8) \approx 1.77$	$1 + 2\sin(\pi/8)$ (tight)	[13]
$4k{+}2$ ($k \geq 1$)	$1 + 2\sin(\pi/(4k{+}2))$ (tight)	$1 + 2\sin(\pi/(4k{+}2))$	[13]
$4k{+}4$ ($k \geq 1$)	$\dfrac{1 + 2\sin(\theta/2)}{\cos(\theta/2) - \sin(\theta/2)}$	$1 + 2\tan(\theta/2) + 2\tan^2(\theta/2)$	[13]

Table 1.1: Known upper and lower bounds on the spanning ratio of θ_k-graphs, where $\theta = 2\pi/k$. A bound listed as "tight" means the upper and lower bounds coincide.

In general, the spanning ratio approaches 1 as $k \to \infty$ [11].

1.2.2 Yao Graphs

Yao graphs are defined similarly to θ_k-graphs. For each point $p \in P$, we partition the plane around p into k cones of equal angle $\frac{2\pi}{k}$ with respect to a fixed reference direction. In each cone C, we add an edge between p and the point $q \in P \cap C$ that minimizes the Euclidean distance $|pq|$.

The resulting graph is called the *Yao-k graph*. The known upper and lower bounds are summarized in Table 1.2.

k	Upper bound	Lower bound	References
1	Not connected	—	[10]
2, 3	Connected, not a spanner	—	[10]
4	≈ 16.54	—	[16]
5	$2 + \sqrt{3} \approx 3.74$	≈ 2.87	[17]
6	≈ 5.8	—	[17]
odd $k \geq 5$	$\dfrac{1}{1 - 2\sin(3\theta/8)}$	—	[17]
$k \geq 7$	$\dfrac{1}{1 - 2\sin(\theta/2)}$	—	[1]

Table 1.2: Known upper and lower bounds on the spanning ratio of Y_k-graphs, where $\theta = 2\pi/k$. The bound for odd $k \geq 5$ subsumes and improves upon the bound for $k \geq 7$ when k is odd.

1.2.3 Delaunay Triangulations

Given a point set P, the *Delaunay triangulation* is the triangulation in which three points form a triangle if and only if their circumscribed circle contains no other point of P in its interior.

The Delaunay triangulation is a planar geometric spanner with constant spanning ratio [18], [19]. The spanning ratio of Delaunay triangulations is at most 1.998 [20] and at least 1.5932 [21].

1.2.4 Empty-Square Delaunay Graphs

The *empty-square Delaunay graph* (also called the L_∞-Delaunay graph) is defined similarly to the Delaunay triangulation, except that circumscribed circles are replaced by axis-aligned squares. That is, two points $p, q \in P$ are connected by an edge if there exists an axis-aligned square having p and q on its boundary and containing no other point of P in its interior. This graph is a geometric spanner with tight spanning ratio $\sqrt{4 + 2\sqrt{2}} \approx 2.61$ [22]. This definition generalizes to rectangles and parallelograms; replacing the square with a rectangle of aspect ratio $A \geq 1$ yields a tight spanning ratio of $\sqrt{2}\sqrt{1 + A^2 + A\sqrt{A^2 + 1}}$ [23], and replacing it with a parallelogram of aspect ratio A and non-obtuse interior angle θ_0 yields the tight spanning ratio

$$\frac{\sqrt{2}\sqrt{1 + A^2 + 2A\cos\theta_0 + (A + \cos\theta_0)\sqrt{1 + A^2 + 2A\cos\theta_0}}}{\sin\theta_0}.$$

[24].

1.2.5 Greedy Spanners

Let P be a set of points in the plane and let $\sigma > 1$ be a fixed stretch parameter. The *greedy σ-spanner* is constructed by considering all pairs of points $(p, q) \in P \times P$ in order of increasing Euclidean distance $|pq|$. For each pair, we add the edge pq if and only if the current graph does not already contain a path between p and q of length at most $\sigma \cdot |pq|$.

It is known that this construction produces a geometric spanner with optimal properties in terms of sparsity, total weight, and maximum degree, up to constant factors.

Notably, the algorithm for creating Greedy spanners is inspired by Kruskal's minimum spanning tree algorithm [1], [2].

1.3 Local Routing Algorithms

In this section, we describe several general-purpose routing algorithms, as well as routing strategies tailored to specific spanner constructions introduced in Section 1.2.

1.3.1 Greedy Routing

Let v be the current vertex and t the target. Greedy routing selects the neighbour u of v that minimizes the Euclidean distance to t; that is, it chooses $u \in \mathcal{N}(v)$ such that $|ut|$ is minimized [25].

In computational geometry, we usually define a geometric graph as a *triangulation* whenever all faces, except maybe one (usually corresponding to the outer face), is a triangle.

Bose and Morin [25] show that there are triangulations which defeat greedy routing.

1.3.2 Compass Routing

Let v be the current vertex and t the target. Compass routing selects the neighbour u of v such that the angle between the edge vu and the segment vt is minimized [6].

There are triangulations which defeat compass routing [25].

1.3.3 Greedy-Compass Routing

Let v be the current vertex and t the target. Let u_{ccw} be the neighbour of v reached by the first edge encountered in a counterclockwise rotation from vt, and let u_{cw} be the neighbour reached by the first edge encountered in a clockwise rotation from vt. The algorithm selects the neighbour among $\{u_{\text{ccw}}, u_{\text{cw}}\}$ that is closest to t in Euclidean distance. This algorithm succeeds on all triangulations [7].

1.3.4 Face-Routing

Face-routing is a local routing algorithm defined for *planar* geometric graphs [26]. A geometric graph $G = (V, E)$ is *planar* if no two edges of G intersect except at their common endpoints. We use the definition of face-routing provided in [27].

From the current vertex v (initialized with $v = s$), the algorithm identifies the face F on whose boundary v lies and which is intersected by the line segment vt. It then traverses vertices along the boundary of F until reaching a vertex v' such that the edge $v'v''$ intersects vt and $v \neq v'$. The current vertex is then updated to v', and the process repeats until $v = t$.

Face-routing guarantees delivery to the target on any planar geometric graph using only constant memory.

1.3.5 Theta-Routing

θ-routing (also called cone-routing) is a local routing algorithm for θ_k-graphs that, from the current vertex v, follows the edge in the cone containing the target t. This algorithm is simple and memoryless, but is not competitive for all values of k; in particular, it has unbounded routing ratio for $k \leq 6$ [13].

For small values of k, dedicated algorithms are required. Bose et al. [12] present a routing algorithm for θ_4 with routing ratio at most 17. Routing on θ_6-graphs is shown to have a routing ratio of at most 2.89 [28].

For $k \geq 7$, cone-routing is competitive. Bose et al. [13] show that the routing ratio of cone-routing depends on the cone family: θ-graphs with $4k+4$ cones have routing ratio at most $\frac{1+2\sin(\theta/2)}{\cos(\theta/2)-\sin(\theta/2)}$, and those with $4k+3$ or $4k+5$ cones have routing ratio at most $\frac{\cos(\theta/4)(1+2\sin(\theta/2))}{\cos(\theta/2)-\sin(3\theta/4)}$, where $\theta = 2\pi/k$. As k increases, these bounds approach 1, reflecting that cone-routing becomes increasingly efficient as the cones become narrower.

1.3.6 Yao-Graph Routing

Cone-routing is also a valid strategy on Yao-k graphs. For some small values of k dedicated routing algorithms have been shown to have constant routing ratios. Bose et al. [16] present the first routing algorithm for Yao-4 with a constant routing ratio of at most $17 + 9/\sqrt{2} \approx 23.36$. Kalnay et al. show a routing ratio of $1 + \frac{38}{\sqrt{3}}$ [29] on Yao-6 graphs.

1.4 Useful Terminology

Two families of geometric graphs we discuss in this thesis are directly related to the concept of *rays*. A *ray* is an ordered triplet (o, θ, λ), where $o \in \mathbb{R}^2$, $\theta \in [0, 2\pi)$ is an angle, and $\lambda \in \mathbb{R}$ is a strictly positive number. The first element of the triplet, o, is the *origin* of the ray (its starting point). The angle θ is the *direction* the ray takes (starting at o), where an angle of 0 corresponds to the direction of the vector $(1, 0)$ and angles are measured counter-clockwise. Finally, λ is the *speed* at which the ray extends in units per second (u/s). Hence, at time $\tau \geq 0$, the ray $\rho = (o, \theta, \lambda)$ corresponds to the line segment between the points $o = (o_x, o_y)$ and $(o_x + \lambda\tau\cos(\theta), o_y + \lambda\tau\sin(\theta))$.

For the purpose of this work, it is possible to *interrupt* a ray. When a ray gets interrupted, it stops extending forever. Formally, we define interrupted rays as follows.

Definition 1.1 (Interrupted Ray)**.** We say that a ray $\rho = (o, \theta, \lambda)$ is *interrupted at time* τ if

- for all $0 \leq \tau' \leq \tau$, ρ corresponds to the line segment between the points $o = (o_x, o_y)$ and $(o_x + \lambda\tau'\cos(\theta), o_y + \lambda\tau'\sin(\theta))$,
- and for all $\tau' \geq \tau$, ρ corresponds to the line segment between the points $o = (o_x, o_y)$ and $(o_x + \lambda\tau\cos(\theta), o_y + \lambda\tau\sin(\theta))$.

We say that ρ *reaches a point* (a, b) *at time* τ if $(a, b) = (o_x + \lambda\tau\cos(\theta), o_y + \lambda\tau\sin(\theta))$ and ρ was not interrupted before time τ. We say that ρ *reaches* (a, b) if there exists a time τ such that ρ reaches (a, b) at time τ. We say that two rays ρ_1 and ρ_2 *intersect at a point* p if both ρ_1 and ρ_2 reach p. We refer to p as the *intersection point of* ρ_1 *and* ρ_2. We say that *two rays intersect at the same time* if they reach p at the same time. We say that *two rays do not intersect at the same time* if they do not reach p at the same time.

Using rays, we can define motorcycle graphs and emanation graphs, which are the main topic of this thesis. Intuitively, Eppstein and Erickson define Motorcycle graphs as the following.

"Imagine several people riding motorcycles out in the desert. Each motorcycle is specified by an initial location and a velocity. All the bikes start moving simultaneously, and, thereafter, no turning, braking, or acceleration is allowed. The bikes are extremely fragile; if any motorcycle runs over the track previously left by another bike, it immediately crashes. If two motorcycles collide, they both crash. After all the bikes either crash or escape to infinity, their tracks form a planar directed graph, which we call the Motorcycle graph." [5]

In this thesis, the "tracks" from this intuitive definition are formally defined by rays.

Grade-k emanation graphs are constructed in a similar way, except that we deal with intersecting tracks in a different way. We defer the reader to Section 2.2 for a formal definition of these graphs. It was shown by Hamedmohseni et al. that grade-1 emanation graphs have a tight spanning ratio of $\sqrt{10}$ [4].

1.5 Contributions

In this thesis, we show that grade-1 emanation graphs are a subclass of motorcycle graphs. We establish several spanning properties of motorcycle graphs and emanation graphs. In particular we show that motorcycle graphs and connected motorcycle graphs are not σ-spanners for any constant σ. We show that grade-1 emanation graphs do not contain σ-spanning paths between Steiner vertices, and we show that grade-1 emanation graphs do contain σ-spanning paths between a Steiner vertex and a real vertex for $\sigma = \sqrt{10}$.

We analyze several existing local routing strategies on grade-1 emanation graphs in general position, showing that greedy routing, compass routing, and greedy compass routing may fail, while face-routing may have arbitrarily large routing ratio.

We introduce a local routing algorithm for grade-1 emanation graphs, called the Marking Algorithm, and prove that it always succeeds on graphs in general position.

We prove that the Marking Algorithm achieves a routing ratio of at most $2+24\sqrt{2}$ for all routing paths which do not contain a subpath of pattern $G10$.

2

Two Closely Related Families of Graphs

In this section, we define two families of graphs that both depend on the concept of (interrupted) rays, namely *motorcycle graphs* [5] and *emanation graphs* [4]. Both definitions are similar. We start with a (finite) set of rays. At the beginning, i.e., when $\tau = 0$, the set of vertices is equal to the set of origins of all rays. We refer to these vertices as *real vertices*. Then the time begins to elapse and the rays start extending. When some rays intersect at a point p, this creates a *Steiner vertex*. Moreover, some of these intersecting rays may get interrupted. Depending on what rays get interrupted or not, we get a motorcycle graph or an emanation graph.

2.1 Motorcycle Graphs

In this subsection, we provide a formal definition of motorcycle graphs.

Let P be a set of points. Consider a set R of rays such that the set of all origins of all rays in R is equal to P. We say that R is *consistent* if for any two rays $(p, \theta, s), (p, \theta', s') \in R$ sharing the same origin, we have $\theta \neq \theta'$. For the rest of this thesis, we assume that all sets of rays are consistent.

At the beginning, i.e., when $\tau = 0$, let $V = P$ and $S = \varnothing$. Let all the rays extend. If a ray ρ reaches a point $p \in \mathbb{R}^2$ belonging to another ray ρ', we do the following.

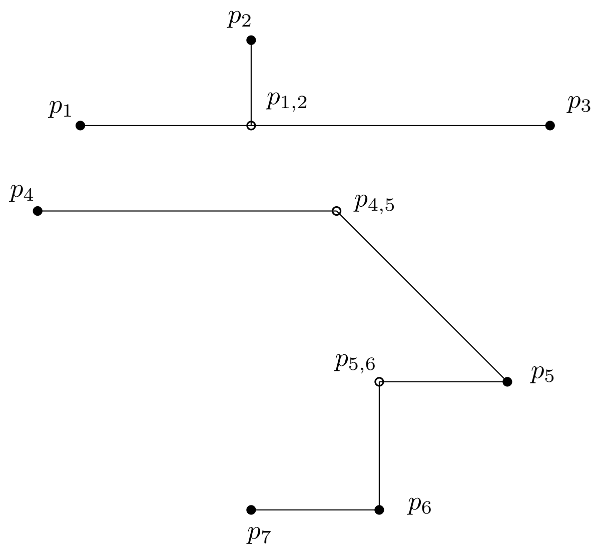

Figure 2.1: An example of a motorcycle graph.

- If ρ reaches p later than ρ', then ρ gets interrupted and ρ' keeps extending.
- If ρ and ρ' reach p at the same time, then both ρ and ρ' get interrupted.

If p is not already in $V \cup S$, we add p to S. The construction terminates when every ray in R has either been interrupted or extends to infinity without crossing the trail of any other ray in R.

The points in V are called *real vertices* and the points in S are called *Steiner vertices*. We now add edges to the graph. Let $E = \varnothing$. For each ray ρ, we do the following. For each pair of consecutive points p, q along ρ such that $p, q \in V \cup S$, we add the edge pq to E.

The motorcycle graph we obtain from R is then $G_R = (V \cup S, E)$. When it is clear from the context, we will write G instead of G_R. Observe that all rays interrupt at intersection, creating a Steiner vertex. Then no edges in motorcycle graphs cross, thus motorcycle graphs are planar graphs. In Figure 2.1, we have an example of a motorcycle graph, where the rays are

$$
\begin{aligned}
\rho_1 &= ((1,9), 0, 2), & \rho_{5_\alpha} &= ((11,3), \frac{3\pi}{4}, \sqrt{2}),\\
\rho_2 &= ((5,11), \frac{3\pi}{2}, 1), & \rho_{5_\beta} &= ((11,3), \pi, 1),\\
\rho_3 &= ((12,9), \pi, 1), & \rho_6 &= ((8,0), \frac{\pi}{2}, 1),\\
\rho_4 &= ((0,7), 0, 2), & \rho_7 &= ((5,0), 0, 1).
\end{aligned}
$$

First, let us look at ρ_1 and ρ_2 which extend from p_1 and p_2 respectively. Ray ρ_1 travels twice the speed of ρ_2, however, ρ_1 must travel twice the distance of ρ_2 before reaching their intersection point. As such, they intersect at the same time. They both become interrupted rays and we create the Steiner vertex $p_{1,2}$. We add $p_{1,2}$ to S, and $p_1p_{1,2}$ and $p_2p_{1,2}$ to E. Ray ρ_3 extends from p_3 travels on course for $p_{1,2}$. Due to its distance and speed it will reach $p_{1,2}$ once ρ_1 and ρ_2 have already been interrupted, and as such once it intersects $p_{1,2}$ it will become an interrupted ray. Since $p_{1,2}$ is already in S then we will not create a new Steiner vertex, but we do need to add $p_3p_{1,2}$ to E.

Rays ρ_4 and ρ_{5_α} intersect at $(7,7)$. Ray ρ_{5_α} will reach point $(7,7)$ after ρ_4 thus when it arrives it will become an interrupted ray and create the Steiner vertex $p_{4,5}$ at $(7,7)$ which will be added to S. We will add $p_4p_{4,5}$ and $p_5p_{4,5}$ to E. Rays ρ_{5_β} and ρ_6 are equidistant from their intersection point and travel at the same speed so they will intersect at the same time and both become interrupted rays creating the Steiner vertex $p_{5,6}$. We will add $p_{5,6}$ to S and we will add $p_6p_{5,6}$ and $p_{5_\beta}p_{5,6}$ to E. Ray ρ_7 is on course to intersect ρ_6 at its origin point p_6. Since p_6 is already in V we do not create a Steiner vertex but we do add p_7p_6 to E.

All the rays except for ρ_4 have now been interrupted. Since ρ_4 is not on course to intersect any more rays after passing $p_{4,5}$ then the construction of the graph is over.

2.2 Emanation Graphs

In this section we define the *grade-k emanation graph*. This was first introduced by Hamedmohseni et al. in [4].

2.2.1 Grade-1 Emanation Graphs

We start by defining *grade-1 emanation graphs*. Consider a set P of points and let R be the following set of rays

$$R = \{(p,0,1) \mid p \in P\} \cup \{(p,\pi/2,1) \mid p \in P\} \cup \{(p,\pi,1) \mid p \in P\} \cup \{(p,3\pi/2,1) \mid p \in P\}.$$

As such, the rays in R are all axis aligned. Moreover, from each point $p \in P$, four rays are emanating from p, one in each of the four directions 0, $\pi/2$, π and $3\pi/2$. Finally, observe that the speed of all rays is 1.

At the beginning, i.e., when $\tau = 0$, let $V = P$ and $S = \varnothing$. Let all the rays extend. If a ray ρ reaches a point $p \in \mathbb{R}^2$ belonging to another ray ρ', we do the following.

- If ρ reaches p later than ρ', then ρ gets interrupted and ρ' keeps extending.

- Otherwise, ρ and ρ' reach p at the same time, say at time τ. Let $\Psi \subset R$ be the set of rays that reach p at time τ. Observe that $2 \leq |\Psi| \leq 4$.
  - If $|\Psi| = 2$ and the two rays in Ψ are collinear, then they both get interrupted. Otherwise, exactly one of them gets interrupted (we can choose arbitrarily).
  - If $|\Psi| = 3$, then two of the rays in Ψ are collinear. The two collinear rays get interrupted. We can choose arbitrarily whether or not to interrupt the third ray.
  - If $|\Psi| = 4$, then all rays in Ψ get interrupted.

In all cases, if p is not already in $V \cup S$, we add p to S. The *bounding box* of a set P of points is the smallest axis-aligned rectangle that contains P. The construction of the set S ends whenever every ray is interrupted or escapes the bounding box of P. The points in V are called *real vertices* and the points in S are called *Steiner vertices*. We now add edges to the graph. Let $E = \varnothing$. For each ray ρ, we do the following. For each pair of consecutive points p, q along ρ such that $p, q \in V \cup S$, we add the edge pq to E.

The grade-1 emanation graph we obtain from R is then $G_R = (V \cup S, E)$. When it is clear from the context, we will write G instead of G_R.

In the analysis of grade-1 emanation graphs, we will use the notion of *shadow edges*, which are defined as follows. Consider a grade-1 emanation graph $G_R = (V \cup S, E)$. In the last step of the construction of S, every ray is either interrupted or escapes the bounding box of P. Consider the set R_b of rays which escaped the bounding box of P. For each ray $r = (o, \theta, 1) \in R_b$ we consider the last vertex $p \in V \cup S$ that was visited before r escaped the bounding box of P. We refer to the ray $(p, \theta, 1)$ as a *shadow edge*. Shadow edges are not part of emanation graphs but they are helpful for proving properties of emanation graphs.

In Figure 2.2 we can see an example of a grade-1 emanation graph.

2.2.2 Grade-k Emanation Graphs

We now define the *grade-k emanation graphs*. Consider a set P of points. Let R be the following set of rays

$$R = \bigcup_{i=0}^{2^{k+1}-1} \left\{ \left(p, i \cdot 2\pi/2^{k+1}, 1\right) \mid p \in P \right\}.$$

At the beginning (at time $\tau = 0$), let $V = P$ and $S = \varnothing$. Let all the rays extend. If a ray ρ reaches a point $p \in \mathbb{R}^2$ belonging to another ray ρ', we do the following.

- If ρ reaches p later than ρ', then ρ gets interrupted and ρ' keeps extending.

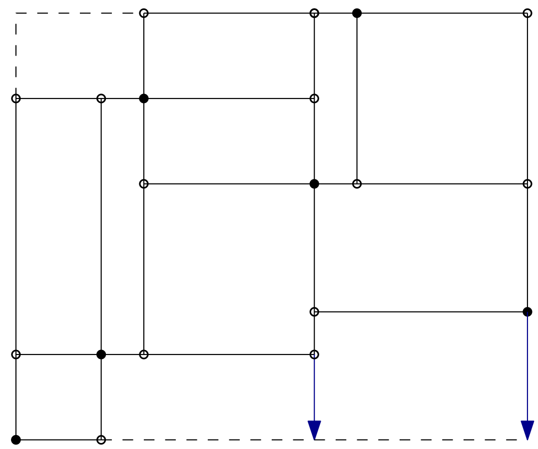

Figure 2.2: A grade-1 emanation graph with the bounding box shown in black dashed lines and shadow edges shown as blue arrows.

- Otherwise, let $\Psi \subset R$ be the set of rays that reach p at time τ. Let us order the rays in Ψ arbitrarily and let ρ^* be the first ray with respect to this ordering. All rays in $\Psi \setminus \{\rho^*\}$ are interrupted. If ρ^* is not collinear with any other ray in Ψ, then ρ^* keeps extending, otherwise, it is interrupted.

In all cases, if p is not already in $V \cup S$, we add p to S. When a ray intersects the bounding box of P, it gets interrupted (without creating any new vertex). The points in V are called *real vertices* and the points in S are called *Steiner vertices*. We now add edges to the graph. Let $E = \varnothing$. For each ray ρ, we do the following. For each pair of consecutive points $p, q \in V \cup S$ belonging to ρ, we add the edge pq to E.

The grade-k emanation graph we obtain from R is then $G_R = (V \cup S, E)$. When it is clear from the context, we will write G instead of G_R. Observe that all rays interrupt at intersection, creating a Steiner vertex. Thus no two edges in an emanation graph cross each other so all emanation graphs are planar graphs.

2.3 The Relationship between Emanation Graphs and Motorcycle Graphs

Looking at the definitions of motorcycle graphs and emanation graphs, a natural question is whether or not these two families of graphs are equivalent or if one is a subfamily of the other. The key distinction between an emanation graph and a motorcycle graph is that in a motorcycle graph, if two or more non-collinear rays intersect simultaneously during construction, all rays will get interrupted, however, in an emanation graph, one ray (chosen arbitrarily) will keep extending.

Let us consider whether motorcycle graphs are a subset of emanation graphs. In a motorcycle graph there is no restriction on the number of rays which originate at a single point p. There is also no restriction on their directions or speeds. However, in a grade-k emanation graph each point will be the origin of 2^{k+1} rays of equal speeds and predetermined direction. As such, motorcycle graphs are not a subset of emanation graph. For an example of a motorcycle graph which is not an emanation graph refer to Figure 2.1.

Now let us consider whether grade-1 emanation graphs are a subfamily of motorcycle graphs. Due to the fact that all rays in an emanation graph have equal speeds and that in a motorcycle graph we can specify the speeds of the rays, then we can always create a speed assignment for the rays of the motorcycle graph such that after construction the motorcycle graph will lead to the same vertex and edge set as any grade-1 emanation graph.

Theorem 2.1. *Every grade-*1 *emanation graph is a motorcycle graph.*

The general approach to prove this theorem is the following. Given an emanation graph G, we show how to build a motorcycle graph G' that is equal to G. *For each ray in G, we define a ray in G' with the same origin, direction and speed.* Unfortunately, this simple approach does not work because of the following case. Consider the following two rays $T_1 = ((0,0), 0, 1)$ and $T_2 = ((1,-1), \pi/2, 1)$. These two rays intersect at $(1,0)$ at time $t = 1$. If T_1 and T_2 are used to build an emanation graph G, one of these two rays, say T_1, will be interrupted and thus T_2 will continue. However, if T_1 and T_2 are used to build a motorcycle graph G', both rays will be interrupted. Therefore, the two rays corresponding to T_1 and T_2 in G' cannot have the same speed. If T_1 is interrupted, then its speed must be smaller than that of T_2. The crux of the proof is then to find a correct speed assignment for all rays we use in the construction.

Proof. Let G be an emanation graph. To simultaneously handle all constraints on the speed assignments, we introduce a *priority graph*. A priority graph $P_G = (V, E)$ is a directed graph defined as follows. For each ray T_a used in the construction of G, there is a vertex a in P_G. The edges of P_G are defined as follows. We consider different cases based on how many rays intersect at a given Steiner vertex.

2 rays intersect Suppose that at a given Steiner vertex, two rays T_a and T_b intersect. If they do not intersect at the same time, then one directed edge is created in P_G. If T_a is interrupted by T_b, there is a directed edge (a, b) in E. Otherwise, if T_b is interrupted by T_a, there is a directed edge (b, a) in E

If T_a and T_b do intersect at the same time, we consider 2 different situations.

1. In Situation 1, we have two collinear rays T_a and T_b that intersect (refer to Figure 2.3a). In this case, we add the edges (a, b) and (b, a) in E. This introduces a directed cycle of length 2 in P_G.

(a) Situation 1. (b) Situation 2 where T_a is interrupted.

Figure 2.3: Situations 1 and 2 where two rays intersect at the same time.

2. In Situation 2, we have two perpendicular rays T_a and T_b that intersect at the same time (refer to Figure 2.3b). In this case, if T_a is interrupted by T_b, we add the edge (a, b) in E. Otherwise, if T_b is interrupted by T_a, we add the edge (b, a) in E.

3 rays intersect Suppose that at a given Steiner vertex, three rays T_a, T_b and T_c intersect. We consider 2 different situations.

3. In Situation 3, we have three rays T_a, T_b and T_c that intersect at the same time. Moreover, T_a, T_b and T_c are all interrupted (refer to Figure 2.4a). In this case, we add the edges (a, b), (b, c) and (c, a) in E. This introduces a directed cycle of length 3 in P_G.

(a) Situation 3 where the three rays are interrupted. (b) Situation 4 where one of the three rays is not interrupted.

Figure 2.4: Situations 3 and 4 where three rays intersect at the same time.

4. In Situation 4, we have three rays T_a, T_b and T_c that intersect at the same time. Moreover, T_a and T_c are interrupted, but not T_b (refer to Figure 2.4b). In this case, we add the edges (a, b) and (c, b) in E.

4 rays intersect Suppose that at a given Steiner vertex, four rays T_a, T_b, T_c and T_d intersect. This leads to the following situation.

5. In Situation 5, we have four rays T_a, T_b, T_c and T_d that intersect at the same time (refer to Figure 2.5). In this case, we add the edges (a, b), (b, c), (c, d) and (d, a) in E. This introduces a directed cycle of length 4 in P_G.

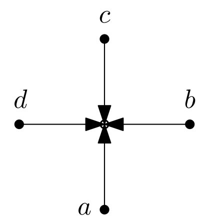

Figure 2.5: Situation 5 where four rays intersect at the same time.

Observe that a ray can be interrupted only once. By this observation and the definition of P_G, each vertex in P_G has out-degree at most 1. As such, each component in the graph we obtain is either

- a directed tree, where each node (except for the root) points to its parent
- or a directed cycle, where each node is the root of a (possibly trivial) directed tree.

We now explain how to use P_G in order to build a motorcycle graph G' that is equal to G. To build G', we first define, for each ray T from G, a ray T' in G' with the same origin and direction as T. It remains to assign a speed to each ray in G'. These speeds will be assigned using P_G. To simplify the discussion, for each vertex a in P_G, we write "the speed of a" instead of "the speed of the ray T_a corresponding to a". Here are the four steps we follow for the speed assignment.

1. Assign a speed of 1 to all vertices belonging to a directed cycle from Situations 1, 3 or 5.
2. Assign speeds to all vertices belonging to the remaining directed cycles (see below).
3. For each directed tree, if no speed has been assigned to the root, assign a speed of 1 to the root.
4. For each remaining vertex v without any speed assignment, observe that v belongs to a directed tree. Let v' be the parent of v. Assign a speed of $\lambda/2$ to v, where λ is the speed assigned to v'.

We now explain how to assign speeds to vertices belonging to directed cycles that are not related to Situations 1, 3 or 5. Assume there is a directed cycle $\mathcal{C}$ that is not defined by Situation 1, 3 or 5. We first describe all the constraints on speed assignments that need to be satisfied. Then, we explain how to design the speed assignment. Let us consider an arbitrary edge (a, b) belonging to $\mathcal{C}$. The existence of this edge implies that in G, T_a is interrupted by T_b. Moreover, since we are not in any of Situations 1, 3 or 5, T_b is not interrupted by T_a. Let $T_a = (o_a, d_a, 1)$ and $T_b = (o_b, d_b, 1)$ and denote by p the intersection point of T_a and T_b.

- Assume T_a and T_b do not intersect at the same time. Observe that in this case we have $|o_a p| > |o_b p|$. Then, in G', the speeds λ_a and λ_b of T_a and T_b must satisfy

$$\frac{|o_a p|}{\lambda_a} > \frac{|o_b p|}{\lambda_b}. \tag{2.1}$$

  This constraint makes sure that T_b reaches p before T_a does. Observe that, since $|o_a p| > |o_b p|$, any speed assignment such that $\lambda_a \leq \lambda_b$ does satisfy (2.1).

- Assume T_a and T_b do intersect at the same time. Observe that in this case we have $|o_a p| = |o_b p|$. Then, in G', the speeds λ_a and λ_b of T_a and T_b must satisfy $\lambda_a < \lambda_b$, from which (2.1) is satisfied. This constraint makes sure that T_b is not interrupted by T_a.

Thus, each edge (a, b) in $\mathcal{C}$ must satisfy (2.1).

Take an arbitrary vertex u_1 belonging to $\mathcal{C}$ and assume $\mathcal{C} = u_1 u_2 ... u_k u_1$. Each pair of consecutive vertices along this directed cycle must satisfy (2.1). We obtain the following sequence of constraints, where o_i is the origin of T_{u_i} and $p_{i,j}$ is the intersection point of T_{u_i} and T_{u_j}.

$$\begin{aligned}
\lambda_1 &< \frac{|o_1 p_{1,2}|}{|o_2 p_{1,2}|}\lambda_2 \\
&< \frac{|o_1 p_{1,2}|}{|o_2 p_{1,2}|}\frac{|o_2 p_{2,3}|}{|o_3 p_{2,3}|}\lambda_3 \\
&< \cdots \\
&< \left(\prod_{i=1}^{k-1} \frac{|o_i p_{i,i+1}|}{|o_{i+1} p_{i,i+1}|}\right)\lambda_k \\
&< \left(\prod_{i=1}^{k-1} \frac{|o_i p_{i,i+1}|}{|o_{i+1} p_{i,i+1}|}\right)\frac{|o_k p_{k,1}|}{|o_1 p_{k,1}|}\lambda_1.
\end{aligned}$$

Let us re-write this sequence of constraints in the following way:

$$\lambda_1 < \gamma_{1,2} \cdot \lambda_2 < \gamma_{2,3} \cdot \lambda_3 < ... < \gamma_{k-1,k} \cdot \lambda_k < \gamma_{k,1} \cdot \lambda_1. \tag{2.2}$$

Observe that, by the previous discussion, each ratio $\frac{|o_i p_{i,i+1}|}{|o_{i+1} p_{i,i+1}|}$ in (2.2) satisfies $\frac{|o_i p_{i,i+1}|}{|o_{i+1} p_{i,i+1}|} \geq 1$. Therefore, the coefficients from $\gamma_{1,2}$ to $\gamma_{k,1}$ are non-decreasing. Therefore, we can always find a speed assignment for all the λ_i's (see below) unless each ratio in (2.2) satisfies $\frac{|o_i p_{i,i+1}|}{|o_{i+1} p_{i,i+1}|} = 1$. Indeed, in this case, we would get $\lambda_1 < \lambda_2 < \lambda_3 < ... < \lambda_k < \lambda_1$, for which of course there does not exist any speed assignment. We argue by contradiction that the situation where each ratio in (2.2) satisfies $\frac{|o_i p_{i,i+1}|}{|o_{i+1} p_{i,i+1}|} = 1$ is not possible.

Assume that such a situation is possible. Since $\gamma_{1,2} = 1$, we need to have $|o_1 p_{1,2}| = |o_2 p_{1,2}|$ and since T_{u_2} is not interrupted by T_{u_1}, but rather by T_{u_3}, then we need to have $|o_2 p_{1,2}| \leq |o_2 p_{2,3}|$. For $2 \leq i < k-1$, since $\gamma_{i,i+1} = 1$, we need to have $|o_i p_{i,i+1}| = |o_{i+1} p_{i,i+1}|$ and since $T_{u_{i+1}}$ is not interrupted by T_{u_i}, but rather by $T_{u_{i+2}}$, then we need to have $|o_{i+1} p_{i,i+1}| \leq |o_{i+1} p_{i+1,i+2}|$. Also, we need to have $|o_{k-1} p_{k-1,k}| = |o_k p_{k-1,k}|$ and since T_{u_k} is not interrupted by $T_{u_{k-1}}$, but rather by T_{u_1}, then we need to have $|o_k p_{k-1,k}| \leq |o_k p_{k,1}|$. Finally, since $\gamma_{k,1} = 1$, we need to have $|o_k p_{k,1}| = |o_1 p_{k,1}|$. Therefore, we find

$$\begin{aligned}
|o_1 p_{1,2}| = |o_2 p_{1,2}| &\leq |o_2 p_{2,3}| = |o_3 p_{2,3}| \\
&\leq \cdots \leq |o_{k-1} p_{k-1,k}| = |o_k p_{k-1,k}| \\
&\leq |o_k p_{k,1}| = |o_1 p_{k,1}| \leq |o_1 p_{1,2}|.
\end{aligned}$$

from which we must have that all $|o_i p_{j,k}|$ are equal. But if this is the case, then we are in Situation 1, 3 or 5, which contradicts our assumption. So we know that

$$\gamma_{k,1} = \left(\prod_{i=1}^{k-1} \frac{|o_i p_{i,i+1}|}{|o_{i+1} p_{i,i+1}|} \right) \frac{|o_k p_{k,1}|}{|o_1 p_{k,1}|} > 1. \tag{2.3}$$

We can now give the speed assignment. We start with $\lambda_1 = 1$. Let $1 \leq i < k$. Then

$$\lambda_{i+1} = \frac{1 + \frac{i\,(\gamma_{k,1} - 1)}{k}}{\gamma_{i,i+1}}. \tag{2.4}$$

From that, we find (everywhere here we use the fact that $\gamma_{k,1} > 1$ by (2.3))

$$\lambda_1 = 1 < \gamma_{1,1+1} \cdot \frac{1 + \frac{(\gamma_{k,1} - 1)}{k}}{\gamma_{1,1+1}} = \gamma_{1,1+1} \cdot \lambda_2.$$

For $1 \leq i < k-1$, we find

$$\begin{aligned}
\gamma_{i,i+1} \cdot \lambda_{i+1} &= \gamma_{i,i+1} \cdot \frac{1 + \frac{i\,(\gamma_{k,1} - 1)}{k}}{\gamma_{i,i+1}} \\
&= 1 + \frac{i\,(\gamma_{k,1} - 1)}{k} \\
&< 1 + \frac{(i+1)(\gamma_{k,1} - 1)}{k} \\
&= \gamma_{i+1,i+2} \cdot \frac{1 + \frac{(i+1)(\gamma_{k,1} - 1)}{k}}{\gamma_{i+1,i+2}} \\
&= \gamma_{i+1,i+2} \cdot \lambda_{i+2}.
\end{aligned}$$

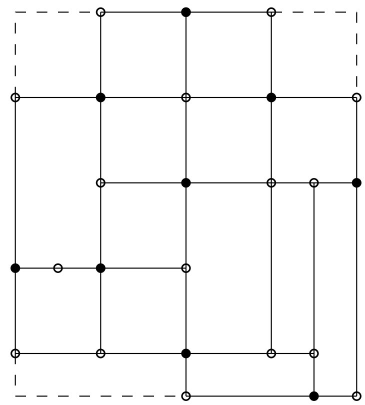

Figure 2.6: A grade-1 emanation graph containing scenarios 1-5.

And finally,

$$\gamma_{k-1,k} \cdot \lambda_k = \gamma_{k-1,k} \cdot \frac{1 + \frac{(k-1)(\gamma_{k,1}-1)}{k}}{\gamma_{k-1,k}} < \gamma_{k,1} \cdot \frac{1 + \frac{k(\gamma_{k,1}-1)}{k}}{\gamma_{k,1}} = \gamma_{k,1} = \gamma_{k,1} \cdot \lambda_1.$$

And hence, the sequence of inequalities (2.2) is satisfied. Thus we can say that every grade-1 emanation graph is a motorcycle graph. □

To illustrate the proof, we show an example of the ray speed assignments for simulating an emanation graph G with a motorcycle graph G'. In Figure 2.6 we can see an emanation graph which includes all the cases identified in the previous section.

In Figure 2.7 we can see the same emanation graph coloured such that it is easier to identify each scenario. Scenario 1 is coloured in green. Scenario 2 is coloured in magenta. Scenario 3 is coloured in red. Scenario 4 is coloured in orange. Scenario 5 is coloured in blue. While some scenarios appear more than once we only colour each scenario one time for clarity.

In Figure 2.8 we can see a version of the emanation graph where each real point has been given a label. When referring to the rays we will refer to the point of origin and include $\mu \in \{0,1,2,3\}$ as a subscript where the direction of the vector is $\frac{(4-\mu)\pi}{2}$. If the indicator of a ray r is denoted by $|r|$. For example, $a_1 = ((a_x, a_y), \frac{3\pi}{2}, |a_1|)$ is the ray that shoots downwards from point a. In the case of the emanation graph all speeds will be 1, however when we are analyzing the equivalent motorcycle graph the speeds will be variable and this notation will help to refer to them.

In Figure 2.9 we can see the priority graph of the emanation graph in Figure 2.6. From this priority graph we will use the previously stated algorithm to generate the speed assignments for each ray.

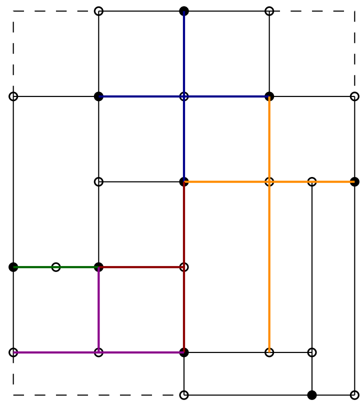

Figure 2.7: A grade-1 emanation graph containing scenarios 1-5, colour-coded.

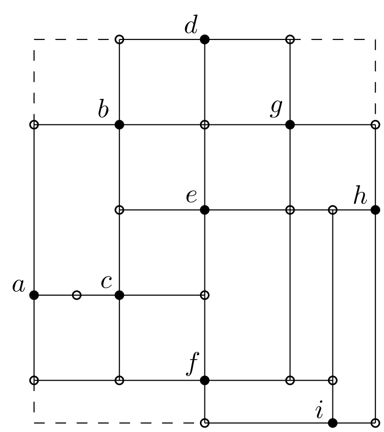

Figure 2.8: A grade-1 emanation graph containing scenarios 1-5 with labelled vertices.

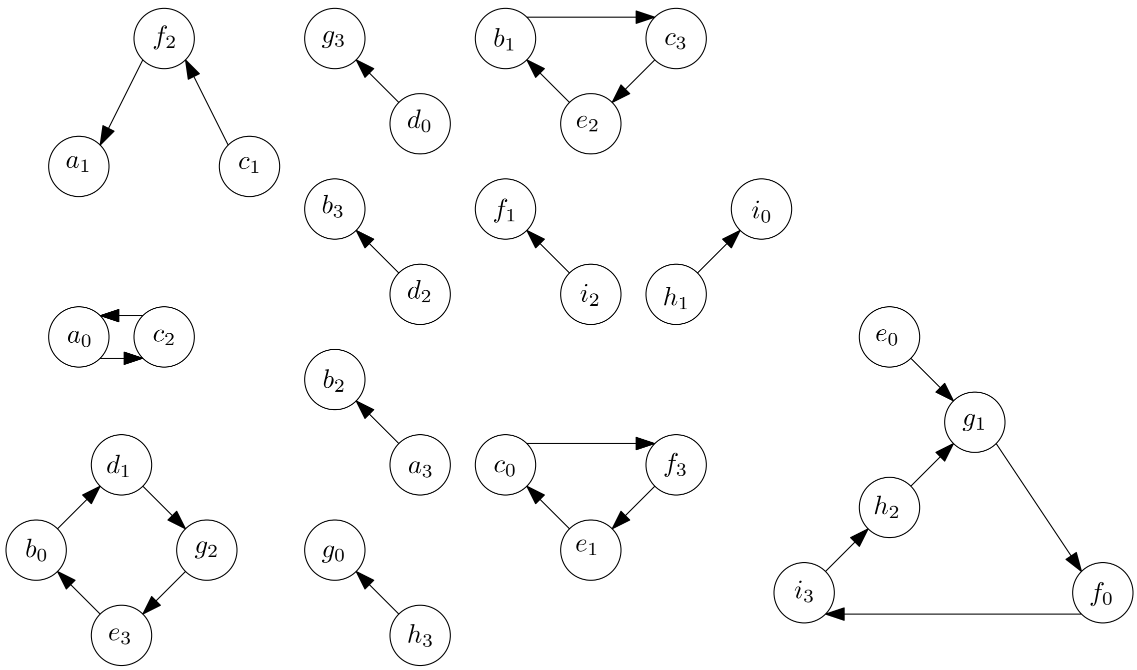

Figure 2.9: A priority graph of the emanation graph in Figure 2.6

We first assign speeds of 1 to all rays belonging to directed cycles in Situations 1, 3, and 5.

$$|b_0| = |d_1| = |g_2| = |e_3| = 1$$

$$|b_1| = |c_3| = |e_2| = 1$$

$$|c_0| = |e_1| = |f_3| = 1$$

$$|a_0| = |c_2| = 1$$

Next we assign speeds to any directed cycles which are not in cases 1, 3, or 5. In our priority graph there is only one such cycle, it is the cycle which contains rays i_3, h_2, g_1, and f_0. Let i_3 be the first ray we consider in the cycle, so $|i_3| = 1$. Next let us establish the coefficients in the inequality (2.2).

$$\gamma_{1,2} = \frac{|ip_{i_3,h_2}|}{|hp_{i_3,h_2}|} = \frac{5}{1} = 5$$

$$\gamma_{2,3} = \frac{|ip_{i_3,h_2}|}{|hp_{i_3,h_2}|} \cdot \frac{|hp_{h_2,g_1}|}{|gp_{h_2,g_1}|} = 5 \cdot \frac{2}{2} = 5$$

$$\gamma_{3,4} = \frac{|ip_{i_3,h_2}|}{|hp_{i_3,h_2}|} \cdot \frac{|hp_{h_2,g_1}|}{|gp_{h_2,g_1}|} \cdot \frac{|gp_{g_1,f_0}|}{|fp_{g_1,f_0}|} = 5 \cdot \frac{6}{2} = 15$$

$$\gamma_{4,1} = \frac{|ip_{i_3,h_2}|}{|hp_{i_3,h_2}|} \cdot \frac{|hp_{h_2,g_1}|}{|gp_{h_2,g_1}|} \cdot \frac{|gp_{g_1,f_0}|}{|fp_{g_1,f_0}|} \cdot \frac{|fp_{f_0,i_3}|}{|ip_{f_0,i_3}|} = 15 \cdot \frac{3}{1} = 45$$

Now that we have the coefficients established we can calculate the speed assignments using equation (2.4). Bearing in mind that we established i_3 to be the "first" ray in the cycle, and the order of the cycle is i_3, h_2, g_1, and f_0 we can get the speeds of each of the rays like so:

$$|h_2| = \frac{1 + \frac{1(\gamma_{4,1}-1)}{4}}{\gamma_{1,2}} = \frac{1 + \frac{1(45-1)}{4}}{5} = \frac{12}{5}$$

$$|g_1| = \frac{1 + \frac{2(\gamma_{4,1}-1)}{4}}{\gamma_{2,3}} = \frac{1 + \frac{2(45-1)}{4}}{5} = \frac{23}{5}$$

$$|f_0| = \frac{1 + \frac{3(\gamma_{4,1}-1)}{4}}{\gamma_{3,4}} = \frac{1 + \frac{3(45-1)}{4}}{15} = \frac{33}{15}$$

Next we calculate the speeds of the rays which are in directed trees, which is an easy task. First we set the speed of any ray at the root of a tree which currently has no assigned speed to 1.

$$|a_1| = |g_3| = |b_3| = |b_2| = |g_0| = |f_1| = |i_0| = 1$$

The remaining rays each receive a speed equal to half their parent's speed. The final speed assignment is:

$$|a_0| = 1$$
$$|a_1| = 1$$
$$|a_3| = \frac{1}{2}$$
$$|b_0| = 1$$
$$|b_1| = 1$$
$$|b_2| = 1$$
$$|b_3| = 1$$

$$|c_0|= 1$$
$$|c_1|= \frac{1}{4}$$
$$|c_2|= 1$$
$$|c_3|= 1$$
$$|d_0|= \frac{1}{2}$$
$$|d_1|= 1$$
$$|d_2|= \frac{1}{2}$$
$$|e_0|= \frac{23}{10}$$
$$|e_1|= 1$$
$$|e_2|= 1$$
$$|e_3|= 1$$
$$|f_0|= \frac{33}{15}$$
$$|f_1|= 1$$
$$|f_2|= \frac{1}{2}$$
$$|f_3|= 1$$
$$|g_0|= 1$$
$$|g_1|= \frac{23}{5}$$
$$|g_2|= 1$$
$$|g_3|= 1$$
$$|h_1|= \frac{1}{2}$$
$$|h_2|= \frac{12}{5}$$
$$|h_3|= \frac{1}{2}$$
$$|i_0|= 1$$
$$|i_2|= \frac{1}{2}$$
$$|i_3|= 1$$

3

Spanning Properties of Motorcycle and Emanation graphs

Hamedmohseni et al. [4] proved that emanation graphs are spanners. Specifically, let $k \geq 1$ be an integer. The showed that there exists a constant α_k (which depends on k) such that for all grade-k emanation graphs G and all real vertices u and v in G, there exists a path between u and v in G whose length is at most $\alpha_k \cdot |uv|$. In this thesis, when we say that emanation graphs are spanners, we refer to the existence of spanning paths between real vertices. As such, a natural question is whether or not there exist spanning paths such that one of the endpoints is a Steiner vertex. Here are two questions we want to study in this Chapter.

1. As shown in Section 2.3, every emanation graph is a motorcycle graph. Are motorcycle graphs spanners? (See Section 3.1.)
2. In an emanation graph, is there a spanning path between a real vertex and a Steiner vertex, or between two Steiner vertices? (See Section 3.2.)

3.1 Motorcycle graphs are not Spanners

Motorcycle graphs are not spanners, as disconnected motorcycle graphs exist.

Lemma 3.1. *There exist disconnected motorcycle graphs.*

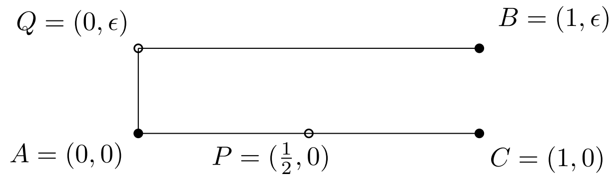

Figure 3.1: Illustration of the proof of Lemma 3.2.

Proof. See Figure 2.1, which shows a disconnected motorcycle graph. $\square$

A natural question is then: are connected motorcycle graphs spanners? The answer is no.

Lemma 3.2. *There exist connected motorcycle graphs with arbitrarily large spanning ratios.*

Proof. Let $\epsilon > 0$ be a real number. Let $A = (0, 0)$, $B = (1, \epsilon)$ and $C = (1, 0)$. Consider the following four rays (refer to Figure 3.1).

$$\rho_1 = (A, 0, 1)$$
$$\rho_2 = (C, \pi, 1)$$
$$\rho_3 = (B, \pi, \epsilon)$$
$$\rho_4 = (A, \pi/2, \epsilon)$$

The rays ρ_1 and ρ_2 meet at $P = (\frac{1}{2}, 0)$ (after $\frac{1}{2}$ s), where a Steiner vertex is created. The rays ρ_3 and ρ_4 meet at $Q = (0, \epsilon)$ (after $\frac{1}{\epsilon}$ s), where a Steiner vertex is created. The spanning ratio between B and C is equal to

$$\frac{1 + \epsilon + 1}{\epsilon} = 1 + \frac{2}{\epsilon} \tag{3.1}$$

which tends to infinity as $\epsilon \to 0$. $\square$

3.2 Spanning Properties of Grade-1 Emanation Graphs

Hamedmohseni et al. [4] proved that a spanning path exists between any two real vertices in emanation graphs. In this section, we want to study the existence of spanning paths between real vertices and Steiner vertices and between two Steiner vertices. We focus on grade-1 emanation graphs.

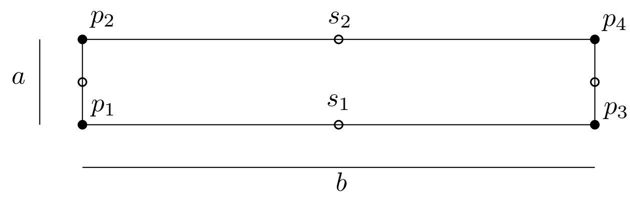

Figure 3.2: A grade-1 emanation graph with an unbounded spanning ratio between two Steiner vertices.

3.2.1 The Spanning Ratio Between Two Steiner Vertices in a Grade-1 Emanation Graph

In general, in a grade-1 emanation graph, there is no spanning path between Steiner vertices.

Lemma 3.3. *There exists a grade-*1 *emanation graph G whose spanning ratio between Steiner vertices is arbitrarily large.*

Proof. Consider the point set $\{p_1, p_2, p_3, p_4\}$ where $p_1 = (0, 0)$, $p_2 = (0, a)$, $p_3 = (b, 0)$, and $p_4 = (b, a)$ where a is arbitrarily small and b is arbitrarily large. After the construction of the emanation graph we will have a Steiner vertex between each pair of collinear vertices. We will show that the spanning ratio between the Steiner vertices s_1 at $(\frac{b}{2}, 0)$ and s_2 at $(\frac{b}{2}, a)$ can be made arbitrarily large.

Since s_1 and s_2 share the same x-coordinate, their Euclidean distance is simply $|s_1s_2|= a$. Their graph distance is

$$|s_1s_2|_G = |s_1p_1| + |p_1p_2| + |p_2s_2| = \frac{b}{2} + a + \frac{b}{2} = a + b.$$

Thus the spanning ratio is $\frac{a+b}{a}$, which is an arbitrarily large number divided by an arbitrarily small number, and so the spanning ratio can be made arbitrarily large.

An example can be seen in Figure 3.2. $\square$

3.2.2 The Spanning Ratio between a Real Vertex and a Steiner Vertex

Let us define four direction vectors $d_0 = (1, 0)$ (rightward), $d_1 = (0, -1)$ (downward), $d_2 = (-1, 0)$ (leftward), and $d_3 = (0, 1)$ (upward).

Definition 3.1 (Bounded Detours Path)**.** Let u be a real vertex in an emanation graph and d_i be one of the four directions. A *bounded detours path from u in direction d_i* is a path we obtained as the result of the following procedure.

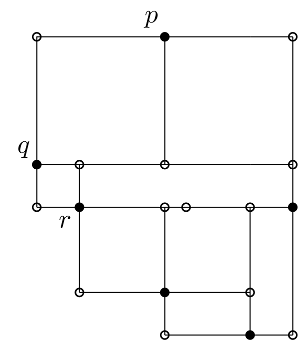

Figure 3.3: A grade-1 emanation graph.

Let v be the current vertex (we start with $v = u$).

1. We move in direction d_i as much as we can. Let w be the last vertex we reach and let v' be the last real vertex we encountered. If $w = v'$, STOP. Otherwise, proceed with Step 2.

2. Let W be the set of real vertices w' such that $|ww'| \leq |wv'|$, ww' is in direction $d_{i\pm1}$ and ww' does not contain any real vertex in its interior. If $W \neq \varnothing$, pick an arbitrary $w' \in W$, move to w' and proceed with Step 1 with $v = w'$. Otherwise, STOP.

Since we make an arbitrary decision in Step 2, there may exist more than one bounded detours path from u in direction d_i. Also observe that, by definition, a bounded detours path in direction d_i is monotonic with respect to direction d_i.

We will use the graph in Figure 3.3 to show several examples of bounded detours paths.

The first example is a bounded detours path consisting of a single vertex: the upward bounded detours path from vertex p contains only p.

The second example is the rightward bounded detours path from r, highlighted in orange in Figure 3.4, which ends at a real vertex.

The third example is the downwards bounded detours path from p.

Observe that by definition, each real vertex u has at least one bounded detours path in each of the four directions. Such a path may consist of only u itself.

We define the subpath of a path $\mathcal{P}$ which begins at a vertex u and ends at a vertex v by $\mathcal{P}_{u,v}$.

Lemma 3.4. *Let u be a real vertex and $\mathcal{P}$ be a bounded detours path from u in direction d_0 or d_2 (respectively d_1 or d_3). Consider a vertex v along $\mathcal{P}$ and let $D = |uv|_x$ (respectively $D = |uv|_y$). The subpath $\mathcal{P}_{u,v}$ has length at most $2D$.*

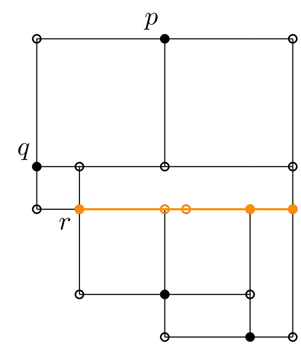

Figure 3.4: The rightwards bounded detours path from r.

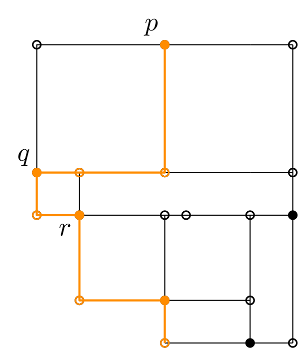

Figure 3.5: The downwards bounded detours path from p.

Proof. By definition of the bounded detours path the edges added to $\mathcal{P}_{u,v}$ in Step 1 are all in direction d_i. Thus the total length of these paths will be D. Consider that Step 2 is only executed after an execution of Step 1 and consider that the edges added to $\mathcal{P}$ in step 2 are in a direction perpendicular to d_i. Thus the path composed of these edges is restricted to being at most as long as the path produced immediately before in Step 1. Thus $\mathcal{P}_{u,v}$ has a length at most $2D$. □

Lemma 3.5. *Let u be a real vertex and $\mathcal{P}$ be a bounded detours path from u in direction d_i. Let v be the last vertex on $\mathcal{P}$. Then v has a shadow edge in direction d_i.*

Proof. We begin with two cases; either (1) v is a real vertex, or (2) v is a Steiner vertex.

1. Assume v is a real vertex. Since v is the last vertex on $\mathcal{P}$ then v does not have a neighbour in direction d_i. This implies the ray $r = (v, -i\frac{\pi}{2}, 1)$ was not interrupted. Which implies v having a shadow edge in direction d_i.
2. Assume v is a Steiner vertex. This implies the existence of a real vertex w such that v is in direction d_i from w. Since v is the last vertex in a bounded detours path, then v does not have a real neighbour v' in direction $d_{i\pm1}$ such that $|vv'| \leq |vw|$. If the ray $r = (v, -i\frac{\pi}{2}, 1)$ was interrupted then such a v' must exist or v would have a neighbour in direction d_i (which it does not). Thus r is not interrupted. So v has a shadow edge in direction d_i.

□

We will prove that the spanning ratio between a Steiner vertex and a real vertex is at most $\sqrt{10}$ (refer to Theorem 3.9). Prior to that, we need some preparatory lemmas.

Lemma 3.6. *Let v be a Steiner vertex. If there is not a pair of collinear edges incident to v, then there is an edge incident to v that is collinear with a shadow edge incident to v.*

Proof. A Steiner vertex is created when two rays intersect. There are two cases depending on how many rays are interrupted at the intersection.

1. **Exactly one ray is interrupted.** The interrupted ray terminates at v, while the other ray continues through v. There are two subcases depending on whether the two rays are collinear or perpendicular.
   (a) **The two rays are collinear.** The continuing ray passes through v in the same direction, so v has two collinear incident edges.

(b) **The two rays are perpendicular.** The interrupted ray terminates at v, and the continuing ray passes through v. If the continuing ray is later interrupted by another ray, then v has an edge in the direction of the continuing ray, giving v a collinear pair of incident edges. If the continuing ray is never interrupted, it extends to infinity from v, forming a shadow edge collinear with the terminated ray.

2. **Both rays are interrupted.** Since both rays are interrupted at v, they must be collinear and travelling in opposite directions, meeting head-on. Thus v has two collinear incident edges.

In every case, v either has two collinear incident edges or has a shadow edge collinear to an incident edge. □

Observation 3.1. Let $G = (V \cup S, E)$ be an emanation graph. Consider two arbitrary vertices $u \in S$ and $v \in V$. Without loss of generality, we can assume that u is at the origin, v is in the first quadrant and there exist two collinear edges or shadow edges e_1 and e_2 incident to u satisfying the following property. At most one of e_1 and e_2 is a shadow edge, and at least one of e_1 and e_2 is vertical and in the first quadrant.

Definition 3.2 (Staircase Paths)**.** Let u be a vertex, and x and y be two directions such that x and y are perpendicular. An *x-y-staircase path from u* is a path produced by the following steps. Let v be the current vertex (at the beginning, $v = u$).

1. Starting at v, move as far as possible in direction x. Let w be the current vertex. Then, if there is an edge from w in direction y, proceed with step 2. Otherwise stop.

2. Starting at w, move as far as possible in direction y. Let v be the current vertex. Then, if there is an edge from v in direction x, proceed with step 1. Otherwise stop.

Lemma 3.7. *Let $\mathcal{S}$ be a x-y-Staircase path from u. Let v be the last vertex on $\mathcal{S}$. Then v has a shadow edge in direction x or direction y.*

Proof. Consider that a x-y-Staircase path ends when there is no edge in direction x or y. Since x and y must by definition be perpendicular directions then by Lemma 3.6 there must be a shadow edge incident to v in either direction x or direction y. □

Lemma 3.8. *Let $e = (v, \theta, 1)$ be a shadow edge of a grade-1 emanation graph G. Then e does not intersect any edge or shadow edge of G.*

Proof. Suppose for contradiction that e intersects an edge or shadow edge e' of G at a point q. Recall that v is the last vertex visited by the original construction ray r before it escaped the bounding box, and that e is the ray $(v, \theta, 1)$ shooting from v in the same

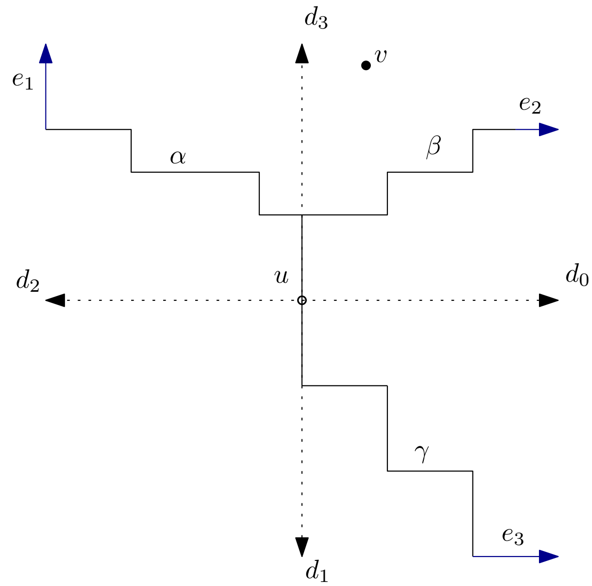

Figure 3.6: An illustration of the staircase paths α, β, and γ along with their corresponding shadow edges e_1, e_2, and e_3. In this figure we show v such that a half-line extending in direction d_1 with origin at v intersects β. This is not always the case.

direction as r. Since v is the last vertex on r, no ray of G intersected r between v and the bounding box during construction. But if e' is an edge of G, it was created by a ray that passed through q, meaning that ray would have intersected r at q, forcing r to either be interrupted at q or to create a new vertex at q, contradicting the fact that v is the last vertex on r. If e' is a shadow edge, its defining ray also passed through q uninterrupted, meaning it would have intersected r at q during construction, again forcing one of them to be interrupted. Both cases lead to a contradiction. Therefore, e does not intersect any edge or shadow edge of G. □

Theorem 3.9. *The spanning ratio between a Steiner vertex and a real vertex in a grade-*1 *emanation graph is at most* $\sqrt{10}$.

Proof. Let G be a grade-1 emanation graph. Let u be any Steiner vertex in G. Let v be any real vertex in G. By Observation 3.1, we assume that u is at the origin and v is in the first quadrant and an edge or a shadow edge incident to u is vertical and in the first quadrant. Let α be a d_3-d_2-Staircase path from u, consider e_1 to be a shadow edge incident to the last vertex on α. Let β be a d_3-d_0-Staircase path from u, consider e_2 to be a shadow edge incident to the last vertex on β. Let γ be a d_0-d_1-Staircase path from u, consider e_3 to be a shadow edge incident to the last vertex on γ. We provide an example of these paths in Figure 3.6 Let us consider three cases for the position of v.

1. v is on β. Then there exists a path connecting v and u which is xy-monotonic,

with Euclidean distance $|uv|=\sqrt{|uv|_x^2+|uv|_y^2}$ and path length $|uv|_x+|uv|_y$. The ratio $\frac{|uv|_x+|uv|_y}{\sqrt{|uv|_x^2+|uv|_y^2}}$ is maximized when $|uv|_x=|uv|_y$, giving $\sqrt{2}\leq\sqrt{10}$.

2. v is positioned such that a half-line originating at v pointing in direction d_i intersects β or e_2. Let $\mathcal{P}$ be the downward bounded detours path from v.

   We would like to show that $\mathcal{P}$ will intersect β or α. We will assume that such an intersection does not exist and prove that this situation is a contradiction. For this to be true one of the following cases must be true:

   (a) Let w be the last vertex on $\mathcal{P}$. Let h be a half-line starting at w pointing downwards. The half-line h intersects α, e_1, e_2, or β. To show that this case is a contradiction we will recall that a bounded detours path in direction d_i ends with a shadow edge in direction d_i. Since we know there is an edge or shadow edge in direction d_i then this is a contradiction of Lemma 3.8, as it implies that the shadow edge intersects an edge or a shadow edge.

   (b) Let w be the last vertex on $\mathcal{P}$. Let h be a half-line starting at w pointing downwards. The half-line h does not intersect α, e_1, e_2, or β. Recall that there is not a vertex on $\mathcal{P}$ between v and w (inclusive) such that this vertex is also in α or β, as we assume these paths do not intersect. Since $\mathcal{P}$ cannot share a vertex with α or β then this means it must cross e_1 or e_2, otherwise h would intersect α, e_1, e_2, or β. However by Lemma 3.8 a shadow edge cannot intersect an edge, and thus $\mathcal{P}$ cannot intersect e_1 or e_2.

   Using the existence of an intersection between $\mathcal{P}$ and α or β, we break down the total path distance between u and v. The paths α and β are both positively y-monotonic, while $\mathcal{P}$ is negatively y-monotonic. Therefore, their intersection guarantees a path whose vertical segments sum to $|uv|_y$. It remains to bound the horizontal distance. The intersection point is at most $|uv|_x+|uv|_y$ away from u horizontally: the $|uv|_x$ term accounts for travelling along the staircase path to reach the same horizontal coordinate as v, and the $|uv|_y$ term accounts for the fact that $\mathcal{P}$ deviates at most $|uv|_y$ horizontally from v by definition of the bounded detours path. The horizontal path lengths traversed along $\mathcal{P}$ itself also amount to at most $|uv|_y$, again by definition of the bounded detours path. This gives a total path length of $3|uv|_y+|uv|_x$.

3. v is positioned such that a half-line originating at v pointing leftwards intersects β or e_2. This case follows an identical argument to case 2, with $\mathcal{P}$ taken as the leftwards bounded detours path from v and with the roles of the x- and y-coordinates swapped throughout. The resulting total path length is $3|uv|_x+|uv|_y$.

Therefore the spanning ratio is at most either:

$$\frac{|uv|_x+3|uv|_y}{\sqrt{|uv|_x^2+|uv|_y^2}} \quad \text{or} \quad \frac{3|uv|_x+|uv|_y}{\sqrt{|uv|_x^2+|uv|_y^2}}. \tag{3.2}$$

Both expressions attain a maximum value of $\sqrt{10}$, so the spanning ratio is at most $\sqrt{10}$. This argument closely mirrors the proof in [4] for the spanning ratio between two real vertices in a grade-1 emanation graph; since a real vertex has four incident edges, it also serves as an alternate proof for that case. $\square$

4

Local Routing on Grade-1 Emanation Graphs

In this section we explore local routing on grade-1 emanation graphs. Recall from Section 1.3 the analogy of a robot routing through a city. In this chapter we make heavy use of this terminology when discussing the agent routing on a geometric graph.

For the rest of this thesis, we make the following general position assumption for grade-1 emanation graphs unless stated otherwise. We assume that no two real vertices have the same x-coordinate, no two real vertices have the same y-coordinate, and no two real vertices belong to a common line whose slope is ± 1.

4.1 Unsuccessful Routing Algorithms

In this section, we discuss different local routing algorithms from the literature. We show that these routing algorithms fail on grade-1 emanation graphs.

4.1.1 Greedy Routing

Recall that greedy routing works as described in Section 1.3.1. We show that greedy routing can fail on a grade-1 emanation graph; see Figure 4.1 for an example. We can observe the path produced by following the greedy routing algorithm on the graph in Figure 4.1. At vertex s, the robot moves to vertex v_1, as v_1 is the neighbour closest to t. The robot then routes to v_3, as v_3 is closer to t than v_2 and s. From here, the robot routes back to v_1, as v_1 is closer to t than v_4. From this point, the robot continues to alternate between v_1 and v_3, never reaching t.

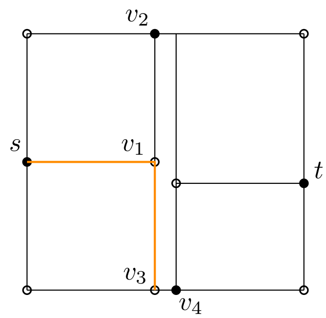

Figure 4.1: An emanation graph which defeats greedy routing with the path produced by greedy routing highlighted in orange.

4.1.2 Compass Routing

Recall that compass routing works as described in Section 1.3.2. Compass Routing can be defeated by grade-1 emanation graphs in general position. Consider the graph in Figure 4.2. The trace is shown in Figure 4.2. From s, the robot routes to v because the angle between the line segment st and sv is minimal among all neighbours of s. The angle between vt and an incident edge of v is then minimal when choosing the edge sv, so the robot routes back to s. From here the robot enters a loop, and t is never reached.

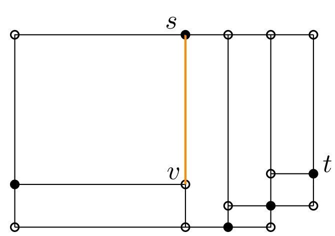

Figure 4.2: An emanation graph which defeats compass routing with the path produced by compass routing highlighted in orange.

4.1.3 Greedy-Compass Routing

Recall that greedy compass Routing works as described in Section 1.3.3. The graph in Figure 4.1 also defeats this algorithm: from s the robot routes to v_1, then to v_3, and then back to v_1, entering an infinite loop. The trace matches Figure 4.1.

4.2 Successful Routing Algorithms With a Proven Arbitrarily Large Routing Ratio

4.2.1 Face-Routing

Recall the definition of face-routing from Section 1.3. We show that Face Routing has an arbitrarily large routing ratio on grade-1 emanation graphs.

Our strategy is to construct two grade-1 emanation graphs, G_A (Figure 4.3) and G_B (Figure 4.4), that are *locally consistent* up to a vertex p. In particular, for every vertex v_i visited by face routing from s to p, the local neighbourhood is identical in both graphs, so the robot cannot distinguish whether it is traversing G_A or G_B. Upon reaching p, we *instantiate* the underlying graph based on the robot's choice of the next vertex. This allows us to ensure that, regardless of which neighbour is selected at p, the resulting path has arbitrarily large length.

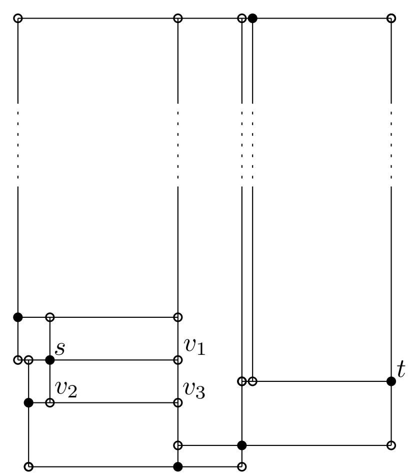

Figure 4.3: The grade-1 emanation graph G_A used in the lower bound for face routing.

Let F_1 be the face in G_A or G_B which contains the edge v_1v_3 and the vertex s. The robot begins at s and routes along the face F_1 until it reaches either v_1 (if it traverses F_1 clockwise) or v_3 (if it traverses F_1 counter-clockwise). In either case, the robot then begins routing along the boundary of the face F_2 (where F_2 is the face opposite of F_1 relative to the edge v_1v_3), which we construct to have an arbitrarily large perimeter. Note that, as defined in [25], from a vertex v the robot traverses a face boundary only until reaching an edge of that face which intersects the segment vt and does not contain the vertex v; however, we construct F_2 so that this portion of its boundary is itself arbitrarily long.

We now instantiate the graph as follows. If the robot routes along F_2 clockwise (regardless of whether it arrived at v_1 or v_3), we use G_A. Otherwise, if the robot routes along

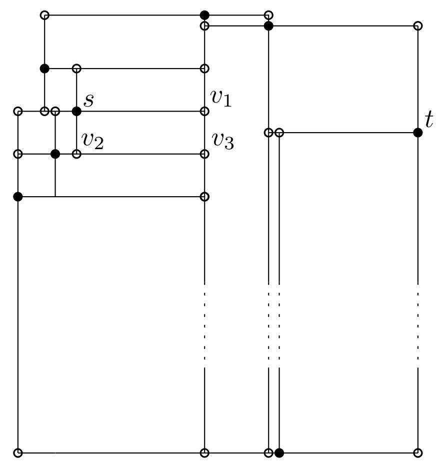

Figure 4.4: The grade-1 emanation graph G_B used in the lower bound for face routing.

F_2 counter-clockwise, we use G_B. In each case, the chosen graph is constructed so that the traversal forces the robot along a path whose length can be made arbitrarily large relative to $|st|$.

4.3 A Successful Routing Algorithm for Grade-1 Emanation Graphs

In this section we describe an algorithm for routing in grade-1 emanation graphs in general position, which we call the Marking Algorithm. Given a grade-1 emanation graph $G = (V \cup S, E)$ and two real vertices $s, t \in V$, the Marking Algorithm routes from s to t. We begin by stating some necessary definitions.

Let us consider an axis-aligned square $Q_{t,v}$ centred at a real vertex t with a real vertex v on its boundary. We denote the boundary of $Q_{t,v}$ by $\partial Q_{t,v}$ and the interior of $Q_{t,v}$ by $\text{int}(Q_{t,v})$. As such, we have $Q_{t,v} = \partial Q_{t,v} \cup \text{int}(Q_{t,v})$ and $\partial Q_{t,v} \cap \text{int}(Q_{t,v}) = \varnothing$.

Consider a point u and let L_u^i ($i \in \{0, 1, 2, 3\}$) be the half-line extending in direction $d_{i-1} + d_i$ from u (all indices are taken modulo 4). Let C_u^i be the cone with apex u bounded by L_u^i and L_u^{i+1} (included). We refer to the half-lines L_u^i and L_u^{i+1} as the *boundary* of C_u^i. As such, a point (different than u) on L_u^i belongs to C_u^{i-1} and C_u^i and u belongs to all of the C_u^i's (refer to Figure 4.5).

We also define a *straight path* to be a path composed of edges such that every edge in the path is vertical or every edge in the path is horizontal. Observe that in a straight path, all edges belong to a common line.

Let v be a Steiner vertex. A *real neighbour of* v is a real vertex v' such that the shortest path between v and v' is a straight path which does not contain any real vertex other than

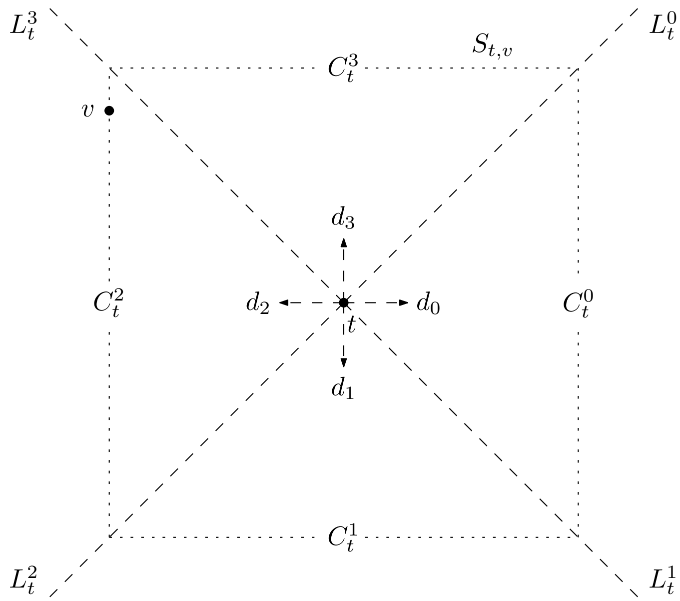

Figure 4.5: Illustration of the definitions of the different subspaces.

v'. Observe that a real neighbour of v is not necessarily a neighbour of v. We denote by $\mathcal{N}_r(v)$ the set of real neighbours of v. Following the analogy that the target is a large landmark that can be seen from anywhere in the city (such as the CN Tower in Toronto), we can say that each real vertex is a smaller landmark which is only visible from spots with a straight road to the landmark (though one cannot see any other landmarks past these smaller landmarks). Since we assumed general position, we have the following property about real neighbours.

Lemma 4.1. *For any Steiner vertex u, we have $|\mathcal{N}_r(u)| = 2$.*

Proof. Let v_1 and v_2 be two real vertices such that the Steiner vertex u is created when two rays shooting from v_1 and v_2 intersect. Thus, there is a set of edges between u and v_1 forming a straight path and a set of edges between u and v_2 forming a straight path. By the general position assumption, v_1 and v_2 are the two real neighbours of u. □

Now we describe the Marking Algorithm. We add the assumption that while executing the Marking Algorithm the robot is able to view the real neighbours of a Steiner vertex u when the robot is at u.

The Marking Algorithm receives as input: the target $t \in V$, the *current vertex* $u \in V \cup S$, a *direction vector* d, and a *navigator vertex* $v \in V$. At the beginning, the Marking Algorithm is called with $u = s$, $d = d_0$ (but we can use any arbitrary direction) and $v = s$. Each time we call the Marking Algorithm, u gets updated to the next vertex in a walk which ends at t. The algorithm identifies the direction to move from

u, then advances to the next vertex in that direction. The description of the MARKING ALGORITHM can be seen in Algorithm 1.

Algorithm 1 The MARKING ALGORITHM

Require: Data: three real vertices $s, t, v \in V$, a vertex $u \in V \cup S$ and a direction $d \in \{d_0, d_1, d_2, d_3\}$.
Ensure: Result: Computes the neighbour u' of u to walk to.

if $u \in V$ **then**
    if $u = t$ **then**
        DONE.
    else
        Set d to the direction from u to $\text{int}(Q_{t,u})$.
        Let u' be the neighbour of u in direction d.
    end if
else
    if $\mathcal{N}(u)$ contains a vertex in direction d **then**
        Let u' be the neighbour of u in direction d.
    else
        Let w be the vertex such that $w \in \mathcal{N}_r(u) \setminus \{v\}$.
        Let $v = w$.
        if $u \notin \text{int}(Q_{t,v})$ **then**
            Let d be the direction from u to v.
            Let u' be the neighbour of u in direction d.
        else
            Let d be the direction from v to u.
            Let u' be the neighbour of u in direction d.
        end if
    end if
end if
Set $u = u'$.

Figure 4.6 illustrates the MARKING ALGORITHM on a grade-1 emanation graph.

We now describe the path constructed via the MARKING ALGORITHM in Figure 4.6. Beginning at vertex $s \in C_t^2$, the robot moves in direction d_0, passing by Steiner vertex u_1, until it reaches the Steiner vertex u_2 such that u_2 does not have a real neighbour in direction d_0. Then, at u_2 the robot observes the real neighbours of u_2. It has one real neighbour in $\mathcal{N}_r(u_2) \setminus \{s\}$, which we call v_1. The real vertex v_1 is in direction d_3 from u_2 and $u_2 \in \text{int}(Q_{t,v_1})$, thus the robot moves in the direction d_1 opposite of v_1, again, continuing until it reaches a vertex u_3 such that u_3 does not have a neighbour in direction d_1. Due to the real neighbour of u_3 in direction d_2 the robot moves in direction d_0 until reaching u_5. Upon reaching u_5 the robot observes that u_5 has a real neighbour v_2 such that

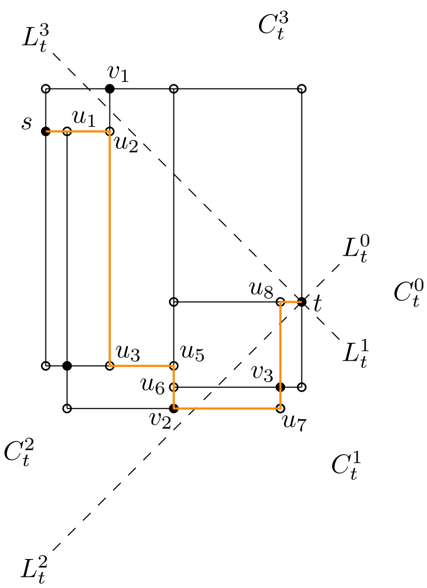

Figure 4.6: Illustration of a path constructed using the MARKING ALGORITHM on a grade-1 emanation graph in general position.

$u_5 \notin \text{int}(Q_{t,v_2})$, thus the robot moves towards v_2. Since $v_2 \in C_t^2$ then the robot will move in direction d_0 until it reaches u_7. At u_7 the robot observes that u_7 has a real neighbour v_3 such that $u_7 \notin \text{int}(Q_{t,v_3})$. Thus it moves towards v_3. Once at $v_3 \in C_t^1$ the robot will move in direction d_3 until reaching u_8 which has a real neighbour t such that $u_8 \notin \text{int}(Q_{t,t})$, thus the robot will move towards t, finally reaching the target.

4.3.1 Proving the Marking Algorithm is Well-Defined

We begin by proving that the MARKING ALGORITHM is well-defined, i.e., that for all grade-1 emanation graphs G in general position, every step of the MARKING ALGORITHM can be executed.

In Algorithm 1, Lines 6, 16 and 19 rely on the existence of a neighbour of u in direction d. Moreover, Line 12 relies on the existence of a *real* neighbour of u that is distinct from v. Therefore, to prove that Algorithm 1 is well-defined, we need to prove the existence of all these neighbours. Prior to this, we prove two fundamental properties in Lemma 4.2 and Corollary 4.4.

Lemma 4.2. *Let $\mathcal{C}$ be a cone with angle $\frac{\pi}{2}$ and apex c. Let p be a point outside of $\mathcal{C}$ whose projection p' onto the bisector of $\mathcal{C}$ belongs to $\mathcal{C}$. Then $|pp'| > |cp'|$.*

Proof. Let b denote the bisector of $\mathcal{C}$. Without loss of generality, assume the direction from c to p' is d_3. We note that the angle between b and either side of $\mathcal{C}$ is $\frac{\pi}{4}$. Let us denote

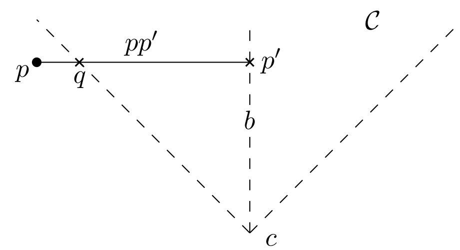

Figure 4.7: Illustration of Lemma 4.2 for the case where $i = 3$.

the point of intersection between pp' and $\partial\mathcal{C}$ by q. Refer to Figure 4.7 for an illustration of the case. Observe that $\triangle cp'q$ forms an isosceles right triangle. Thus, cp' and qp' have the same length. Since $|pq| > 0$, then $|pp'| > |cp'|$. □

Corollary 4.3. *Let $u, v \in V$ be two real vertices such that $u \neq v$. Then for any ray ρ_u shooting from u in direction d where $d \in \{d_0, d_1, d_2, d_3\}$ if $\rho_u \cap L_v^i \neq \varnothing$ then $\rho_u \cap L_v^{i-1} = \varnothing$ and $\rho_u \cap L_v^{i+1} = \varnothing$.*

Proof. Without loss of generality assume that $i = 3$ and $u \in C_v^2$. As such, $d = d_0$ or $d = d_3$.

If $d = d_3$ and ρ_u intersects L_v^3, then ρ_u will not intersect any other line in $\{L_v^0, L_v^1, L_v^2\}$.

If $d = d_0$ and ρ_u intersects L_v^3, then we will show that ρ_u cannot intersect L_v^0.

Let ℓ be the supporting line of ρ_u and $\triangle_{v,\ell}^3$ be the triangle defined by L_v^3, L_v^0, and ℓ. Refer to Figure 4.8. Consider the real vertex w in $\triangle_{v,\ell}^3$ that is closest to ℓ (we possibly have $w = v$). Therefore, the triangle $\triangle_{w,\ell}^3$, defined by L_w^3, L_w^0, and ℓ, is empty of real vertices.

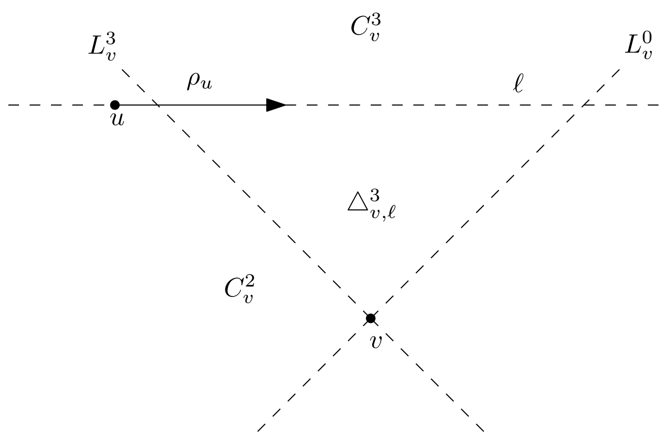

Figure 4.8: Illustration of Corollary 4.3 for the case where $i = 3$.

Let us consider the contribution of the ray ρ_w shot from w, in direction d_3, during the construction of the graph. Since $\triangle_{w,\ell}^3$ is empty of real vertex. Then, by Lemma 4.2, any ray which intersects ρ_w before ρ_w reaches ℓ cannot interrupt ρ_w. Let p be the intersection point of ℓ and ρ_w.

Consider now the ray ρ_u shot from u, in direction d_0, during the construction of the graph. Note that ρ_u will not intersect v, as this would imply u and v have the same y coordinate, which contradicts the general position assumption. We consider two cases: (1) ρ_u reaches p during the construction of the graph or (2) ρ_u does not reach p.

1. Suppose ρ_u reaches p during the construction of the graph. Since u is not in $\triangle^3_{v,\ell}$ then it is also not in $\triangle^3_{w,\ell}$. Therefore, by Lemma 4.2, we have $|up| > |wp|$. As such, ρ_u gets interrupted by ρ_w at p.
2. Suppose ρ_u does not reach p during the construction of the graph. Then it is interrupted earlier in C^3_v.

In both cases, we obtain $\rho_u \cap L^0_v = \varnothing$.

□

Corollary 4.4. *Consider a straight path* Π *that is perpendicular to the bisector of* C^i_v*. If there is no real vertex in* $\Pi \cap C^i_v$*, then* Π *cannot* span C^i_v*, i.e.,* $\Pi \cap L^i_u = \varnothing$ *or* $\Pi \cap L^{i+1}_u = \varnothing$*.*

Proof. This proof follows trivially from Corollary 4.3. If Π spans a cone C^i_v this would imply that a ray shooting from a real vertex u, where $u \in \Pi$ and $u \notin C^i_v$, intersected L^i_v and L^{i+1}_v. By Corollary 4.3 this is not possible. □

The following Lemma states that Line 6 of Algorithm 1 is well-defined.

Lemma 4.5. *Let* $u, t \in V$ *be two different real vertices such that* $u \in C^i_t$*. Then* u *has a Steiner neighbour in direction* d_{i+2}*.*

Proof. Without loss of generality assume that u is in C^2_t and u has a greater y-coordinate than t. Consider the ray ρ_u shot from u, in direction d_0, during the construction of the graph. If u does not have a Steiner neighbour in direction d_0, then, during the construction of the graph, ρ_u was not intersected by any other ray. As such, it was uninterrupted during the construction of the graph. However, By Corollary 4.3, ρ_u will be interrupted before it can span C^2_t. This is a contradiction. As such, u has a Steiner neighbour u' in direction d_0. □

In Line 12 of Algorithm 1 we assume that if u is a Steiner vertex and u has no neighbour in direction d, then there must be at least two real neighbours of u, namely the vertex stored in v and a real neighbour distinct from v which we call w. Line 12 of Algorithm 1 is well-defined by Lemma 4.1.

In Line 6 of Algorithm 1 we assume that a Steiner vertex u has a neighbour u' in the direction of a real neighbour. The following lemma shows that u' exists.

Lemma 4.6. *If a vertex u has a real neighbour v in direction d then it has a neighbour u' in direction d.*

Proof. If u has a real neighbour v in direction d, then there is a straight path in direction d between u and v which does not contain any real vertices aside from v. Thus there is an edge incident to u in direction d. Therefore, u has a neighbour u' in direction d. It is possible that $u' = v$. □

We have the following observation about Algorithm 1.

Observation 4.1. While executing Algorithm 1, if u is a Steiner vertex and $u \in \text{int}(Q_{t,v})$, then we move away from v. In such a case, $d = d_i$ if and only if $v \in C_t^{i+2}$. If $u \notin \text{int}(Q_{t,v})$, then we move towards v.

Let us now analyze the situation of Line 19. Our goal is to argue that v and w are in two adjacent cones of t. In Line 19, the robot just reached a Steiner vertex u by travelling in direction d_i away from a real vertex v. By the previous observation, we have that $v \in C_t^{i+2}$. Moreover, u does not have any neighbour in direction d_i. As such, $\{v, w\} = \mathcal{N}_r(u)$, where the direction from w to u is $d_{i\pm1}$. Observe that $u \notin C_t^i$ otherwise this would contradict Corollary 4.4. In Line 19 we also have that $u \in \text{int}(Q_{t,w})$. Let us consider two cases: (1) $u \in C_t^{i+2}$ or (2) $u \in C_t^{i\pm1}$.

1. If $u \in C_t^{i+2}$, we argue that $w \notin C_t^{i+2}$. Consider that w must be on the line perpendicular to the bisector of C_t^{i+2} that intersects u. If w is on this line *and* in C_t^{i+2} then $u \notin \text{int}(Q_{t,w})$, which is a contradiction. Therefore, $w \in C_t^{i\pm1}$. We illustrate this case in Figure 4.9a.

2. If $u \in C_t^{i\pm1}$, then we argue that w and u belong to the same cone of t. Without loss of generality assume that u is in C_t^{i+1}. Let ℓ be the line perpendicular to the bisector of C_t^{i+2} that intersects u. The real vertex w must be on ℓ. If w is in direction d_{i-1} from u, then $u \notin \text{int}(Q_{t,w})$, which is a contradiction. Therefore, w is in direction d_{i+1} from u. Thus, $w \in C_t^{i+1}$. We illustrate this case in Figure 4.9b.

In all cases, we get that v and w are in two adjacent cones of t.

The following lemma implies that Line 19 is well-defined.

Lemma 4.7. *Let t be a real vertex. Let u be a Steiner vertex in C_t^i. Assume $\mathcal{N}_r(u) = \{v_1, v_2\}$, where $v_1 \in C_t^i$ and v_2 is in an adjacent cone (without loss of generality assume $v_2 \in C_t^{i-1}$). Moreover, assume v_1 and v_2 are positioned such that v_1u is in direction d_{i+2} and v_2u is in direction d_{i+1}. Then u has a neighbour in direction d_{i+2} or direction d_{i+1}. See Figure 4.10.*

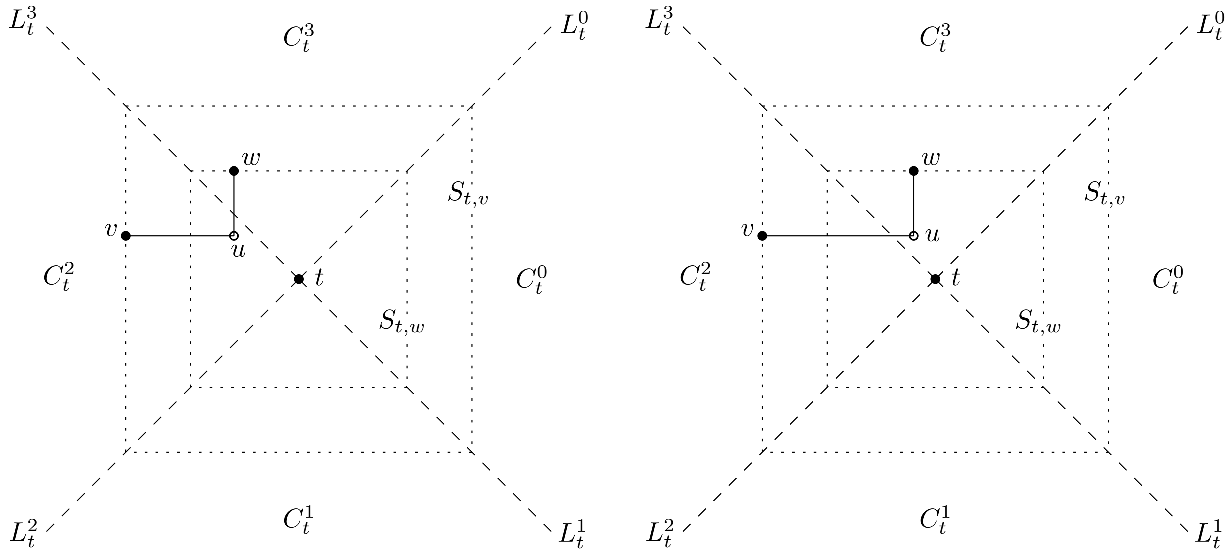

(a) A possible case for Line 19 where $i = 0$. (b) A possible case for Line 19 where $i = 0$.

Figure 4.9: Two figures describing possible cases where Line 19 in the Marking Algorithm gets executed.

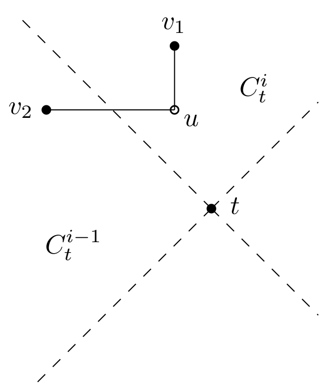

Figure 4.10: Illustration of Lemma 4.7. In this figure $|v_2u| > |v_1u|$, this is not necessarily the case.

Proof. We prove this lemma by contradiction. Assume u does not have a neighbour in d_{i+2} nor in direction d_{i+1}. Let ρ_1 be the ray shooting from v_1 in direction d_{i+2} and ρ_2 be the ray shooting from v_2 in direction d_{i+1}. During the construction of the graph, either ρ_1 interrupted ρ_2 or vice-versa. If ρ_2 interrupted ρ_1 at u, then since u does not have any neighbour in direction d_{i+1}, ρ_2 spans C_t^i, which contradicts Corollary 4.3. If ρ_1 interrupted ρ_2 at u, the same argument yields a contradiction. □

Since at Line 19, u has no neighbour in direction d, Line 19 is well-defined by the previous lemma.

Through Lemmas 4.5, 4.1, 4.6, and 4.7 we have shown that every step in the Marking Algorithm can be executed as described.

4.4 Proving the Marking Algorithm Succeeds

In this section, we show that the Marking Algorithm succeeds. The general strategy is to show that the Marking Algorithm produces a path Π satisfying the following property: if $u \neq t$ is a vertex along Π, then there exists a vertex $u^* \in \Pi$ appearing after u such that $|u^*t|_\infty < |ut|_\infty$. Moreover, we argue we can find u^* such that all vertices along Π leading to u^* stay at the same $\|\cdot\|_\infty$-distance from t. Since the graph has a finite number of vertices, then the algorithm eventually succeeds.

For the rest of the thesis, we denote the path produced by the Marking Algorithm by Π, routing from a real vertex s to a real vertex t.

We start with the following preparatory lemma.

Lemma 4.8. *Let u and u' be two consecutive vertices along Π, where $u \in C_t^i$. Then u' is not in direction d_i from u.*

Proof. First observe that $u \neq t$. Moreover, if u is a real vertex and $u \in C_t^i$, then by Line 5 in Algorithm 1, we have $d = d_{i+2}$.

Let us now consider the case where u is a Steiner vertex. We proceed by contradiction. Assume that $u \in C_t^i$ and u' is in direction d_i from u. From Observation 4.1, we have two cases to consider: (1) $u \in \text{int}(Q_{t,v})$ and u is in direction d_i from v, and (2) $u \notin \text{int}(Q_{t,v})$ and v is in direction d_i from u. In both cases, v is the vertex from Algorithm 1.

Let ℓ be the line which is parallel to the bisector of C_t^i and intersects u. We also consider the square $Q_{t,u}$.

1. Since $u \in \text{int}(Q_{t,v})$ then $v \notin Q_{t,u}$. Moreover, since the direction from v to u is d_i, then $v \in \ell$. Therefore, $v \in C_t^{i+2}$. Therefore, we find a straight path from v to u which spans $C_t^{i\pm1}$. This contradicts Corollary 4.4.
2. Since v is in direction d_i from u, then $v \in C_t^i$. Thus, $v \notin Q_{t,u}$ which consequently gives us $u \in \text{int}(Q_{t,v})$. This is a contradiction.

Therefore we have that if $u \in C_t^i$ then u' is not in direction d_i from u. □

Lemma 4.9. *Let u, u', and u'' be three consecutive vertices along Π, where u' is in direction d_j from u. Then u'' is not in direction d_{j+2} from u'.*

Proof. Assume for contradiction that u'' is in direction d_{j+2} from u'. Assume without loss of generality that $u' \in C_t^i$. Since the robot changed direction at u', we consider two cases. Either (1) u' is a real vertex or (2) u' is a Steiner vertex with no neighbour in direction d_j.

1. Assume u' is a real vertex. By Line 5 of Algorithm 1, the robot moves in direction d_{i+2} from u', so u'' is in direction d_{i+2} from u', meaning $j+2 = i+2$, i.e. $j = i$. But then u is also in direction d_i from u', contradicting Lemma 4.8.

2. Assume u' is a Steiner vertex with no neighbour in direction d_j. By Lemma 4.8, u'' is not in direction d_i from u', so $j \in \{i+1, i-1\}$ and $j+2 \in \{i+1, i-1\}$ respectively. By Observation 4.1, the robot is either travelling towards a real vertex v or away from a real vertex v. Since u' is a Steiner vertex with no neighbour in direction d_j, the robot must have been walking away from v when it reached u'. If the robot then moves in direction d_{j+2} then $u' \notin \text{int}(Q_{t,v})$, so $v \notin C_t^i$. Then the segment vu' spans C_t^i, contradicting Corollary 4.4.

Therefore all cases lead to a contradiction, and u'' is not in direction d_{j+2} from u'. □

Observation 4.2. Let u, u', and u'' be three consecutive vertices along Π, where $u' \in C_t^i$ and u' is in direction $d_{i\pm1}$ from u. If the robot changes direction at u', then u'' is in direction d_{i+2} from u'.

Proof. By Lemma 4.8, u'' is not in direction d_i from u'. By Lemma 4.9, u'' is not in direction d_{j+2} from u', where $j \in \{i+1, i-1\}$, so u'' is not in direction $d_{i\pm1}$ from u'. Since the robot changed direction at u', we have u'' is not in direction $d_{i\pm1}$ from u'. Therefore the only remaining direction is d_{i+2}. □

In the rest of the thesis, this observation is subsumed in a large number of arguments. As such, to improve readability, we do not make explicit mention of Observation 4.2 each time it is used.

Lemma 4.10. *Let u and u' be two consecutive vertices along Π, where $u \in C_t^i$. If u is a real vertex, then $|u't|_\infty < |ut|_\infty$.*

Proof. First observe that $u \neq t$. By Line 5 and Line 6 of Algorithm 1, u' is in direction d_{i+2} from u. Assume $|u't|_\infty \geq |ut|_\infty$. Then $u' \in C_t^{i+2}$. Therefore, we find a straight path from u to u' which spans $C_t^{i\pm1}$. This contradicts Corollary 4.4. □

Lemma 4.11. *Let $u \in S$ and $u' \in V \cup S$ be two consecutive vertices along Π, where $u \in int(C_t^i)$ and u' is in direction d_{i+2} from u. Then $|u't|_\infty < |ut|_\infty$.*

Proof. Assume $|u't|_\infty \geq |ut|_\infty$. Then $u' \in C_t^{i+2}$. Therefore, we find a straight path from u to u' which spans $C_t^{i\pm1}$. This contradicts Corollary 4.4. □

Lemma 4.12. *Let $u \in S$ and $u' \in S \cup V$ be two consecutive vertices along Π, where $u \in \partial C_t^i = L_t^i \cup L_t^{i+1}$. Then there exists a vertex $u^* \in \Pi$ appearing after u' such that the following two properties are satisfied:*

- $|u^*t|_\infty < |ut|_\infty$
- *and for all vertices $u^\# \in \Pi$ between u and u^*, we have $|u^\# t|_\infty = |ut|_\infty$.*

Proof. Without loss of generality, assume $u \in L_t^{i+1}$ and u' is in direction d_{i+2} from u. By the definition of Algorithm 1, the robot keeps moving in direction d_{i+2} from u until either: (1) it reaches a real vertex v or (2) it reaches a Steiner vertex $\overline{u}$ that does not have a neighbour in direction d_{i+2}.

1. If the robot reaches a real vertex v, observe that $v \in C_t^{i+1}$, otherwise we found a straight path from u to v spanning C_t^{i+1} contradicting Corollary 4.4. By Lemma 4.10, the next vertex after v along Π is a vertex u^* such that $|u^*t|_\infty < |vt|_\infty = |ut|_\infty$.
2. If the robot reaches a Steiner vertex $\overline{u}$ that does not have a neighbour in direction d_{i+2}, observe that $\overline{u} \in \text{int}(C_t^{i+1})$, otherwise we found a straight path from u to $\overline{u}$ spanning C_t^{i+1} contradicting Corollary 4.4. The next vertex after $\overline{u}$ along Π is in direction d_{i-1} from $\overline{u}$. Therefore, by Lemma 4.11, the next vertex after $\overline{u}$ along Π is a vertex u^* such that $|u^*t|_\infty < |\overline{u}t|_\infty = |ut|_\infty$.

Observe that in both cases, the robot keeps moving in direction d_{i+2} and does not exit C_t^{i+1}. As such, it travels along one side of $Q_{t,u}$. Thus, in Case (1), all the vertices $u^\# \in \Pi$ visited by the robot until reaching v (and including v) satisfy $|u^\# t|_\infty = |ut|_\infty$. And in Case (2), all the vertices $u^\# \in \Pi$ visited by the robot until reaching $\overline{u}$ (and including $\overline{u}$) satisfy $|u^\# t|_\infty = |ut|_\infty$. □

Lemma 4.13. *Let $u \in S$ and $u' \in V \cup S$ be two consecutive vertices along Π, where $u \in$ int(C_t^i). Let u' be in direction $d_{i\pm1}$ from u. Then there exists a vertex $u^* \in \Pi$ appearing after u' such that the following two properties are satisfied:*

- $|u^*t|_\infty < |ut|_\infty$
- *and for all vertices $u^\# \in \Pi$ between u and u^*, we have $|u^\# t|_\infty = |ut|_\infty$.*

Proof. Without loss of generality, assume u' is in direction d_{i+1} from u.

By Observation 4.1 either (1) u has a real neighbour v in direction d_{i+1} or (2) u has a real neighbour v in direction d_{i-1}.

1. If v is in direction d_{i+1} from u then $v \in \text{int}(C_t^i)$ by Observation 4.1. Thus, by the definition of Algorithm 1, the robot will reach v. By Lemma 4.10, after reaching v the robot will then move to a vertex u^* such that $|u^*t|_\infty < |vt|_\infty = |ut|_\infty$.

2. If v is in direction d_{i-1} from u then $v \in \text{int}(C_t^{i-1})$ by Observation 4.1. Thus, by the definition of Algorithm 1, the robot keeps moving in direction d_{i+1} from u until it reaches a Steiner vertex $\overline{u}$ that does not have a neighbour in direction d_{i+1}. Observe that $\overline{u} \in \text{int}(C_t^i)$, otherwise we found a straight path from v to $\overline{u}$ spanning C_t^i contradicting Corollary 4.4. The next vertex after $\overline{u}$ along Π is in direction d_{i+2} from $\overline{u}$. Therefore, by Lemma 4.11, the next vertex after $\overline{u}$ along Π is a vertex u^* such that $|u^*t|_\infty < |\overline{u}t|_\infty = |ut|_\infty$.

Observe that in both cases, the robot keeps moving in direction d_{i+1} and does not exit C_t^i. As such, it travels along one side of $Q_{t,u}$. Thus, in Case (1), all the vertices $u^\# \in \Pi$ visited by the robot until reaching v (and including v) satisfy $|u^\# t|_\infty = |ut|_\infty$. And in Case (2), all the vertices $u^\# \in \Pi$ visited by the robot until reaching $\overline{u}$ (and including $\overline{u}$) satisfy $|u^\# t|_\infty = |ut|_\infty$. □

Theorem 4.14. *Let $u \in \Pi$ be in the cone C_t^i. For each vertex $u \neq t$ there exists a vertex $u^* \in \Pi$ which appears after u such that the following two properties are satisfied:*

- $|u^*t|_\infty < |ut|_\infty$
- *and for all vertices $u^\# \in \Pi$ between u and u^*, we have $|u^\# t|_\infty = |ut|_\infty$.*

Proof. We consider two cases: either (1) u is a real vertex or (2) u is a Steiner vertex.

1. If u is a real vertex then by Lemma 4.10 there exists a vertex u^* which appears directly after u in Π such that $|u^*t|_\infty < |ut|_\infty$. Thus the set of vertices between u and u^* is empty.

2. If u is a Steiner vertex then we consider two cases (a) $u \in \partial C_t^i = L_t^i \cup L_t^{i+1}$ or (b) $u \in \text{int}(C_t^i)$.

   (a) If $u \in \partial C_t^i$, assume without loss of generality that $u \in L_t^i$. By Lemma 4.12, there exists a vertex u^* which appears after u on Π such that $|u^*t|_\infty < |ut|_\infty$. Moreover, by Lemma 4.12, for all vertices $u^\#$ between u and u^* we have $|u^\# t|_\infty = |ut|_\infty$.

   (b) If $u \in \text{int}(C_t^i)$ then we consider the vertex u' which appears directly after u in Π. By Lemma 4.8 we have that u' is not in direction d_i from u. So we consider (i) u' is in direction d_{i+2} from u, or (ii) u' is in direction $d_{i\pm1}$ from u.

      i. If u' is in direction d_{i+2} from u then by Lemma 4.11 there exists a vertex u^* which appears directly after u in Π such that $|u^*t|_\infty < |ut|_\infty$. Thus the set of vertices between u and u^* is empty.

ii. If u' is in direction $d_{i\pm1}$ from u then by Lemma 4.13 there exists a vertex u^* which appears after u in Π such that $|u^*t|_\infty < |ut|_\infty$. Moreover, by Lemma 4.13, for all vertices $u^\#$ between u and u^* we have $|u^\#t|_\infty = |ut|_\infty$.

□

Since there is a finite number of vertices in the graph and the $\|\cdot\|_\infty$-distance keeps decreasing by the previous theorem, we have the following corollary.

Corollary 4.15. *Given an emanation graph of grade-*1*, the* Marking Algorithm *constructs a path from any real vertex s to any real vertex t. Moreover for any two vertices u and u' on Π such that u precedes u' on Π we have $|u't|_\infty \leq |ut|_\infty$.*

In its current form, the Marking Algorithm is not well defined when the starting vertex satisfies $s \in S$. We cannot simply allow this case without further modification of the algorithm. Indeed, the Steiner vertices appearing in Lemmas 4.8 through 4.13 are not arbitrary. In each instance, they are vertices that were visited during the construction of a path containing $s \in V$. Consequently, additional steps must be incorporated into the Marking Algorithm in order for it to succeed when $s \in S$. Such additional steps are in discussed in Section 5.2.2.

4.5 On the Competitiveness of the Marking Algorithm

Since we have described a routing algorithm which works for grade-1 emanation graphs in general position it is natural to ask whether this algorithm is competitive: does there exist a constant r such that for any path Π produced by the Marking Algorithm from s to t, $\frac{|\Pi|}{|st|} \leq r$?

Recall the analogy of the robot travelling through a city from Section 1.3. We say that the robot *travels across edge ab* if the current position of the robot u is changed from a to b.

We begin by defining the concept of *marks*. Marks are points on the lines L_t^0, L_t^1, L_t^2, L_t^3 created as we follow Π. Specifically, we create a mark whenever one of the following two situations occurs.

- When the robot intersects a line $L \in \{L_t^0, L_t^1, L_t^2, L_t^3\}$ at a point p, we add a mark m at p. See Figure 4.11. We refer to such a mark as a *visitation mark*. By default, when the robot reaches t it intersects all lines in $\{L_t^0, L_t^1, L_t^2, L_t^3\}$ simultaneously. In this case we consider only one mark being created, which happens to exist on all lines in $\{L_t^0, L_t^1, L_t^2, L_t^3\}$.

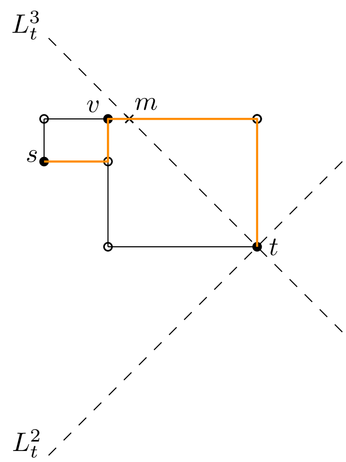

Figure 4.11: Illustration of the definition of *marks*. By following the Marking Algorithm, the robot intersects L_t^3 when moving from v. The mark m is then created.

- A mark is also created in the following situation. Following the notation from Algorithm 1, assume u is a vertex in $\mathrm{int}(C_t^i)$ with a neighbour $u' \in \mathrm{int}(C_t^i)$ such that u' is in direction d_{i+2} from u. If the robot moves from u to u' and u' does not have a neighbour in direction d_{i+2}. Moreover, u' has a real neighbour v in direction $d_{i\pm1}$ such that $u' \in \mathrm{int}(Q_{t,v})$. Then a mark is created at the intersection of L_t^{i-1} (respectively L_t^i) and uv, if $v \in C_t^{i-1}$ (respectively if $v \in C_t^{i+1}$). See Figure 4.12. We refer to such

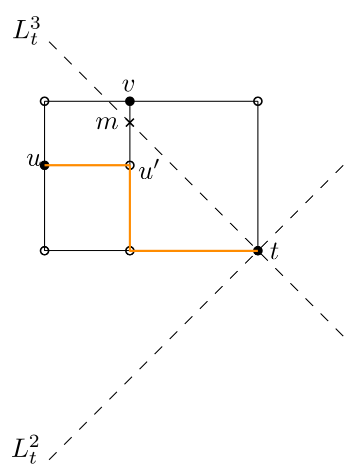

Figure 4.12: Illustration of the definition of *remote marks*. By following the Marking Algorithm, the robot reaches a vertex u' which satisfies the conditions for a remote mark to be created.

a mark as a *remote mark*.

Here is the general strategy to prove that the Marking Algorithm is competitive.

Denote by Π the path produced by the MARKING ALGORITHM and by $\Pi_{a,b}$ the subpath of Π from a to b, where b appears after a along Π. In this notation, a and b can be any point in the plane belonging to Π. Consider two marks m and m', where m' was created after m. Let p (respectively p') be the location of the robot when m (respectively m') was created. We first prove that $|mt| > |m't|$. Then, our goal will be to prove that there exists a constant c such that

$$|\Pi_{p,p'}| \leq c(|mt| - |m't|).$$

The following corollary follows directly from Theorem 4.14.

Corollary 4.16. *Let uu' be an edge along Π, where u' appears after u along Π. Then for any two points $p_1, p_2 \in uu'$ such that p_1 is visited before p_2, we have*

$$|u't|_\infty \leq |p_2 t|_\infty \leq |p_1 t|_\infty \leq |ut|_\infty.$$

This corollary implies that, by following Π, the $\|\cdot\|_\infty$-distance never increases.

Lemma 4.17. *Consider two visitation marks m and m' such that m' is visited after m along Π and $\Pi_{m,m'}$ does not contain any visitation mark other than m and m'. Then $|mt|_\infty > |m't|_\infty$.*

Proof. Let $p_1, p_2 \in \Pi$ be two points visited by the robot between m and m', where p_1 was visited before p_2. By Corollary 4.16, we have $|p_1 t|_\infty \geq |p_2 t|_\infty$. Since p_1 and p_2 are arbitrary, and m and m' are visitation marks, we find $|mt|_\infty \geq |m't|_\infty$. We now prove that the inequality is strict.

We proceed by contradiction. Assume $|mt|_\infty = |m't|_\infty$. We consider two cases: (1) $m = m'$ or (2) $m \neq m'$.

1. We argue that the case where $m = m'$ is impossible. Without loss of generality, $m \in L_t^3$ and the robot is moving in direction d_0. By the definition of the algorithm, the robot keeps moving in direction d_0 from m until either: (1) it reaches a real vertex v or (2) it reaches a Steiner vertex $\overline{u}$ that does not have a neighbour in direction d_0. In both cases, the robot then moves in direction d_1. By Lemma 4.10 and 4.11 it will reach a vertex whose $\|\cdot\|_\infty$-distance to t is strictly smaller than $|mt|_\infty$. Afterwards, by Corollary 4.16, the robot will never visit a point at $\|\cdot\|_\infty$-distance $|mt|_\infty$ from t. Therefore, it will never visit m again. So we must have $m \neq m'$.

2. Assume $m \neq m'$ and let $m \in L_t^i$. Therefore, if $|mt|_\infty = |m't|_\infty$ then $m' \in L_t^{i \pm 1}$. Without loss of generality, assume $m' \in L_t^{i+1}$. Since $|mt|_\infty = |m't|_\infty$, we have a straight path which spans C_t^i contradicting Corollary 4.4.

□

Lemma 4.18. *Let $u \in C_t^i$ and $u' \in C_t^i$ be two consecutive vertices along Π. Assume u' is in direction d_{i+2} from u. Assume u' has a real neighbour v in direction d_i and a real neighbour v' is in direction $d_{i\pm1}$. Then $|vu'|> |v'u'|$.*

In the above lemma we can state that v exists due to the fact that $\mathcal{N}_r(u') = 2$ by Lemma 4.1.

Proof. By the general position assumption we have $|vu'|\neq |v'u'|$, otherwise v and v' would belong to the same diagonal. Let ρ_1 (respectively ρ_2) be the ray shot from v (respectively from v') during construction which intersects u'. Assume that $|vu'|< |v'u'|$ then ρ_2 does not interrupt ρ_1. Yet u' has no neighbour in direction d_{i+2}. This would imply that ρ_1 continued uninterrupted and spanned $C_t^{i\pm1}$, contradicting Corollary 4.3. Therefore we have $|vu'|> |v'u'|$. □

Lemma 4.19. *Let $v \in \Pi$ be a real vertex. Let m be the first mark created when walking along Π from v. Let p be the location of the robot when m is created. Moreover assume $\Pi_{v,p}$ does not contain any real vertex other than v and let $L = |vt|_\infty - |mt|_\infty$. Then $|\Pi_{v,p}|+|pm|\leq 2L$.*

In the statement of the previous lemma, note that if m is a visitation mark, then $p = m$, otherwise, $p \neq m$.

Proof. Assume that $v \in C_t^i$. We begin by observing that from v the robot will move in direction d_{i+2} by the definition of Algorithm 1. It will continue to move in this direction until it reaches a vertex u such that u has no neighbour in direction d_{i+2}. Either (1) $u \notin \mathrm{int}(C_t^i)$ or (2) $u \in \mathrm{int}(C_t^i)$.

1. If $u \notin \mathrm{int}(C_t^i)$, then a visitation mark m is created on vu. Therefore, $p = m$ and there is a straight path from v to m. This implies

$$|\Pi_{v,p}|+|pm|= |\Pi_{v,p}|= |vt|_\infty - |mt|_\infty = L \leq 2L.$$

2. If $u \in \mathrm{int}(C_t^i)$, we have that u is a Steiner vertex so $|\mathcal{N}_r(u)|= 2$ by Lemma 4.1. Let $v' \neq v$ be the real neighbour of u in direction $d_{i\pm1}$. By Lemma 4.18 we have $|uv'|< |uv|$.

   We consider two cases (a) $v' \notin C_t^i$ or (b) $v' \in C_t^i$.

   (a) If $v' \notin C_t^i$, then a remote mark m is created on uv'. Therefore, $p = u$ and $\Pi_{v,p}$ is a straight path from v to $p = u$. Since $|uv'|< |uv|$, we have

$$|\Pi_{v,p}|+|pm|= |vu|+|um|\leq |vu|+|uv'|< 2|uv|= 2\left(|vt|_\infty - |mt|_\infty\right) = 2L.$$

(b) If $v' \in C_t^i$, then by the definition of Algorithm 1, we walk to v'. As such, we walked from v to v' without creating any mark. Thus, v' belongs to $\Pi_{v,p}$. This contradicts the assumptions of the lemma.

□

Lemma 4.20. *Let $v, v^* \in \Pi$ be real vertices in C_t^i, where v^* appears after v along Π. Assume no marks are created while the robot walks along Π_{v,v^*}. Also assume Π_{v,v^*} contains no real vertices other than v and v^* and let $L = |vt|_\infty - |v^*t|_\infty$. Then $|\Pi_{v,v^*}| \leq 2L$.*

Proof. We begin by observing that from v the robot will move in direction d_{i+2} by the definition of Algorithm 1. It will continue to move in this direction until it reaches a vertex u such that u has no neighbour in direction d_{i+2}. Either (1) $u \notin \text{int}(C_t^i)$ or (2) $u \in \text{int}(C_t^i)$.

1. If $u \notin \text{int}(C_t^i)$, then a visitation mark m is created on vu. This contradicts our assumption that no mark is created while the robot walks $\Pi_{v,v'}$.
2. If $u \in \text{int}(C_t^i)$, we have that u is a Steiner vertex so $|\mathcal{N}_r(u)| = 2$ by Lemma 4.1. Let $v' \neq v$ be the real neighbour of u in direction $d_{i\pm1}$. By Lemma 4.18 we have $|uv'| < |uv|$.

   We consider two cases (a) $v' \notin C_t^i$ or (b) $v' \in C_t^i$.

   (a) If $v' \notin C_t^i$, then a remote mark m is created in uv'. This contradicts the assumptions of the lemma.

   (b) If $v' \in C_t^i$, then by the definition of Algorithm 1, we walk to v'. As such, we walked from v to v'. Therefore, $\Pi_{v,u}$ is a straight path from v to u. Since $|uv'| < |uv|$, we have

   $$|\Pi_{v,v'}| = |vu| + |uv'| < 2|uv| = 2\left(|vt|_\infty - |v't|_\infty\right) = 2L.$$

   Since v' is the first real vertex visited after v in Π then we have $v' = v^*$. Thus we have $|\Pi_{v,v^*}| \leq 2L$.

□

Corollary 4.21. *Let $v, v^* \in \Pi$ be real vertices in C_t^i, where v^* appears after v along Π. Assume no marks are created while the robot walks along Π_{v,v^*} and let $L = |vt|_\infty - |v^*t|_\infty$. Then $|\Pi_{v,v^*}| \leq 2L$.*

Proof. Assume that Π_{v,v^*} contains n real vertices $v = v_1, v_2, \ldots, v_n = v^*$. Observe that all v_j's belong to C_t^i otherwise a visitation mark would be created while walking along Π_{v,v^*}. For $1 \leq j \leq n-1$, let $L_j = |v_j v_{j+1}|_\infty$. By Lemma 4.20, we have $|\Pi_{v_j,v_{j+1}}| \leq 2L_j$ for all

$1 \leq j \leq n-1$. Moreover, by Lemma 4.8, we never walk in direction d_i while walking along Π_{v,v^*}. Therefore, we have

$$|\Pi_{v,v^*}|=\sum_{j=1}^{n-1}|\Pi_{v_j,v_{j+1}}|\leq 2\sum_{j=1}^{n-1}L_j = 2L.$$

$\square$

Corollary 4.22. *Let $v \in \Pi$ be a real vertex. Let m be the first mark created when walking along Π from v. Let p be the location of the robot when m is created and let $L = |vt|_\infty - |mt|_\infty$. Then $|\Pi_{v,p}|+|pm|\leq 2L$.*

Proof. Consider the last real vertex v^* visited before the creation of m. Let $x = |vv^*|_\infty$. By Corollary 4.21 we have that $|\Pi_{v,v^*}|\leq 2x$. Then we have $|v^*p|_\infty = L - x$. Now consider the path $\Pi_{v^*,p}$. By Lemma 4.19 we have that $|\Pi_{v^*,p}|+|pm|\leq 2(L-x)$. Then we have

$$|\Pi_{v,p}|+|pm|= |\Pi_{v,v^*}|+|\Pi_{v^*,p}|+|pm|\leq 2x + 2(L-x) = 2L.$$

$\square$

The following Corollary immediately follows from Corollary 4.22.

Corollary 4.23. *Let $v \in C_t^i$ be a real vertex on Π. Let m be the first mark created after the robot reaches v and let p be the location of the robot when m is created. For each path segment in $\Pi_{v,p}$ parallel to d_i the robot walks a path segment of greater than or equal length in direction d_{i+2} and the sum of the lengths of each path segment perpendicular to d_i in addition to $|mp|$ is less than or equal the sum of the path segments parallel to d_i. Moreover the mark $m \in C_v^{i+2}$.*

Observe that the corollary is equivalent to saying that from v until the creation of m when the robot is at a point p, the robot traverses the bounded detours path from v in direction d_{i+2}, with no marks created while the robot walks along $\mathrm{int}(\Pi_{v,p})$.

In the following lemma, we observe that if a visitation mark is created when travelling from a vertex u to a vertex $u' \in C_t^i$, then uu' is perpendicular to the bisector of C_t^i.

Lemma 4.24. *Let uu' be an edge of Π, where u' appears after u along Π. Assume a visitation mark m is created when the robot walks from u to u'. Assume $u' \in C_t^i$. Then uu' and mu' are perpendicular to the bisector of C_t^i.*

Proof. Assume uu' is parallel to the bisector of C_t^i. Since uu' intersects $L_t^{i-1} \cup L_t^i$, then $|u't|_\infty > |ut|_\infty$, contradicting Corollary 4.15. Therefore, uu' is perpendicular to the bisector of C_t^i. Since $m \in uu'$, then mu' is perpendicular to the bisector of C_t^i. $\square$

Lemma 4.25. *Let uu' be an edge of Π, where u' appears after u along Π. Assume a remote mark m is created when the robot reaches u. Also assume that $u' \in C_t^i$. Then uu' and mu' are perpendicular to the bisector of C_t^i.*

The following proof heavily depends on the definition of a remote mark.

Proof. By Lemma 4.8, since $u' \in C_t^i$, the direction from u to u' cannot be d_i. Assume the direction from u to u' is d_{i+2}.

Let d be the direction taken by the robot to reach u. Since a remote mark is created when the robot reaches u, then u does not have any neighbour in direction d. Since the direction from u to u' is d_{i+2}, then $d = d_{i\pm1}$.

Since a remote mark is created when the robot reaches u, and since the direction from u to u' is d_{i+2}, then u has a real neighbour v in direction d_i. Therefore, there is a line ℓ containing v, u and u'. Since the direction from u to u' is d_{i+2}, then $v, u, u' \in C_t^i$. But since a remote mark is created when the robot reaches u, then v and u are not in the same cone. This is a contradiction.

Therefore, the direction from u to u' is $d_{i\pm1}$. In other words, uu' is perpendicular to the bisector of C_t^i, and so is mu'. □

Lemma 4.26. *Let m and m' be two consecutive marks. Let p (respectively p') be the location of the robot when m (respectively m') was created. Assume m' is a remote mark. Then $|mt|_\infty > |m't|_\infty$.*

Proof. By Lemma 4.24 and Lemma 4.25 the first path segment of $\Pi_{p,p'}$ is perpendicular to the bisector of a cone C_t^i. Moreover, we assume that $p' \in C_t^i$. By the definition of remote marks a m' can only be created while moving in direction d_{i+2}. Moreover it is not possible for the robot to move in direction d_i while in a cone C_t^i. Thus the $||\cdot||_\infty$ distance between the robot and t strictly decreases between the creation of m and the creation of m'. Moreover, observe that since m' is on a line L_t^i then $|m't|_\infty = |p't|_\infty$. Therefore $|mt|_\infty > |m't|_\infty$. □

Lemma 4.27. *Let m and m' be two consecutive marks. Then $|mt|_\infty > |m't|_\infty$.*

Proof. Assume m and m' are visitation marks, then by Lemma 4.17 $|mt|_\infty > |m't|_\infty$ holds true. Assume m' is a remote mark. Then by Lemma 4.26 $|mt|_\infty > |m't|_\infty$ holds true. Assume m is a remote mark, and m' is a visitation mark. Let p be the location of the robot when m was created. Assume $p \in C_t^i$. Then by Lemma 4.25, from p, the robot will walk perpendicular to the bisector of C_t^i. Without loss of generality let this direction be d_{i-1}. From p the robot will continue to walk in direction d_{i-1} until it reaches either a real vertex v or a Steiner vertex v such that v does not have a neighbour in direction d_{i-1}. In either case the vertex must be in C_t^i. Otherwise we would have a straight path from m to v which spans C_t^i contradicting Corollary 4.4. If v is in C_t^i then since v is a real vertex the robot will move in direction d_{i+2} decreasing its $\|\cdot\|_\infty$ to t. By Corollary 4.15, the robot's distance from t will not increase. So upon creating the next mark we will have $|mt|_\infty > |m't|_\infty$. If v is a Steiner vertex then since it cannot move in direction d_i, then it will move in direction d_{i+2} and by the same argument when m' is created we will have $|mt|_\infty > |m't|_\infty$. □

We now introduce two properties of path segments of Π which do not contain real vertices.

Proposition 4.28. *Let m and m' be two consecutive marks such that $m \in L_t^i$. Let p (respectively p') be the location of the robot when m (respectively m') was created. Assume $\Pi_{p,p'}$ does not contain any real vertex. Then $m' \in L_t^i$ or $m' = t$.*

Proof. Assume $m' \neq t$. Observe that $\Pi_{p,p'}$ has at least one edge in $\mathrm{int}(C_t^i)$ or $\mathrm{int}(C_t^{i+1})$. We assume without loss of generality that $\Pi_{p,p'} \cap \mathrm{int}(C_t^i) \neq \varnothing$. Observe that this implies that $\Pi_{p,p'}$ is contained in C_t^i. Indeed if it is not contained in C_t^i then the path would exist in two cones, meaning that along this path a visitation mark is created before reaching p', contradicting the assumption of our proposition. By Observation 4.1, when the robot is at p it is either walking toward a real vertex v or walking away from v.

Suppose that the robot is walking toward v. By the definition of Marking Algorithm, the robot must then reach v. Furthermore, we must have $v \in C_t^i$, since otherwise the straight path from m to v would span C_t^i, contradicting Corollary 4.4. Consequently, the robot would reach the real vertex v before creating a new mark, contradicting the assumption that $\Pi_{p,p'}$ contains no real vertices.

Therefore, the robot cannot be walking toward v. It follows that $v \in C_t^{i+1}$ and that the robot is walking away from v. If m is a remote mark, then there exists a straight path from m to p; moreover, by Lemma 4.25, the segment mp is perpendicular to the bisector of C_t^i. If m is a visitation mark then by Lemma 4.24 the first vertex visited after the creation of m is in C_t^i and in direction d_{i-1} from m. In particular, the vertices v, m, and the location p lie on the same straight path.

Starting from p, the robot moves in direction d_{i-1} until it reaches a vertex u such that u has no neighbour in direction d_{i-1}. We consider two cases.

1. $u \notin \mathrm{int}(C_t^i)$.

   In this case, there exists a straight path from m to u that spans C_t^i, contradicting Corollary 4.4. Thus, this case is impossible.

2. $u \in \mathrm{int}(C_t^i)$.

From u, the robot moves in direction d_{i+2} until it reaches a vertex u' such that u' is either a Steiner vertex with no neighbour in direction d_{i+2} or u' is a real vertex. We analyze the possible locations of u'.

(a) $u' \in C_t^{i+1}$.
In this case, the traversal from u to u' creates a visitation mark on L_t^i, and thus $m' \in L_t^i$.

(b) $u' \in C_t^{i-1}$.
Let ℓ be the line perpendicular to the bisector of C_t^i that passes through u, and let $\triangle_{t,\ell}^i$ be the triangle bounded by L_t^i, L_t^{i-1}, and ℓ. Let w be the real vertex in $\triangle_{t,\ell}^i$ closest to ℓ that has a projection w' onto the straight path from m to u. Such a vertex exists, since t itself satisfies this property. Since $v \notin C_t^i$ then $v \notin C_w^i$. Similarly to $\triangle_{t,\ell}^i$ let $\triangle_{w,\ell}^i$ be the triangle defined by L_w^i, L_w^{i-1}, and ℓ. Consider the ray ρ_1 emitted from v in direction d_{i-1} during the construction of the graph. Also consider the ray ρ_2 emitted from w in direction d_i.
We first argue that ρ_2 must be interrupted before it reaches w'. Observe that ρ_1 remains uninterrupted until it reaches u. Moreover, ρ_2 reaches w' before ρ_1 reaches u. Since $v \notin C_w^i$ then by Lemma 4.2 we have $ww' < vw'$. Thereby we have ρ_2 interrupting ρ_1 before it reaches u, a contradiction.
We now argue that ρ_2 cannot be interrupted before it reaches w, leading to a contradiction. By the minimality of w no vertex with a projection onto the straight path from m to u can produce a ray interrupting ρ_2 before it reaches w'. Consider a vertex without a projection on $\Pi_{p,u}$ which produces a ray which interrupts ρ_2 before it reaches w'. Observe that this vertex must lie in $\triangle_{w,\ell}^i$. However, a ray from such a vertex would also interrupt the ray defining the straight path $\Pi_{u,u'}$, contradicting the existence of this path. Thus, this case cannot occur.

(c) $u' \in C_t^i$.
The robot reaches u' before creating a mark. Since $\Pi_{p,p'}$ contains no real vertices, u' must be a Steiner vertex with no neighbour in direction d_{i+2}. From u', the robot moves either in direction d_{i-1} or d_{i+1}.

i. The robot moves in direction d_{i-1}.
If there exists a real neighbour v' in direction d_{i-1} such that $u' \notin \mathrm{int}(Q_{t,v'})$, then the robot walks to v' without creating a mark, contradicting the assumption that $\Pi_{p,p'}$ contains no real vertices. Otherwise, v' is in direction d_{i+1} from u' and $u' \in \mathrm{int}(Q_{t,v'})$, which implies $v' \in C_t^{i+1}$ and thus the segment $u'v'$ intersects L_t^i, creating a remote mark $m' \in L_t^i$.

ii. The robot moves in direction d_{i+1}.
If there exists a real neighbour v' in direction d_{i+1} such that $u' \notin \mathrm{int}(Q_{t,v'})$,

then the robot walks to v' without creating a mark, contradicting the assumption that $\Pi_{p,p'}$ contains no real vertices.

Otherwise, v' is in direction d_{i-1} from u' and $u' \in \mathrm{int}(Q_{t,v'})$, which implies $v' \in C_t^{i-1}$ and thus the segment $u'v'$ intersects L_t^{i-1}, creating a remote mark $m' \in L_t^{i-1}$. We would like to show that this scenario is impossible.

In this case, consider the line ℓ perpendicular to the bisector of C_t^i that passes through u', and let $\triangle_{t,\ell}^i$ denote the triangle bounded by L_t^i, L_t^{i-1}, and ℓ. Let w be the real vertex in $\triangle_{t,\ell}^i$ that is closest to ℓ and has a projection w' onto the straight path from m to u. Next, let ℓ' be the line perpendicular to the bisector of C_t^i that passes through u, and let $\triangle_{t,\ell'}^i$ denote the triangle bounded by L_t^i, L_t^{i-1}, and ℓ'.

We consider two subcases.

A. Suppose that w exists. If $\mathrm{int}(\triangle_{t,\ell}^i)$ contains no real vertices, then during the construction the ray ρ_1 emitted from w in direction d_i would intersect the ray ρ_2 emitted from v' in direction d_{i+1} at the point w', thereby interrupting ρ_2. This would imply that the path $v'u'$ does not exist, contradicting the case under consideration. If instead $\mathrm{int}(\triangle_{t,\ell}^i)$ is not empty of real vertices, then there exists a real vertex c in $\triangle_{t,\ell}^i$ that admits a projection onto t.

B. Suppose that no such vertex w exists. Then there exists a real vertex b that is closest to ℓ' and has a projection b' onto ℓ'. Such a vertex exists, since if w does not exist then t itself satisfies this property.

If either $\mathrm{int}(\triangle_{t,\ell}^i)$ is not empty of real vertices or w does not exist, we take b to be the closest real vertex to ℓ'. If $\mathrm{int}(\triangle_{b,\ell}^i)$ is empty of real vertices, during construction the ray ρ_3 emitted from b in direction d_i would intersect the ray ρ_4 emitted from v' in direction d_{i+1} at the point b', thereby interrupting ρ_4. This implies that the path vu does not exist, contradicting the case under consideration.

Otherwise, if $\mathrm{int}(\triangle_{b,\ell}^i)$ is not empty of real vertices then a real vertex in the triangle could produce a ray which interrupts ρ_3 before it reaches b'. Observe that such a real vertex does not have a projection onto the straight path from m to u, and thus such a ray would interrupt the ray which defines $\Pi_{u,u'}$, contradicting the case under consideration.

In conclusion, in all possible cases we either have $m' \in L_t^i$ or a contradiction. Therefore, if $\Pi_{p,p'}$ does not contain any real vertex, then $m' \in L_t^i$.

□

Observe from the proof of the previous proposition we can make the following observation about subpaths of Π which do not contain real vertices.

Corollary 4.29. *Let m and m' be two consecutive marks such that $m \in L_t^i$. Let p (respectively p') be the location of the robot when m (respectively m') was created. Assume $\Pi_{p,p'}$ does not contain any real vertex. Then $\Pi_{p,p'}$ is xy-monotonic.*

Proof. In the proof of Proposition 4.28, we explore all possible cases of a path $\Pi_{p,p'}$ between p and p'. The proof shows that all paths which break xy-monotonicity do not exist. □

Proposition 4.30. *Let $\Pi_{a,b}$ be a section of Π such that $int(\Pi_{a,b})$ does not contain real vertices. Moreover, assume that a is the point where a mark m was created. Then $\Pi_{a,b}$ is xy-monotonic.*

Proof. Without loss of generality assume that $a \in C_t^i$ and $m \in L_t^i$.

Let $m = m_1, m_2, ..., m_n$ be the sequence of marks created while the robot walks along $\Pi_{a,b}$. Let $p_i \in \Pi_{a,b}$ $(1 \leq i \leq n)$ be the location of the robot when m_i was created, where $p_1 = a$. By Corollary 4.29 we have that each subpath $\Pi_{p_j,p_{j+1}}$ is xy-monotonic. Moreover, for each subpath $\Pi_{p_j,p_{j+1}}$ if the mark $m_j \in C_t^i$ then $m_{j+1} \in L_t^i$ by Proposition 4.28. Therefore, since $m = m_1 \in L_t^i$, all marks $m_1, m_2, ..., m_n$ belong to L_t^i. We first show that Π_{p_1,p_n} is xy-monotonic. To this end, we show that for all $\Pi_{p_j,p_{j+1}}$'s, the robot moves in the same two directions.

By Proposition 4.28 applied on each $\Pi_{p_j,p_{j+1}}$, all marks created while the robot walks from a to b are created on L_t^i. This means that Π_{p_1,p_n} is contained in $C_t^i \cup C_t^{i+1}$. Observe that by the definition of the p_j's, each $\Pi_{p_j,p_{j+1}}$ belongs to one cone. Assume $\Pi_{p_j,p_{j+1}}$ belongs to C_t^i. Since $m_j \in L_t^i$ then by Lemmas 4.24 and 4.25 the robot will move perpendicular to the bisector of C_t^i from p_j. If m_j is a visitation mark then this direction must be d_{i-1}, otherwise it would not be in C_t^i. If m is a remote mark then again the robot will move in direction d_{i-1}, otherwise it would walk to the remote mark, contradicting the definition of remote marks. The robot will continue to move in direction d_{i-1} until it reaches a vertex with no neighbour in direction d_{i-1}. At this vertex it will move in direction d_{i+2}. So the two directions the robot will move in while walking along a path $\Pi_{p_j,p_{j+1}}$ which belongs to C_t^i is d_{i-1} and d_{i+2}.

Assume $\Pi_{p_j,p_{j+1}}$ belongs to C_t^{i+1}. Since $m_j \in L_t^i$ then by Lemmas 4.24 and 4.25 the robot will move perpendicular to the bisector of C_t^{i+1} from p_j. If m_j is a visitation mark then this direction must be d_{i+2}, otherwise it would not be in C_t^{i+1}. If m is a remote mark then again the robot will move in direction d_{i+2}, otherwise it would walk to the remote mark, contradicting the definition of remote marks. The robot will continue to move in direction d_{i+2} until it reaches a vertex with no neighbour in direction d_{i+2}. At this vertex it will move in direction d_{i-1}. So the two directions the robot will move in while walking along a path $\Pi_{p_j,p_{j+1}}$ which belongs to C_t^{i+1} is d_{i-1} and d_{i+2}.

Finally we must argue that upon reaching p_n the robot will not move in d_i or d_{i+1} before reaching b. If m_n is a visitation mark then the robot cannot move in direction d_i or d_{i+1} from p_n, as both cases would contradict Lemma 4.8.

Without loss of generality assume that $p_n \in C_t^i$ and the robot moves in direction d_{i-1} from p_n. Note that there exists a real vertex v such that there is a straight path vp_n parallel to d_{i-1}. From p_n the robot moves in direction d_{i-1} until it reaches a vertex u. After reaching u the robot moves in direction d_{i+2} until it reaches a vertex u' such that u' does not have a neighbour in direction d_{i+2}. Note that $u' \in C_t^i$, otherwise there is a mark created, and so p_n is not the last point where a mark is created while walking $\Pi_{a,b}$.

We proceed by contradiction to prove that the robot will not move in direction d_{i+1} from u'. Assume that from u' the robot moves in direction d_{i+1}. This can happen for two reasons: either (1) there is a real neighbour v' of u' in direction d_{i-1} such that $u' \in \text{int}(C_t^i)$ implying $v' \in C_t^{i-1}$ or (2) there is a real neighbour v' of u' in direction d_{i+1} such that $u' \notin \text{int}(C_t^i)$ implying $v' \in C_t^i$.

1. Case 1 implies the creation of a remote mark on L_t^{i-1} contradicting Proposition 4.28.
2. Consider case 2. Let ℓ be the line perpendicular to the bisector of C_t^i that passes through u, and let $\triangle_{t,\ell}^i$ be the triangle bounded by L_t^i, L_t^{i-1}, and ℓ. Let w be the real vertex in $\triangle_{t,\ell}^i$ closest to ℓ that has a projection w' onto $\Pi_{m,u}$. Such a vertex exists, since v' itself satisfies this property. Since $v \notin C_t^i$ then $v \notin C_w^i$. Consider the ray ρ_1 emitted from v in direction d_{i-1} during the construction of the graph. Ray ρ_1 remains uninterrupted until it reaches u. Now consider the ray ρ_2 emitted from w in direction d_i. If ρ_2 were uninterrupted, it would reach w' before ρ_1 reaches u. Since $v \notin C_w^i$ then by Lemma 4.2 we have $ww' < vw'$. Thereby we have ρ_2 interrupting ρ_1, a contradiction. No other real vertex with a projection onto $\Pi_{m,u}$ can interrupt ρ_2 earlier by the minimality of w. Any real vertex without such a projection must lie in $C_w^i \subseteq C_t^i$, and a ray from such a vertex interrupting ρ_2 would also interrupt the ray defining the path $\Pi_{u,u'}$, contradicting the existence of this path. Thus, this case cannot occur.

□

We now begin the discussion of the competitiveness of the Marking Algorithm. We will choose a sequence of marks $m_1, m_2, ..., m_n$ such that $m_n = t$, and for all $1 \leq \nu < n$, $m_{\nu+1}$ is created after[1] m_ν. Let p_ν be the position of the robot when m_ν is created (observe that $m_n = t = p_n$). We will then break $\Pi_{s,t}$ into the subpaths Π_{s,p_1} and $\Pi_{p_\nu,p_{\nu+1}}$ and analyze each subpath independently. Our goal is to show that there exists a constant c such that

$$|\Pi_{p_\nu,p_{\nu+1}}| \leq c(|m_\nu t| - |m_{\nu+1} t|) \tag{4.1}$$

[1]The m_ν's are not necessarily consecutive, in the sense that multiple marks may be created between m_ν and $m_{\nu+1}$.

for all $1 \leq \nu < n$. From (4.1), we can show the following. First observe that $|\Pi_{s,p_1}| \leq 2|sp_1|_\infty \leq 2|st|_\infty \leq 2|st|$ by Corollary 4.22 and Theorem 4.16. As such, we have

$$\begin{aligned}
|\Pi_{st}| &= |\Pi_{s,p_1}| + \sum_{\nu=1}^{n-1} |\Pi_{p_\nu,p_{\nu+1}}| \\
&\leq 2|st| + \sum_{\nu=1}^{n-1} c(|m_\nu t| - |m_{\nu+1} t|) \\
&= 2|st| + c(|m_1 t| - |m_n t|) \\
&= 2|st| + c(|m_1 t| - |tt|) \\
&= 2|st| + c|m_1 t| \\
&\leq 2|st| + c|st| \\
&= (c+2)|st|.
\end{aligned}$$

The second inequality follows from (4.1). The inequality before the final equality follows from Corollary 4.23: when $s \in C_t^i$, the mark m_1 satisfies $m_1 \in C_s^{i+2} \cap (L_t^i \cup L_t^{i-1})$.

Our next step is to explain how to choose the m_ν's and to prove (4.1). Without loss of generality assume $m_\nu \in L_t^i$.

We consider two cases, each of which is split into two sub cases.

1. $\Pi_{p_\nu,p_{\nu+1}}$ does not contain a real vertex.
   (a) $m_{\nu+1}$ is on L_t^i. Refer to Lemma 4.31.
   (b) Without loss of generality $m_{\nu+1}$ is on L_t^{i-1}. Refer to Lemma 4.32.
2. $\Pi_{p_\nu,p_{\nu+1}}$ contains at least one real vertex.
   (a) $m_{\nu+1}$ is on L_t^i. Refer to Lemma 4.33
   (b) Without loss of generality $m_{\nu+1}$ is on L_t^{i-1}. Refer to Section 4.5.1.

In what follows, in order to simplify the notation we denote m_ν, p_ν, $m_{\nu+1}$ and $p_{\nu+1}$ by m, p, m' and p', respectively.

We start with the following lemma (corresponding to Case 1(a) described above).

Lemma 4.31. *Let $m \in L_t^i$ and $m' \in L_t^i$ be two marks created by the robot while executing the* Marking Algorithm. *Let p (respectively p') be the locations of the robot when m (respectively m') was created. Assume m' is the first visitation mark created after the creation of m. Assume $\Pi_{p,p'}$ does not contain any real vertex. Then $\frac{|\Pi_{p,p'}|}{|mt|-|m't|} \leq \sqrt{2}$.*

For the rest of this section, we denote the sum of the lengths of all the horizontal (respectively vertical) edges in $\Pi_{p,p'}$ by $|\Pi_{p,p'}|_x$ (respectively by $|\Pi_{p,p'}|_y$).

Proof. We assume that m' is the first visitation mark created after the creation of m. Observe that m' is well-defined since the robot must eventually reach t, thus creating a visitation mark at t. Observe that this implies that $\Pi_{p,p'} \subset C_t^i$.

By Corollary 4.30 we have that $\Pi_{p,p'}$ is an xy-monotonic path. Thus we have that $|\Pi_{p,p'}| = |\Pi_{p,p'}|_x + |\Pi_{p,p'}|_y$. Assume without loss of generality that the straight path from m to p is parallel to the y-axis. Using the xy-monotonicity of $\Pi_{p,p'}$, we also have the following: If m is a visitation mark, then $m = p$ and $|\Pi_{p,p'}|_x = |\Pi_{p,p'}|_y = |\Pi_{p,p'}|_y + |mp|$. Otherwise, if m is a remote mark, then $|\Pi_{p,p'}|_x = |\Pi_{p,p'}|_y + |mp|$. As such, since m and m' are along the same line which makes an angle of $\frac{\pi}{4}$ with the x-axis, we get

$$|mm'|^2 = |\Pi_{p,p'}|_x^2 + (|\Pi_{p,p'}|_y + |mp|)^2.$$

Therefore,

$$\frac{|\Pi_{p,p'}|}{|mt| - |m't|} = \frac{|\Pi_{p,p'}|}{|mm'|} = \frac{|\Pi_{p,p'}|_x + |\Pi_{p,p'}|_y}{\sqrt{|\Pi_{p,p'}|_x^2 + (|\Pi_{p,p'}|_y + |mp|)^2}} \leq \frac{|\Pi_{p,p'}|_x + |\Pi_{p,p'}|_y}{\sqrt{|\Pi_{p,p'}|_x^2 + |\Pi_{p,p'}|_y^2}} \leq \sqrt{2},$$

where the last inequality can be obtained by basic calculus. □

We now explore the case where $\Pi_{p,p'}$ does not contain any real vertices and m and m' belong to different lines (corresponding to Case 1(b) described above).

Lemma 4.32. *Let $m \in L_t^i$ and $m' \in L_t^{i-1}$ be two marks created by the robot while executing the* MARKING ALGORITHM*. Let p (respectively p') be the locations of the robot when m (respectively m') was created. Assume m' is the first mark created after the creation of m. Assume $\Pi_{p,p'}$ does not contain any real vertex. Then $\Pi_{p,p'}$ does not exist.*

Proof. This follows directly from Proposition 4.28. □

Now we consider case 2(a).

Lemma 4.33. *Let $m \in L_t^i$ and $m' \in L_t^i$ be two marks created by the robot while executing the* MARKING ALGORITHM*. Let p (respectively p') be the location of the robot when m (respectively m') was created. Assume $\Pi_{p,p'}$ contains a real vertex v. Assume that no visitation marks are created while the robot walks along $int(\Pi_{p,v})$. Moreover, assume that while the robot walks along $\Pi_{v,p'}$ no marks are created except for m'. Then $\frac{|\Pi_{p,p'}|}{|mt|-|m't|} \leq 2\sqrt{2}$.*

Proof. By the assumptions, no visitation marks are created while walking along $\mathrm{int}(\Pi_{p,p'})$. Therefore, the interior of $\Pi_{p,p'}$ lies entirely inside a single cone. Without loss of generality, let this cone be C_t^i. Without loss of generality assume d_i is parallel with the x-axis.

Let

$$L = |mt|_\infty - |m't|_\infty = |mm'|_\infty.$$

Because $\mathrm{int}(\Pi_{p,p'})$ remains inside one cone, the total horizontal displacement of the path satisfies $|\Pi_{p,p'}|_x = |\Pi_{p,v}|_x + |\Pi_{v,p'}|_x = L$ (by Lemma 4.8).

Let us denote $|\Pi_{p,v}|_x$ by α. By Corollary 4.23, we have

$$|\Pi_{v,p'}|_y + |p'm'| \le |\Pi_{v,p'}|_x = L - \alpha,$$

from which

$$|\Pi_{v,p'}|_y \le L - \alpha - |p'm'|. \tag{4.2}$$

Observe a possible example of the path $\Pi_{p,p'}$ in Figure 4.13.

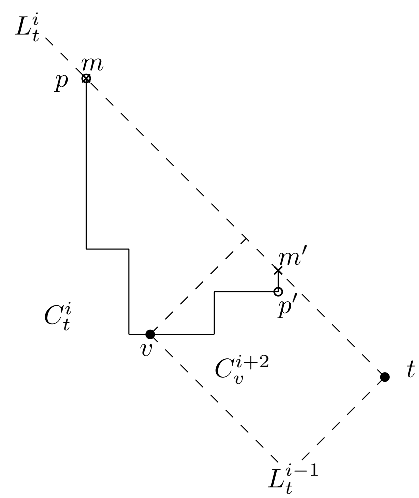

Figure 4.13: Illustration of a possible such path $\Pi_{p,p'}$ from Lemma 4.33.

Let the line L_v^{i+1} be the result of translating L_t^{i+1} such that its endpoint is at v. Let q be the point of intersection between L_v^{i+1} and L_t^i. Let γ be the intersection between L_t^i and the line which intersects v and is parallel to the y-axis. Let the rectangle of width α in direction d_i from $v\gamma$ be

$$R = \{r + \beta d_i | r \in v\gamma, 0 \le \beta \le \alpha\}.$$

Note that it is possible for R to be a degenerate rectangle when $\alpha = 0$. We allow for this case.

Figure 4.14 shows the path from Figure 4.13 along with the defined rectangle R. We will

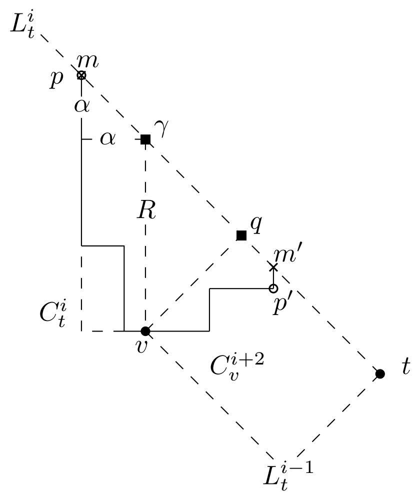

Figure 4.14: Illustration of a possible such path $\Pi_{p,p'}$ from Lemma 4.33 along with the rectangle R.

use this rectangle to find $|\Pi_{p,v}|_y$. Consider the triangle $\triangle(\gamma + \alpha d_i)\gamma m$. Observe that due to γ and m being two corners of the triangle lying on a line which makes an angle $\frac{\pi}{4}$ with the x-axis, and since γ and $(\gamma + \alpha d_i)$ form a line parallel to the x-axis that $\triangle(\gamma + \alpha d_i)\gamma m$ is an isosceles right triangle. Then $|\Pi_{p,v}|_y + |mp| = |v\gamma|_y + \alpha$ or,

$$|\Pi_{p,v}|_y + |mp| - \alpha = |v\gamma|_y$$

Observe from the restriction that $m' \in C_v^{i+2} \cap L_t^i$ then

$$|mm'|_y = L \geq \frac{|v\gamma|_y}{2} + \alpha = \frac{|\Pi_{p,v}|_y + |mp| - \alpha}{2} + \alpha.$$

We isolate for $|\Pi_{p,v}|_y$,

$$|\Pi_{p,v}|_y \leq 2L - \alpha - |mp|.$$

We now bound the total length of the path:

$$|\Pi_{p,p'}| = |\Pi_{p,v}| + |\Pi_{v,p'}| = |\Pi_{p,v}|_x + |\Pi_{p,v}|_y + |\Pi_{v,p'}|_x + |\Pi_{v,p'}|_y.$$

Substituting the bounds obtained above,

$$|\Pi_{p,p'}| \leq \alpha + (2L - \alpha - |mp|) + (L - \alpha) + ((L - \alpha) - |p'm'|) = 4L - 2\alpha - |mp| - |p'm'| \leq 4L$$

since $\alpha \geq 0$, $|mp| \geq 0$ and $|p'm'| \geq 0$.

Finally, because m and m' lie on the same line L_t^i, which forms an angle of $\frac{\pi}{4}$ with the x-axis, we have

$$|mt| - |m't| = |mm'| = \sqrt{2}\,|mm'|_\infty = \sqrt{2}\,L.$$

Therefore

$$\frac{|\Pi_{p,p'}|}{|mt| - |m't|} \leq \frac{4L}{\sqrt{2}L} = 2\sqrt{2}.$$

□

4.5.1 Cases with a Real Vertex and Marks on Adjacent Lines

We now consider the case where the path $\Pi_{p,p'}$ contains at least one real vertex and the consecutive marks m and m' lie on different lines L_t^i and L_t^{i-1}.

Unlike the case where both marks lie on the same line, the ratio

$$\frac{|\Pi_{p,p'}|}{|mt| - |m't|}$$

cannot be bounded by a constant in general. Indeed, consider the example depicted in Figure 4.15. In this figure we see that m and m' are visitation marks, thus we have $p = m$ and $p' = m'$. Let $|mu| + \epsilon = 1$, where $\epsilon > 0$ is an arbitrarily small real number. Since $|up'| = \epsilon$ then $|\Pi_{p,p'}| = |mu| + \epsilon = 1$. Observe that

$$|mt| - |m't| = \sqrt{2}\epsilon.$$

Therefore

$$\frac{|\Pi_{p,p'}|}{|mt| - |m't|} = \frac{1}{\sqrt{2}\epsilon}. \tag{4.3}$$

Since ϵ can be made arbitrarily small, the ratio can become arbitrarily large.

This shows that if we select m and m' as two marks in the sequence $m_1, \ldots, m_\nu$, then the strategy we discussed previously which consists of proving Inequality 4.1 fails. In fact, regardless of whether m or m' are remote marks, one can construct a path between these two consecutive marks such that the ratio (4.3) above becomes arbitrarily large.

Although the ratio (4.3) cannot be bounded, the path length itself can still be bounded.

Lemma 4.34. *Let m (respectively m') be a mark created when the robot is at location p (respectively p') while walking along Π. Assume that no visitation marks are created while*

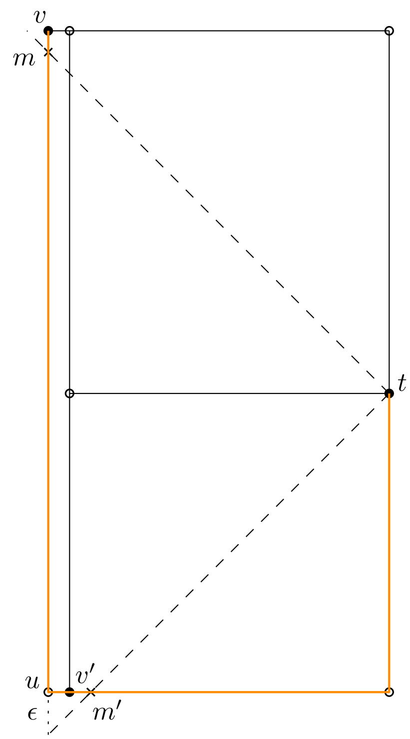

Figure 4.15: Illustration of a case where two marks are on different lines and the path length is not bounded by a constant factor of $|mt| - |m't|$.

the robot walks along int$(\Pi_{p,p'})$. *Suppose* $m \in L_t^i$ *and* $m' \in L_t^{i-1}$. *Moreover, let* m' *be the first mark created on* L_t^{i-1} *after the creation of* m. *Then*

$$|\Pi_{p,p'}| \leq 2\sqrt{2}\,|mt|.$$

Proof. Without loss of generality assume that d_i is parallel to the x-axis. While the robot remains in C_t^i, it never moves in direction d_i (by Lemma 4.8). Therefore,

$$|\Pi_{p,p'}|_x = |mt|_\infty - |m't|_\infty.$$

By Proposition 4.28, $\Pi_{p,p'}$ contains at least one real vertex. Let v be the first real vertex encountered along this path. Let

$$|\Pi_{p,v}|_x = \alpha.$$

Then

$$|\Pi_{v,p'}|_x = (|mt|_\infty - |m't|_\infty) - \alpha.$$

By Corollary 4.23,

$$|\Pi_{v,p'}|_y \leq |\Pi_{v,p'}|_x = (|mt|_\infty - |m't|_\infty) - \alpha.$$

By Corollary 4.30, the path $\Pi_{p,v}$ is xy-monotone. Hence

$$|\Pi_{p,v}|_y \leq 2|mt|_\infty,$$

since otherwise the path would exit the cone C_t^i, contradicting Proposition 4.28.

Moreover,

$$|mt|_\infty - |m't|_\infty \leq |mt|_\infty.$$

Therefore,

$$\begin{aligned}
|\Pi_{p,p'}| &= |\Pi_{p,p'}|_x + |\Pi_{p,p'}|_y \\
&= |\Pi_{p,v}|_x + |\Pi_{p,v}|_y + |\Pi_{v,p'}|_x + |\Pi_{v,p'}|_y \\
&\leq \alpha + 2|mt|_\infty + (|mt|_\infty - |m't|_\infty - \alpha) + (|mt|_\infty - |m't|_\infty - \alpha) \\
&\leq 4|mt|_\infty \\
&= \frac{4|mt|}{\sqrt{2}} \\
&= 2\sqrt{2}\,|mt|.
\end{aligned}$$

□

Although the lemma bounds the length of a single such path, this alone is insufficient. If the robot could traverse such paths an arbitrary number of times while making arbitrarily small progress toward t, then the total length of Π could still be unbounded.

We therefore introduce the following notion. We call two marks m and m' a *pair of problematic marks* if

- m was created while the robot was at p and m' while at p',
- $m \in L_t^i$ and $m' \in L_t^{i-1}$, and
- no visitation marks are created while the robot walks along $\text{int}(\Pi_{p,p'})$.

We say that this pair of problematic marks *belongs* to the cone C_t^i. We refer to $\Pi_{p,p'}$ as a *problematic path with respect to m and m'* (or simply *problematic path* when m and m' are clear from the context).

To help with further analysis, we define 10 distinct patterns of subpaths. We then argue that every path produced by the Marking Algorithm can be broken into a path consisting of Π_{s,m_1}, followed by a finite sequence of subpaths belonging to one of these 10 patterns, where m_1 is the first mark created while executing the Marking Algorithm.

Let p (respectively p') be the location of the robot when a mark m (respectively m') is created. We describe how to partition the path into subpaths of type $(L_t^i)^*$ and $[C_t^i]$. The definitions below specify which pair of marks is used to represent each subpath.

Subpaths of type $(L_t^i)^*$. Suppose that a (maximal) sequence of consecutive marks is created on a line L_t^i.

If this sequence contains at least one visitation mark, let m be the first mark in the sequence such that the mark preceding m is not on L_t^i, and let m' be the last visitation mark in the sequence such that the mark following m' is not on L_t^i. In this case, we represent the corresponding subpath $\Pi_{p,p'}$ by $(L_t^i)^*$.

If no visitation marks are created on L_t^i, then the path segment corresponding to $(L_t^i)^*$ is empty; instead, these marks are incorporated into the adjacent problematic segment (defined below).

Subpaths of type $[C_t^i]$. Consider two marks m and m', where m was created on L_t^i and m' was created after m and on L_t^{i-1}. Moreover, assume that no visitation marks were created while the robot was walking between p and p'. We define subpaths of type $[C_t^i]$ in the following way.

Let m' be the first mark created on L_t^{i-1}. We define m as follows:

- If there exists at least one visitation mark on L_t^i before m', then let m be the last such visitation mark.
- Otherwise, consider the (maximal) sequence of remote marks created on L_t^i immediately before creating m'. We let m be the first mark of this sequence.

In both cases, we represent the corresponding path segment $\Pi_{p,p'}$ by $[C_t^i]$, provided that the mark m is on L_t^i and m' is on L_t^{i-1}.

Every pattern is assumed to terminate either when the robot reaches t or when a subpath has two problematic path segments belonging to one cone. We denote the end of Π in the following patterns as END. For instance, consider the following sequence of subpaths corresponding to pattern $G4$ (see below).

$$(L_t^3)^* \to [C_t^3] \to (L_t^2)^* \to [C_t^2] \to (L_t^1)^* \to \text{END}$$

This sequence represents a path which begins at a point p such that p is the location of the robot when a mark $m \in L_t^3$ was created.

From p, the robot may create an arbitrary (but finite) number of marks on L_t^3. If at least one visitation mark is created on L_t^3 before the creation of a mark on L_t^2, then the corresponding maximal subpath on L_t^3 is represented by $(L_t^3)^*$. When the first mark on L_t^2 associated with this portion of the path is created, the intervening problematic path segment is represented by $[C_t^3]$.

Otherwise, if no visitation marks are created on L_t^3 before the creation of a mark on L_t^2, then $(L_t^3)^*$ represents an empty path segment, and the corresponding problematic path segment is incorporated into $[C_t^3]$.

Similarly, an arbitrary number of marks may be created on L_t^2 until a mark is created on L_t^1, forming a problematic path segment corresponding to $[C_t^2]$. This segment is defined analogously: if visitation marks are created on L_t^2 before the creation of a mark on L_t^1, then we use the last such visitation mark; otherwise, we use the first mark on L_t^2 associated with this portion of the path.

Finally, an arbitrary number of marks may be created on L_t^1. Since there are no further problematic path segments in this pattern, the robot eventually reaches t, completing the path.

We now count all the patterns. Without loss of generality we assume the robot begins on L_t^3, and that the first pair of problematic marks belong to C_t^3.

G1.
$$(L_t^3)^* \to \text{END}$$

G2.
$$(L_t^3)^* \to [C_t^3] \to (L_t^2)^* \to \text{END}$$

G3.
$$(L_t^3)^* \to [C_t^3] \to (L_t^2)^* \to [C_t^3]$$

G4.
$$(L_t^3)^* \to [C_t^3] \to (L_t^2)^* \to [C_t^2] \to (L_t^1)^* \to \text{END}$$

G5.
$$(L_t^3)^* \to [C_t^3] \to (L_t^2)^* \to [C_t^2] \to (L_t^1)^* \to [C_t^2]$$

G6.
$$(L_t^3)^* \to [C_t^3] \to (L_t^2)^* \to [C_t^2] \to (L_t^1)^* \to [C_t^1] \to (L_t^0)^* \to \text{END}$$

G7.
$$(L_t^3)^* \to [C_t^3] \to (L_t^2)^* \to [C_t^2] \to (L_t^1)^* \to [C_t^1] \to (L_t^0)^* \to [C_t^2]$$

G8.
$$(L_t^3)^* \to [C_t^3] \to (L_t^2)^* \to [C_t^2] \to (L_t^1)^* \to [C_t^1] \to (L_t^0)^* \to [C_t^0] \to (L_t^3)^* \to \text{END}$$

G9.
$$(L_t^3)^* \to [C_t^3] \to (L_t^2)^* \to [C_t^2] \to (L_t^1)^* \to [C_t^1] \to (L_t^0)^* \to [C_t^0] \to (L_t^3)^* \to [C_t^0]$$

G10.

$$(L_t^3)^* \to [C_t^3] \to (L_t^2)^* \to [C_t^2] \to (L_t^1)^* \to [C_t^1] \to (L_t^0)^* \to [C_t^0] \to (L_t^3)^* \to [C_t^3]$$

We show rudimentary *shapes* for each of these cases in Figure 4.16.

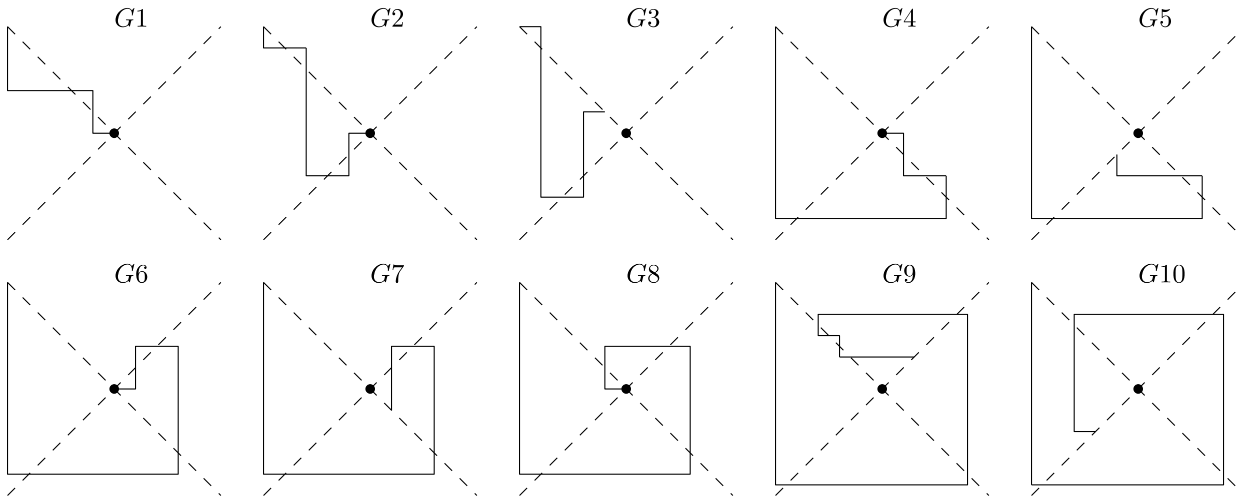

Figure 4.16: Examples of the 10 patterns of paths we discuss.

We now argue that any path produced by Marking Algorithm can be decomposed into an initial subpath Π_{s,m_1} followed by a sequence of subpaths, each belonging to one of the ten patterns described above.

Consider the sequence of marks created while the robot walks along Π. The robot begins at s and then walks until creating the first mark m_1. From here, if the robot reaches t without creating 2 problematic pairs in one cone then $\Pi_{p_1,t}$ belongs to one of the terminating patterns $G1$, $G2$, $G4$, $G6$, $G8$. If the robot instead creates 2 problematic pairs in one cone, the portion of the path from p_1 to the point of creating the second pair contains exactly the sequence of marks described by one of the non-terminating patterns $G3$, $G5$, $G7$, $G9$, and $G10$. We therefore classify this portion of the path as belonging to that patterns.

After such a segment ends, we begin a new segment starting from the point where the second problematic pair was created. The same reasoning applies again: the next portion of the path must follow one of the ten patterns until either the robot reaches t or a cone accumulates two problematic pairs.

Since each segment either reaches t or creates a second problematic pair in some cone, and since only finitely many marks are created along Π, this process yields a finite decomposition of Π into segments. Therefore every path produced by Marking Algorithm can be written as

$$\Pi = \Pi_{s,p_1} \circ \Pi_1 \circ \Pi_2 \circ \ldots \circ \Pi_k,$$

where each subpath Π_j belongs to one of the patterns $G1, \ldots, G10$.

We now show that patterns $G1$, $G2$, $G4$, $G6$, and $G8$ contain paths with bounded length. In each of these cases the path terminates at the target. None of these patterns contain paths with more than one pair of problematic marks per cone. Since there are four cones, these patterns contain at most four pairs of problematic marks, which is the case for $G8$. Observe that $G1$ can be seen as being a subpath of $G2$, which can be seen as being a subpath of $G4$, which can be seen as being a subpath of $G6$, which can be seen as being a subpath of $G8$. Therefore, we only bound the length of a path segment in $G8$. The total length of such a path can be expressed as the sum of two components: the upper bound on the distance traversed during the creation of a pair of problematic marks (given by Lemma 4.34), and the ratio between the path length and the infinity distance between two marks on the same line (bounded using Lemma 4.33).

Let m be the mark created at the beginning of a path segment belonging to pattern $G8$. Note that paths in $G8$ end at t. Let $L = |mt|_\infty$.

For each symbol $(L_t^i)^*$, if at least one visitation mark is created we denote the first mark in the sequence of marks representative of (L_t^i) as μ. Let μ' be the last visitation mark created in the representative sequence. For each symbol $(L_t^i)^*$ let $x_j = |\mu t|_\infty - |\mu' t|_\infty$.

We now bound the length of a path in pattern $G8$.

$$\begin{aligned}|G8| &= |(L_t^3)^* \to [C_t^3] \to (L_t^2)^* \to [C_t^2] \to (L_t^1)^* \to [C_t^1] \to (L_t^0)^* \to [C_t^0] \to (L_t^3)^* \to \text{END}| \\ &= |(L_t^3)^*| + |[C_t^3]| + |(L_t^2)^*| + |[C_t^2]| + |(L_t^1)^*| + |[C_t^1]| + |(L_t^0)^*| + |[C_t^0]| + |(L_t^3)^*|.\end{aligned}$$

By Lemma 4.34 we have

$$|[C_t^i]| \leq 2\sqrt{2}\, L.$$

Furthermore, by Lemmas 4.31 and 4.33,

$$|(L_t^i)^*| \leq 2\sqrt{2}\, x_j.$$

$$
\begin{aligned}
|G8| &= 2\sqrt{2}(L - x_1) + 2\sqrt{2}(L - x_1 - x_2) + 2\sqrt{2}(L - x_1 - x_2 - x_3) \\
&\quad + 2\sqrt{2}(L - x_1 - x_2 - x_3 - x_4) + 2\sqrt{2}(x_1 + x_2 + x_3 + x_4 + x_5) \\
&= 2\sqrt{2}\Big[(L - x_1) + (L - x_1 - x_2) + (L - x_1 - x_2 - x_3) \\
&\qquad + (L - x_1 - x_2 - x_3 - x_4) + (x_1 + x_2 + x_3 + x_4 + x_5)\Big] \\
&= 2\sqrt{2}\Big[4L - (4x_1 + 3x_2 + 2x_3 + x_4) + (x_1 + x_2 + x_3 + x_4 + x_5)\Big] \\
&= 2\sqrt{2}\Big[4L - (3x_1 + 2x_2 + x_3) + x_5\Big] \\
&\le 2\sqrt{2}\Big[4L - (3x_1 + 2x_2 + x_3) + (L - x_1 - x_2 - x_3 - x_4)\Big] \quad \text{since } x_1 + \cdots + x_5 \le L \\
&= 2\sqrt{2}\Big[5L - (4x_1 + 3x_2 + 2x_3 + x_4)\Big] \\
&\le 2\sqrt{2} \cdot 5L \quad \text{since } x_j \ge 0 \text{ for all } j \\
&= 10\sqrt{2}\,L.
\end{aligned}
$$

Thus any path segment belonging to pattern $G8$ has length at most

$$|G8| \le 10\sqrt{2}\,L = 10\sqrt{2}\,|mt|_\infty.$$

Thus, the length of any path segment in patterns $G1$, $G2$, $G4$, $G6$, and $G8$ is bounded by $10\sqrt{2}\,|mt|_\infty$.

Our hope would be to prove that all other patterns contain a similar bound as well. Unfortunately, we can show this only for $G3$, $G5$, $G7$ and $G9$, i.e., we do not know how to bound the case $G10$.

Before proving the bound on path lengths for subpaths in $G3$, $G5$, $G7$ and $G9$ we first prove the following preparatory lemma and proposition.

Lemma 4.35. *Let p (respectively p') be the location of the robot when a mark m (respectively m') was created as the robot walks along Π. Assume $m \in L_t^i$ and $m' \in L_t^{i-1}$. Moreover assume that no other marks are created while the robot walks along $\Pi_{p,p'}$ and that m' is created after m. Then m' is created while the robot is moving in direction d_{i+2}, away from a real vertex.*

Proof. If m' is a remote mark, then by definition, m' is created while the robot moves in direction d_{i+2}. If m' is a visitation mark, then m' can only be created while the robot moves in direction d_{i+2}. Otherwise, this would violate Lemma 4.24.

By Observation 4.1 when the robot reaches p' it reaches it by either moving towards a real vertex or away from one. We will prove that it happens as the robot moves away from a real vertex.

By Proposition 4.28, $\Pi_{p,p'}$ contains at least one real vertex v. Upon reaching v observe that the robot will move in direction d_{i+2} until it reaches a vertex u^* that does not have a neighbour in direction d_{i+2}.

If u^* is not in C_t^i then m' was created when the robot intersected L_t^{i-1} thus m' was created while the robot moves away from v, a real vertex. Otherwise, we observe that vertex u^* has a real neighbour v^* in direction $d_{i\pm1}$. Either v^* is not in C_t^i or it is. If v^* is not in C_t^i, then a remote mark is created at the intersection between L_t^{i-1} and u^*v^*. Therefore m' was created while the robot is moving away from v, a real vertex.

If v^* is in C_t^i, then the robot will reach this vertex which is inside of C_t^i. Therefore from this point the robot will either create m' while moving away from v^* or it will reach another real vertex in C_t^i. Thus the robot will not create m' while moving towards a real vertex. □

Observe that in patterns $G3$, $G5$, $G7$ and $G9$, the problematic pairs of marks are situated such that the first mark m_1 in the first pair belongs to the same line as the second mark m_4 of the second pair. In the following lemma, we show that $|m_1m_4| \geq |m_4t|$.

Proposition 4.36. *Let m_1 and m_2 be a pair of problematic marks belonging to C_t^i. Let m_3 and m_4 be a pair of problematic marks belonging to C_t^i created after the pair m_1 and m_2. Let p_2 (respectively p_3) be the location of the robot when m_2 (respectively m_3 was created. Assume no problematic pairs of marks was created while the robot walked along Π_{p_2,p_3}. Then $\frac{|m_4t|}{|m_1t|} \leq \frac{1}{2}$.*

Proof. Let p_1 (respectively p_2, p_3 and p_4) be the location of the robot when m_1 (respectively m_2, m_3, and m_4) is created. Moreover, observe that p_2 and p_3 need not be distinct from one another. Indeed, if m_2 is a remote mark, and the next mark created after m_2 is on L_t^i then m_2 satisfies the conditions for m_3. This is taken into account in the following proof.

By Proposition 4.28 Π_{p_1,p_2} contains a real vertex. Let v be the first real vertex visited after p_1 while walking along Π. By Corollary 4.30 $\Pi_{p_1,v}$ is xy-monotonic.

By Lemma 4.35 we have that there exists a real vertex $v' \in \Pi_{p_3,p_4}$ that the robot walks away from before creating m_4. By Corollary 4.23 and the assumption of this proposition we have $m_4 \in C_{v'}^{i+2} \cap L_t^i$.

Let $q \in L_t^i$ be the point such that $|m_1q| = |qt|$. We consider C_q^i. Refer to figure 4.17.

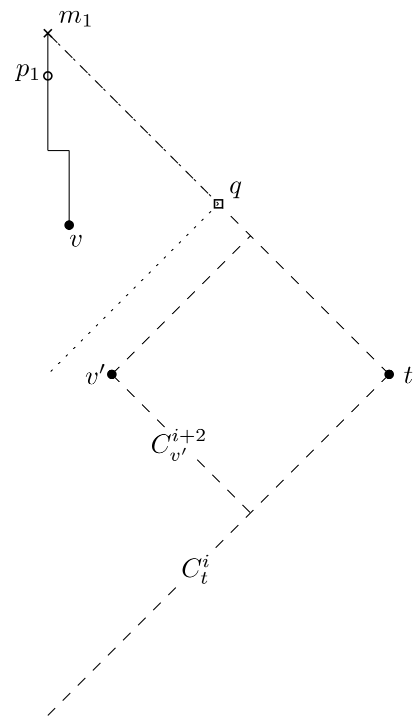

Figure 4.17: An example of some points, paths, and cones in consideration in this proposition. Notably with $v' \notin C_q^i$.

Observe that if $v' \notin C_q^i$, then all points in $C_{v'}^{i+2} \cap L_t^i$ lie closer to t than they do to m_1. Since $m_4 \in C_{v'}^{i+2} \cap L_t^i$, it follows that $|m_1m_4| \geq |m_4t|$, which establishes the statement of the proposition.

Therefore, in the remainder of the proof we may assume that $v' \in C_q^i$.

Observe that $\Pi_{p,v}$ is an xy-monotonic path by Corollary 4.30. By Lemmas 4.24 and 4.25 the robot will walk in direction d_{i-1} from p_1. Since by Lemma 4.8 the robot cannot move in direction d_i then we can say that while walking across $\Pi_{p,v}$ the robot will only move in directions d_{i-1} and d_{i+2}.

We now show that $v \in C_q^i$. We consider two cases: either (1) m_4 does not have a projection onto $m_1p_1 \cup \Pi_{p_1,v}$ in direction d_i or (2) m_4 has a projection $\widehat{m}_4$ onto $m_1p_1 \cup \Pi_{p_1,v}$ in direction d_i.

1. Assume m_4 does not have a projection onto $m_1p_1 \cup \Pi_{p_1,v}$ in direction d_i.

   If $m_1 \neq p_1$ then m_1 is a remote mark and m_1p_1 is perpendicular to the bisector of C_t^i by Lemma 4.25. Moreover, by the definition of remote marks, and since m_1p_1 and $\Pi_{p_1,v}$ intersect only at p_1, we have that $m_1p_1 \cup \Pi_{p_1,v}$ forms an xy-monotonic path.

   If $m_1 = p_1$ then $m_1p_1 \cup \Pi_{p_1,v}$ is an xy-monotonic path.

If m_4 does not have a projection onto $m_1p_1 \cup \Pi_{p_1,v}$ in direction d_i, but q does have a projection onto $m_1p_1 \cup \Pi_{p_1,v}$ in direction d_i then $|m_1m_4|> |m_1q|$ thus $|m_1m_4|\geq |m_4t|$. So for the rest of this case we consider q does not have a projection onto $m_1p_1 \cup \Pi_{p_1,v}$ in direction d_i.

Let r be the point of intersection between the line perpendicular to the bisector of C_t^i which passes through m_1 and the line parallel to the bisector of C_t^i which passes through q. Let $\triangle m_1qr$ be the right triangle which has m_1q as its hypotenuse and r at its right angle (refer to Figure 4.18).

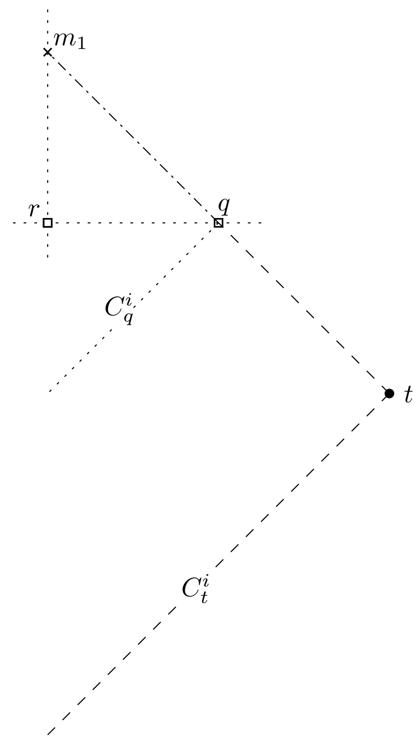

Figure 4.18: An example of the triangle $\triangle m_1qr$ used in Proposition 4.36.

Observe that since q does not have a projection on $m_1p_1 \cup \Pi_{p_1,v}$ in direction d_i, then $v \in \triangle m_1qr$. Indeed, if v was outside of $\triangle m_1qr$, then qr would intersect $m_1p_1 \cup \Pi_{p_1,v}$, which would create a projection in direction d_i.

Since $\triangle m_1qr \subset C_q^i$ then $v \in C_q^i$.

2. Assume m_4 has a projection $\widehat{m}_4$ onto $m_1p_1 \cup \Pi_{p_1,v}$ in direction d_i or d_{i+2}. Then v' also has a projection $\widehat{v}'$ onto $m_1p_1 \cup \Pi_{p_1,v}$ in direction d_i or d_{i+2}, otherwise we have $v \in C_q^i$ (and the proof is complete for this case). We consider two subcases: either (a) $|v't|_\infty> |\widehat{v}'t|_\infty$ or (b) $|v't|_\infty< |\widehat{v}'t|_\infty$. Observe that $|\widehat{v}'t|_\infty= |v't|_\infty$ is not possible as $\Pi_{p_1,v}$ does not contain a real vertex other than v.

(a) Assume $|v't|_\infty > |\widehat{v}'t|_\infty$. In this case, observe that $p_4 \notin \Pi_{p_1,v}$ as this would imply m_4 is created before m_2. Then we have that Π_{v',p_4} intersects $m_1p_1 \cup \Pi_{p_1,v}$. Otherwise $|p_4t|_\infty > |vt|_\infty$, contradicting Corollary 4.15.

If $v'p_4$ intersects $m_1p_1 \cup \Pi_{p_1,v}$ at a path segment perpendicular to d_i then this would imply the existence of two rays which cross each other, a contradiction to the definition of emanation graphs.

If the intersection is at a path segment parallel to d_i then this would imply that the robot walks along this path segment but does not continue to p_4, a contradiction of the MARKING ALGORITHM. Therefore this case is not possible.

(b) Assume $|v't|_\infty < |\widehat{v}'t|_\infty$ (refer to Figure 4.19). Recall that our goal is to show

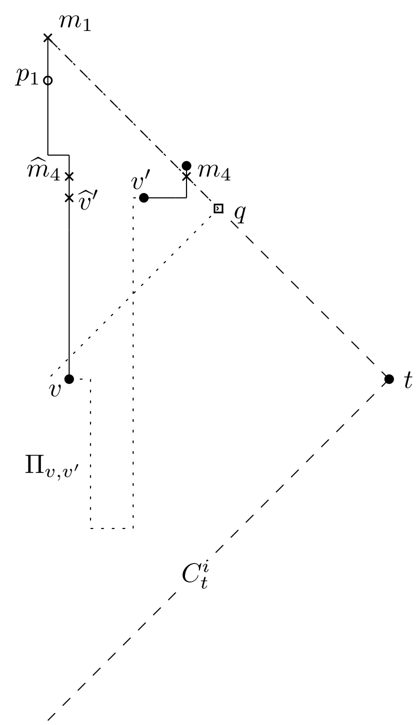

Figure 4.19: An example of the points, paths, and projections, discussed in case 2(b) of Proposition 4.36.

$v \in C_q^i$. We proceed by contradiction. Assume $v \notin C_q^i$.

Then, since $C_{v'}^i \subseteq C_q^i$ and v' has a projection onto $mp \cup \Pi_{p_1,v}$ in direction d_i, we have $mp \cup \Pi_{p_1,v} \cap L_{v'}^i \neq \varnothing$ and $mp \cup \Pi_{p_1,v} \cap L_{v'}^{i-1} \neq \varnothing$. From p_1 the robot moves in direction d_{i-1} until it reaches a vertex u such that u does not have a neighbour in direction d_{i-1} or u is a real vertex.

For the rest of the proof, we will need the following observation.

Observation. We have $u \in \mathrm{int}(C_{v'}^i)$.

Proof of the observation. If $u \notin \text{int}(C^i_{v'})$, then either we have a straight path from m to u which spans a cone $C^i_{v'}$ contradicting Corollary 4.4, or $m_1u \cap C^i_{v'} = \varnothing$. We will argue that $m_1u \cap C^i_{v'} = \varnothing$ also leads to a contradiction. From u the robot will move in direction d_{i+2} until it reaches a vertex u' such that u' is a Steiner vertex that does not have any neighbours in direction d_{i+2}. If $u' \notin \text{int}(C^i_t)$ then we create a visitation mark where the straight path from u to u' intersects $L^i_t \cup L^{i-1}_t$. If u' is in C^i_t, then from u' the robot will move in direction d_{i-1}, either towards a real vertex, or away from a real vertex. If it is moving away from a real vertex then we create a remote mark on L^i_t, contradicting the creation of m_2 on L^{i-1}_t. If it is moving towards a real vertex then if this vertex is in C^q_t then we contradict the assumption that $v \notin C^q_t$. If it is not in C^q_t then the path from u' to this vertex is a straight path which spans $C^i_{v'}$, contradicting Corollary 4.4. □

Let us continue with the proof of the proposition. The vertex u is not a real vertex, since this would imply $u = v$, and we assume $v \notin C^i_q$. Then, from u the robot will walk in direction d_{i+2} until it reaches a vertex u' such that u' does not have a neighbour in direction d_{i+2}. Then we have four subcases: i. uu' intersects $L^{i-1}_{v'}$, ii. uu' intersects $L^i_{v'}$, iii. $u' \in C^i_{v'}$.

i. Assume uu' intersects $L^{i-1}_{v'}$. Let ℓ be the line perpendicular to the bisector of $C^i_{v'}$ that passes through u, and let $\triangle^i_{v',\ell}$ be the triangle bounded by $L^i_{v'}$, $L^{i-1}_{v'}$, and ℓ.
   Let w be the real vertex in $\triangle^i_{v',\ell}$ closest to ℓ that has a projection w' onto the straight path from m_1 to u in direction d_i. Such a vertex exists, since v' itself satisfies this property. Similarly to $\triangle^i_{v',\ell}$ let $\triangle^i_{w,\ell}$ be the triangle defined by L^i_w, L^{i-1}_w, and ℓ.
   Consider the ray ρ_1 which supports the path m_1u. Observe that the real vertex v_1 from which ρ_1 is shot is not in $C^i_{v'}$, because otherwise the robot would have reached v_1, making $v_1 = v$, but we assume $v \notin C^i_q$ and ρ_1 cannot span C^i_q by Corollary 4.3.
   Also consider the ray ρ_2 emitted from w in direction d_i. We first argue that ρ_2 must be interrupted before it reaches w'. Observe that ρ_1 remains uninterrupted until it reaches u. Moreover, ρ_2 reaches w' before ρ_1 reaches w'. Since the origin of ρ_1 is not in C^i_w then we have ρ_2 interrupting ρ_1 before it reaches u, a contradiction.
   We now argue that ρ_2 cannot be interrupted before it reaches w', leading to a contradiction. By the definition of w no vertex with a projection in direction d_i onto the straight path from m_1 to u can produce a ray interrupting ρ_2 before it reaches w'. Consider a vertex without a projection in direction d_i on m_1u which produces a ray which interrupts ρ_2 before it reaches w'. Observe that this vertex must lie in $\triangle^i_{w,\ell}$. However, a ray from such a vertex

would also interrupt the ray defining the straight path uu', contradicting the existence of this path.
Thus, this case cannot occur.

ii. Assume uu' intersects $L^i_{v'}$. Then $u' \notin C^i_{v'}$ but $u' \in C^i_t$ (otherwise we would create the mark m_2 on L^i_t). Upon reaching u' the robot must move in direction d_{i-1}. Either the robot is moving away from a real vertex w or it is moving towards a real vertex w.
If the robot is moving away from w, then w must be in C^{i+1}_t, but this situation would create a mark on L^i_t contradicting the assumption that m_2 is on L^{i-1}_t. If the robot is moving towards w then w is in C^i_t. Either w is in $C^i_{v'}$ or it is not. If w is in $C^i_{v'}$ then the robot will reach this vertex, contradicting our assumption that $v \notin C^i_q$. If w is not in $C^i_{v'}$ then we have a straight path from w to u' spanning $C^i_{v'}$ contradicting Corollary 4.4 or we have that v' does not have a projection in direction d_i on $m_1p_1 \cup \Pi_{p_1,v}$ contradicting our assumptions.
Thus, this case cannot occur.

iii. Assume $u' \in C^i_{v'}$. Upon reaching u' the robot must move in direction d_{i-1}. Either the robot is moving away from a real vertex w or it is moving towards a real vertex w. If the robot is moving away from w, then w must be in C^{i+1}_t, but this situation would create a mark on L^i_t contradicting the assumption that $m_2 \in L^{i-1}_t$. If the robot is moving towards w then w is in C^i_t. Either w is in $C^i_{v'}$ or it is not. If w is in $C^i_{v'}$ then the robot will reach this vertex, contradicting our assumption that $v \notin C^i_q$. Thus the straight path from u' to w intersects $L^{i-1}_{v'}$.
We also have that m_1u intersects $L^i_{v'}$. As such, consider the line ℓ perpendicular to the bisector of $C^i_{v'}$ that passes through u', and let $\triangle^i_{v',\ell}$ denote the triangle bounded by $L^i_{v'}$, $L^{i-1}_{v'}$, and ℓ. Let ℓ' be the line perpendicular to the bisector of $C^i_{v'}$ that passes through u, and let $\triangle^i_{v',\ell'}$ denote the triangle bounded by $L^i_{v'}$, $L^{i-1}_{v'}$, and ℓ'.
Suppose there is a real vertex b in $\triangle^i_{v',\ell}$ that is closest to ℓ and has a projection in direction d_i b' onto the straight path from u' to w. If $\mathrm{int}(\triangle^i_{b,\ell})$ contains no real vertices, then during the construction of the graph the ray ρ_1 emitted from b in direction d_i would intersect the ray ρ_2 emitted from w in direction d_{i+1} at the point w', thereby interrupting ρ_2. This would imply that the straight path from w to u' does not exist, contradicting the assumption that the path exists. If instead $\mathrm{int}(\triangle^i_{b,\ell})$ is not empty of real vertices, then there exists a real vertex in $\triangle^i_{v',\ell}$ that admits a projection in direction d_i onto m_1u.
Now consider the subcase where b does not exist. Observe that v' is in $\triangle^i_{v',\ell}$ and has a projection in direction d_i onto ℓ'.
If either $\mathrm{int}(\triangle^i_{b,\ell})$ is not empty of real vertices or b does not exist, we take

c to be the closest real vertex to ℓ' such that c has a projection in direction d_i c' on ℓ'.
If $\mathrm{int}(\triangle^i_{c,\ell})$ is empty of real vertices, during construction the ray ρ_3 emitted from c in direction d_i would intersect the ray ρ_4 supporting mu at the point c', thereby interrupting ρ_4.
This implies that the path m_1u does not exist, contradicting the assumption that such a path exists.
Otherwise, if $\mathrm{int}(\triangle^i_{c,\ell})$ is not empty of real vertices then a real vertex in the triangle could produce a ray which interrupts ρ_3 before it reaches c'.
Observe that such a real vertex does not have a projection in direction d_i onto the straight path from m_1 to u in direction d_i, and thus such a ray would interrupt the ray which defines $\Pi_{u,u'}$, contradicting the assumption that such a path exists.

All cases explored in case 2b lead to a contradiction. Therefore, $v \in C^i_q$.

Consider the line ℓ passing through m_1 which is perpendicular to the bisector of C^i_t. Let $\triangle^i_{q,\ell}$ be the triangle bounded by ℓ, L^i_q, and L^{i-1}_q. Observe that due to the xy-monotonicity of $\Pi_{p,v}$ that v is in $\triangle^i_{q,\ell}$. Let q^* be the projection of q onto L^{i-1}_t.

In order to satisfy $|m_2t| > |m_4t|$ we must have $q^* \in \mathrm{int}(C^{i+1}_v)$. Otherwise we would have $|m_2t| < |m_4t|$ which contradicts Lemma 4.27. This is equivalent to showing $v \in \mathrm{int}(C^i_{q^*})$. Which is equivalent to showing $\triangle^i_{q,\ell} \cap \mathrm{int}(C^i_{q^*}) \neq \varnothing$. Observe that this is not true. Therefore $|m_1m_4| \geq |m_4t|$. Since m_1, m_4 and t appear on the same line, and in this order, we now have $|m_1t| = |m_1m_4| + |m_4t| \geq 2|m_4t|$ and the result follows. □

By definition, each of the patterns $G3$, $G5$, $G7$ and $G9$ begin at a point p such that a mark m is created at p and end at a point p' such that a mark m' is created at p'. Proposition 4.36 shows that m' is at least a factor of 2 closer to t than m, i.e. $\frac{|mt|_\infty}{|m't|_\infty} \geq 2$. In each of these patterns the path terminates after creating a second pair of problematic marks belonging to one cone. Consequently, none of these patterns contain paths with more than one pair of problematic marks per cone, aside from the terminating problematic pair. Since there are four cones, subpaths from these patterns contain at most 5 pairs of problematic marks (namely, it is $G9$ which contains 5 pairs of problematic marks). Observe that $G3$ can be seen as being a subpath of $G5$, which can be seen as being a subpath of $G7$, which can be seen as being a subpath of $G9$. Therefore, we only bound the length of a path segment in $G9$. The total length of such a path can be expressed as the sum of two components: the upper bound on the distance traversed during the creation of problematic marks (given by Lemma 4.34), and the ratio between path length and the distance between two marks on the same line (bounded using Lemma 4.33).

Let us focus on $G9$ and let $L = |mm'|_\infty$. Consider a symbol $(L^i_t)^*$ in $G9$ together with the sequence of marks created while the robot walks along the subpath corresponding to this symbol. If this sequence of marks is not empty, then let μ (respectively μ') be the first (respectively the last) one. For the j-th symbol $(L_t^i)^*$ in $G9$, let $x_j = |\mu t|_\infty - |\mu' t|_\infty$.

$$\begin{aligned}
|G9| &= 2\sqrt{2}(L - x_1) + 2\sqrt{2}(L - x_1 - x_2) + 2\sqrt{2}(L - x_1 - x_2 - x_3) \\
&\quad + 2\sqrt{2}(L - x_1 - x_2 - x_3 - x_4) + 2\sqrt{2}(x_1 + x_2 + x_3 + x_4 + x_5) \\
&\quad + 2\sqrt{2}(L - x_1 - x_2 - x_3 - x_4 - x_5) \\
&= 2\sqrt{2}\Big[(L - x_1) + (L - x_1 - x_2) + (L - x_1 - x_2 - x_3) \\
&\qquad + (L - x_1 - x_2 - x_3 - x_4) + (L - x_1 - x_2 - x_3 - x_4 - x_5) \\
&\qquad + (x_1 + x_2 + x_3 + x_4 + x_5)\Big] \\
&= 2\sqrt{2}\Big[5L - (5x_1 + 4x_2 + 3x_3 + 2x_4 + x_5) + (x_1 + x_2 + x_3 + x_4 + x_5)\Big] \\
&= 2\sqrt{2}\Big[5L - (4x_1 + 3x_2 + 2x_3 + x_4) + x_5\Big] \\
&\leq 2\sqrt{2}\Big[5L - (4x_1 + 3x_2 + 2x_3 + x_4) + (L - x_1 - x_2 - x_3 - x_4)\Big] \\
&\qquad\qquad \text{since } x_1 + \cdots + x_5 \leq L \\
&= 2\sqrt{2}\Big[6L - (5x_1 + 4x_2 + 3x_3 + 2x_4)\Big] \\
&\leq 2\sqrt{2} \cdot 6L \quad \text{since } x_j \geq 0 \text{ for all } j \\
&= 12\sqrt{2}\, L.
\end{aligned}$$

Thus any path segment belonging to pattern $G9$ satisfies

$$|G9| \leq 12\sqrt{2}\,|mm'|_\infty.$$

We can bound the length of a path Π produced by the MARKING ALGORITHM, provided Π does not contain path segments in $G10$.

Theorem 4.37. *Let $s, t \in V$ and Π be a path from s to t produced by the* MARKING ALGORITHM*. Assume Π does not contain path segments in $G10$. Then $|\Pi| \leq (2 + 24\sqrt{2})|st|$.*

Proof. Observe that from the patterns $G1$ through $G9$ the largest bound on a path terminating at t is $G8$. The largest bound on a path terminating with a second problematic pair in the same cone is $G9$. As such, without loss of generality, assume $\Pi = \Pi_{s,p_1} \circ \Pi_1 \circ \Pi_2 \circ \ldots \circ \Pi_{k-1} \circ \Pi_k$, where Π_j is a path in $G9$ for $1 \leq j \leq k-1$.

By Proposition 4.36, each $G9$ subpath reduces the $\|\cdot\|_\infty$-distance to t by at least a factor of 2, since $|pt|_\infty = |mt|_\infty$ and $|p't|_\infty = |m't|_\infty$. Therefore,

$$\begin{aligned}
|\Pi| &= |\Pi_{s,p_1} \circ \Pi_1 \circ \Pi_2 \circ \ldots \circ \Pi_k| \\
&= |\Pi_{s,p_1}| + |\Pi_1| + |\Pi_2| + \cdots + |\Pi_k| \\
&= 2|sm_1|_\infty + 12\sqrt{2}\sum_{i=0}^{n} \frac{|m_1 t|_\infty}{2^i} + 10\sqrt{2}|m_{k-1}t|_\infty
\end{aligned}$$

where n is the number subpaths in Π belonging to pattern G9.

By Corollary 4.23, when $s \in C_t^i$ the mark $m_1 \in C_s^{i+2} \cap (L_t^i \cup L_t^{i-1})$ so $|sm_1| \leq |st|_\infty \leq |st|$. Moreover, by Lemma 4.27 we have $|m_1 t|_\infty > |m_i t|_\infty$ for all m_i where $i > 1$. Thus the bound can be expressed as

$$2|st| + 12\sqrt{2}\sum_{i=0}^{n} \frac{|st|}{2^i} + 10\sqrt{2}\frac{|st|}{2^n}.$$

We proceed with the simplification.

$$\begin{aligned}
&2|st| + 12\sqrt{2}\,|st|\sum_{i=0}^{n} \frac{1}{2^i} + 10\sqrt{2}\frac{|st|}{2^n} \\
&\quad = 2|st| + 12\sqrt{2}\,|st| \cdot 2\left(1 - \frac{1}{2^{n+1}}\right) + 10\sqrt{2}\frac{|st|}{2^n} \\
&\quad = 2|st| + 24\sqrt{2}\,|st|\left(1 - \frac{1}{2^{n+1}}\right) + 10\sqrt{2}\frac{|st|}{2^n} \\
&\quad = 2|st| + 24\sqrt{2}\,|st| - \frac{24\sqrt{2}}{2^{n+1}}|st| + \frac{10\sqrt{2}}{2^n}|st| \\
&\quad = |st|\left(2 + 24\sqrt{2} - \frac{12\sqrt{2}}{2^n} + \frac{10\sqrt{2}}{2^n}\right) \\
&\quad = |st|\left(2 + 24\sqrt{2} - \frac{2\sqrt{2}}{2^n}\right).
\end{aligned}$$

As $n \to \infty$ this expression converges to $|st|(2 + 24\sqrt{2})$. Thus the routing ratio of the Marking Algorithm on grade-1 emanation graphs in general position, for paths not containing a subpath in $G10$, is at most

$$2 + 24\sqrt{2}.$$

$\square$

5

Conclusion

To conclude this thesis, we summarize our results, offer additional observations and remarks that did not fit cleanly into any preceding section, and discuss open problems for future research, along with our intuition for the most promising approaches to each.

5.1 Summary of Results

5.1.1 Grade-1 Emanation Graphs

In this thesis we first showed an interesting property that *grade-k emanation graphs* are a subset of motorcycle graphs, at least for $k = 1$. We used a priority graph in order to provide a speed assignment as part of our proof.

5.1.2 Spanning Properties

We followed by proving some spanning properties. We showed that motorcycle graphs are not spanners, a trivial observation followed by the fact that not all motorcycle graphs are connected. But then we also proved that *connected* motorcycle graphs are also not t-spanners for a constant t.

Next, we showed some spanning properties of grade-1 emanation graphs. Namely, that for Steiner vertices to Steiner vertices, grade-1 emanation graphs are not t-spanners for some constant t and for Steiner vertices to real vertices grade-1 emanation graphs are $\sqrt{10}$-spanners.

5.1.3 Local Routing

We've explored several general purpose routing algorithms on grade-1 emanation graphs in general position. In this exploration we showed how greedy routing fails, compass routing fails, and greedy compass routing fails. We also showed that face-routing is proven to have an arbitrarily large routing ratio.

We then introduced a routing algorithm for grade-1 emanation graphs called the Marking Algorithm defined in Algorithm 1. We showed that this algorithm is well-defined for grade-1 emanation graphs in general position. We also showed that it *succeeds* on such graphs, using a key observation that this algorithm provides a path with non-increasing $\|\cdot\|_\infty$ from t.

We then show that this routing algorithm has a routing ratio of $2 + 24\sqrt{2}$ for all paths which do not contain a pattern we identify as $G10$.

5.2 Observations and Remarks

In this subsection we discuss some observations.

5.2.1 Routing from a Steiner Vertex to a Steiner Vertex in Grade-1 Emanation Graphs

We consider the problem of local routing from s to t in grade-1 emanation graphs when s and t are both Steiner vertices. We note that such a routing algorithm cannot have a bounded routing ratio, as we have shown in Lemma 3.3 there does not exist a bound on the spanning path between two Steiner vertices. Thus, for a *successful* routing algorithm between two Steiner vertices we can use face-routing.

5.2.2 Routing from a Steiner Vertex to a Real Vertex in Grade-1 Emanation Graphs

Recall that Algorithm 1 has the precondition that the input vertex is a real vertex. In particular, it is not defined for $s \in S$. We now describe an initialization step which extends Algorithm 1 to handle the case where $s \in S$.

If s is a Steiner vertex, we initialize v to be an arbitrary vertex from $\mathcal{N}_r(s)$. Assume v is in direction d_i from s. If $s \in \mathrm{int}(Q_{t,v})$, let $d = d_{i+2}$. Otherwise, let $d = d_i$.

Observe that with this extra initialization step, $\Pi_{s,t}$ is a subpath of $\Pi_{v,t}$, which ends in t. Since $\Pi_{v,t}$ is a valid path, so is $\Pi_{s,t}$.

5.3 Future Work and Open Problems

In this subsection we discuss some problems related to this thesis that remain open and provide some intuition as to the solutions and possible ways to prove them.

5.3.1 Routing on Grade-1 Emanation graphs Outside of General Position

In this thesis, we have provided a routing algorithm for grade-1 emanation graphs *in general position*. It is natural to ask whether the same algorithm succeeds outside of general position. Note that the Marking Algorithm is *not well-defined* outside of general position, as it does not specify which direction the robot should move from a real vertex v when v belongs to more than one cone of t. For the remainder of this section, we augment the Marking Algorithm with the following clarification: if v belongs to more than one cone, we arbitrarily select a cone C_t^i and set $d = d_{i+2}$.

Even with this clarification, the adjusted Marking Algorithm can fail on grade-1 emanation graphs outside of general position. Figure 5.1 shows such a failure. Starting at s, suppose the robot selects direction d_1. It walks in this direction until reaching u_1, at which point it sets $d = d_0$ and continues to v. From v, it may select $d = d_3$ and walk until reaching u_2, after which it returns to s, entering a cycle.

We propose the following additional step to address this failure. If the robot is at a Steiner vertex u with a real neighbour v such that $u \notin Q_{t,v}$, the robot moves to v. Since $u \notin Q_{t,v}$ implies that moving to v strictly reduces the robot's $\|\cdot\|_\infty$-distance to t, this step is always beneficial. One can verify that this addition causes the algorithm to succeed on the graph in Figure 5.1.

However, there is another ambiguity which needs to be addressed. Consider the graph in Figure 5.2. Routing from s to t, the robot first moves in direction d_1 until reaching u_1, then changes direction and moves to u_2. At this point, the robot's next move is undefined: the presence of v_2 suggests moving in direction d_1, while the presence of v_3 suggests moving in direction d_3.

To resolve this ambiguity, we propose a third alteration. If the robot is travelling in direction d_i within cone C_t^i and reaches a Steiner vertex with no neighbour in direction d_i

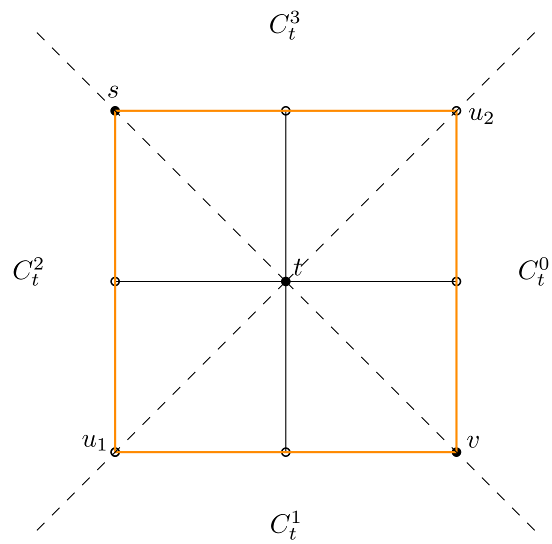

Figure 5.1: A grade-1 emanation graph on which the adjusted Marking Algorithm fails.

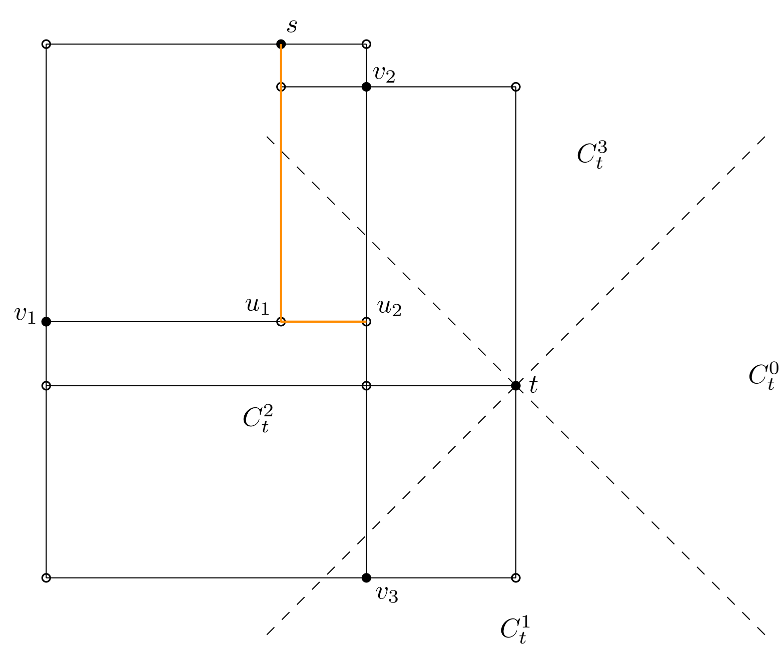

Figure 5.2: A grade-1 emanation graph which exposes undefined behaviour in the adjusted Marking Algorithm.

but with two real neighbours v and v' in adjacent cones, the robot performs a line search along $C_t^i \cap vv'$, without leaving C_t^i. If during this search the robot reaches a Steiner vertex u' with a real neighbour v^* such that $u' \notin Q_{t,v^*}$, it moves to v^*. The existence of such a vertex v^* can be established by an argument analogous to Corollary 4.4.

We conjecture that these three alterations together

1. arbitrarily resolving cone ambiguity at real vertices,

2. always moving to real neighbours when strictly outside their square,

3. and performing a line search in the above case

are sufficient for the MARKING ALGORITHM to succeed on grade-1 emanation graphs outside of general position. A full proof of this conjecture remains an open problem.

5.3.2 Routing Without the Ability to See Real Neighbours

In this thesis we make the assumption that in the MARKING ALGORITHM the robot can see the *real neighbours* of a vertex u when it is located at u. This allows the robot to route toward advantageous real vertices. We now argue informally that this assumption is not strictly necessary, and sketch a variant we call the BLIND MARKING ALGORITHM.

Instead of observing real neighbours directly, the robot maintains two distance variables L and L', and a phase bit b. Upon reaching a real vertex, the robot resets $L = 0$, $L' = 0$, and $b = 0$. While $b = 0$, the robot increments L by the length of each edge it traverses.

When the robot is at a vertex u in a cone C_t^i with $d = d_{i+2}$ but u has no neighbour in direction d_{i+2}, it sets $b = 1$ and walks in an arbitrary direction perpendicular to d_{i+2}, tracking the distance walked from u in L', until one of the following occurs:

1. Walking to the next vertex would cause $L' > L$.

2. Walking to the next vertex would cause the robot to leave C_t^i.

3. The current vertex has no neighbour in the chosen perpendicular direction.

4. The robot reaches a real vertex.

In cases 1–3, the robot reverses direction and walks until it reaches a real vertex. In case 4, the BLIND MARKING ALGORITHM resumes from that real vertex normally.

When the robot is at a vertex u in a cone C_t^i with $d \neq d_{i+2}$ and u has no neighbour in direction d, the robot instead walks in direction d_{i+2}.

The intuition behind the distance bound $L' \leq L$ follows from the existence of the bounded detours path (refer to Definition 3.1). It remains to be shown formally that the BLIND MARKING ALGORITHM is well-defined, always reaches t, and worsens the upper bounds on the competitive cost established for the MARKING ALGORITHM by at most a constant factor.

5.3.3 Competitive Routing on Grade-1 Emanation Graphs with Subpaths of Pattern G10

In this thesis we have set aside subpaths of pattern G10, as they are difficult to handle. We now discuss them briefly. Figure 5.3 shows a trace of the Marking Algorithm which produces a subpath of pattern G10. In this figure, upon completing the second problematic

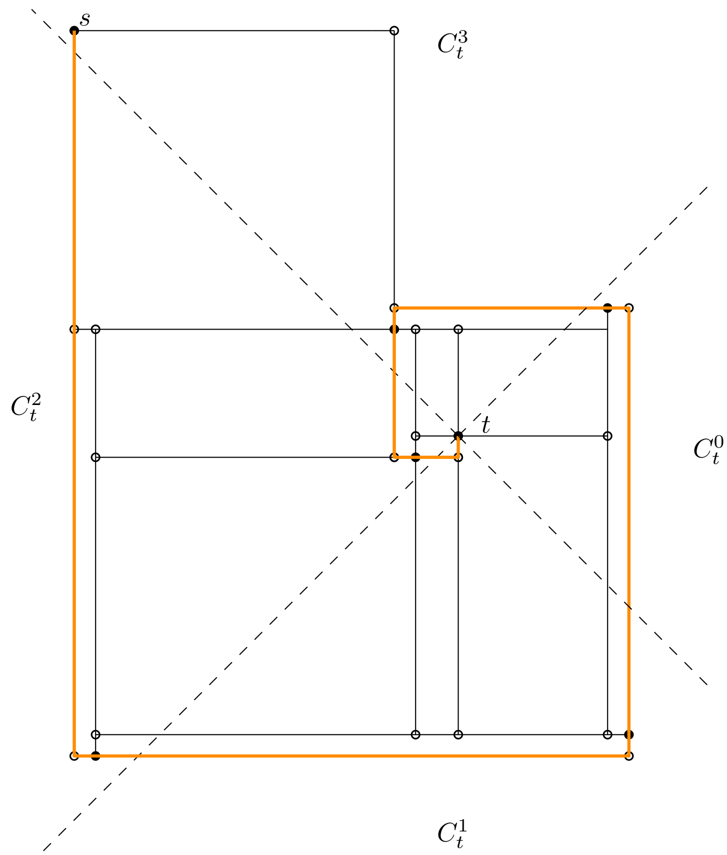

Figure 5.3: A grade-1 emanation graph in which the Marking Algorithm produces a path with a subpath of pattern G10.

path the robot has made *significant* progress toward t. We are confident that it would be possible to prove a progress factor similar to that of Proposition 4.36, but we believe such a factor can only be established when the first problematic path contains exactly *one* real vertex. Figure 5.4 shows an example where the first problematic path contains *two* real vertices. Here the second problematic path makes a substantially smaller factor of progress, and it is not hard to imagine this factor being driven arbitrarily small. We discuss possible avenues for establishing competitiveness in this case. Let $\Pi_{a,b}$ be a subpath of Π belonging to G10.

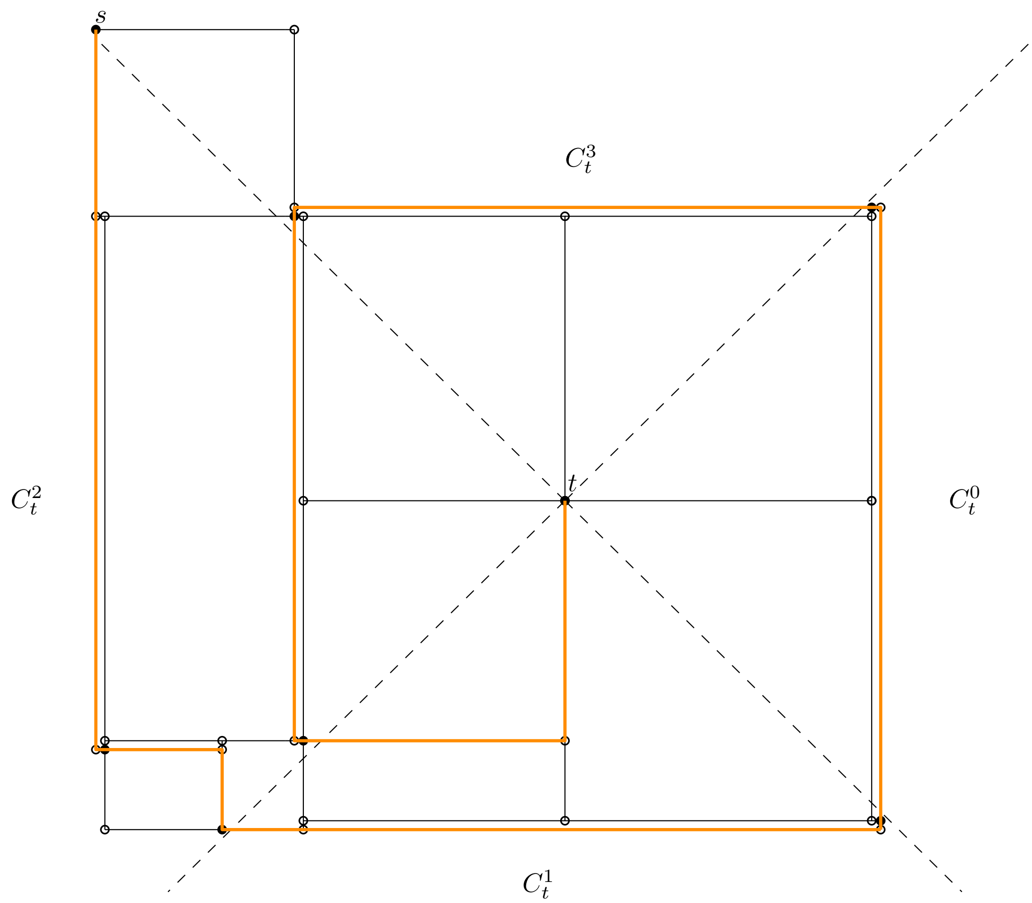

Figure 5.4: A grade-1 emanation graph in which the MARKING ALGORITHM produces a path with a subpath of pattern G10 whose first problematic path contains two real vertices.

1. Prove that if the first problematic path in $\Pi_{a,b}$ contains exactly one real vertex, then $\Pi_{a,b}$ is guaranteed to end a constant factor closer to t.

2. Prove that if the first problematic path in $\Pi_{a,b}$ contains more than one real vertex and the progress made is below some threshold factor, then the robot must pass through a Steiner vertex u with a real neighbour v satisfying $u \notin Q_{t,v}$. One could then augment the MARKING ALGORITHM with the following step: if the robot is at a Steiner vertex u with a real neighbour v such that $u \notin Q_{t,v}$, it moves directly to v. The goal would then be to show that this modification prevents the robot from ever following such a $\Pi_{a,b}$.

As an alternative to step 2, one could instead show that a subpath of pattern G10 with arbitrarily small progress cannot be repeated an unbounded number of times.

References

[1] G. Narasimhan and M. H. M. Smid, *Geometric spanner networks*. Cambridge University Press, 2007.

[2] S. Arya and M. H. M. Smid, “Efficient construction of a bounded-degree spanner with low weight,” *Algorithmica*, vol. 17, no. 1, pp. 33–54, 1997.

[3] J. M. Keil and C. A. Gutwin, “Classes of graphs which approximate the complete euclidean graph,” *Discret. Comput. Geom.*, vol. 7, pp. 13–28, 1992.

[4] B. Hamedmohseni, Z. Rahmati, and D. Mondal, “Emanation graph: A plane geometric spanner with steiner points,” *Graphs Comb.*, vol. 39, no. 2, p. 38, 2023.

[5] D. Eppstein and J. Erickson, “Raising roofs, crashing cycles, and playing pool: Applications of a data structure for finding pairwise interactions,” *Discret. Comput. Geom.*, vol. 22, no. 4, pp. 569–592, 1999.

[6] E. Kranakis, H. Singh, and J. Urrutia, “Compass routing on geometric networks,” in *Proceedings of the 11th Canadian Conference on Computational Geometry, UBC, Vancouver, British Columbia, Canada, August 15-18, 1999*, 1999.

[7] P. Bose, A. Brodnik, S. Carlsson, E. D. Demaine, R. Fleischer, A. López-Ortiz, P. Morin, and J. I. Munro, “Online routing in convex subdivisions,” *Int. J. Comput. Geom. Appl.*, vol. 12, no. 4, pp. 283–296, 2002.

[8] P. Bose, S. Durocher, D. Mondal, M. Peabody, M. Skala, and M. A. Wahid, “Local routing in convex subdivisions,” *Int. J. Comput. Geom. Appl.*, vol. 30, no. 1, pp. 1–17, 2020.

[9] O. Aichholzer, S. W. Bae, L. Barba, P. Bose, M. Korman, A. van Renssen, P. Taslakian, and S. Verdonschot, “Reprint of: Theta-3 is connected,” *Comput. Geom.*, vol. 48, no. 5, pp. 407–414, 2015.

[10] N. M. El Molla, “Yao spanners for wireless ad hoc networks,” Ph.D. dissertation, Villanova University, 2009.

[11] L. Barba, P. Bose, J.-L. De Carufel, A. van Renssen, and S. Verdonschot, “On the stretch factor of the theta-4 graph,” in *Algorithms and Data Structures - 13th International Symposium, WADS 2013, London, ON, Canada, August 12-14, 2013. Proceedings*, F. Dehne, R. Solis-Oba, and J. Sack, Eds., ser. Lecture Notes in Computer Science, Springer, 2013, pp. 109–120.

[12] P. Bose, J.-L. De Carufel, D. Hill, and M. Smid, “On the spanning and routing ratio of the directed theta-four graph,” *Discret. Comput. Geom.*, vol. 71, no. 3, pp. 872–892, 2024.

[13] P. Bose, J.-L. De Carufel, P. Morin, A. van Renssen, and S. Verdonschot, “Towards tight bounds on theta-graphs: More is not always better,” *Theor. Comput. Sci.*, vol. 616, pp. 70–93, 2016.

[14] P. Bose, D. Hill, and A. Ooms, “Improved spanning ratio of the θ-5 graph,” *Journal of Computational Geometry*, vol. 15, no. 1, pp. 66–87, 2024.

[15] N. Bonichon, C. Gavoille, N. Hanusse, and D. Ilcinkas, “Connections between theta-graphs, Delaunay triangulations, and orthogonal surfaces,” in *Graph Theoretic Concepts in Computer Science - 36th International Workshop, WG 2010, Zarós, Crete, Greece, June 28-30, 2010 Revised Papers*, D. M. Thilikos, Ed., ser. Lecture Notes in Computer Science, 2010, pp. 266–278.

[16] P. Bose, D. Hill, M. Smid, and T. Tuttle, "On the spanning and routing ratios of the Yao-Four graph," in *35th International Symposium on Algorithms and Computation, ISAAC 2024, Sydney, Australia, December 8-11, 2024*, J. Mestre and A. Wirth, Eds., ser. LIPIcs, Schloss Dagstuhl - Leibniz-Zentrum für Informatik, 2024, 15:1–15:17.

[17] L. Barba, P. Bose, M. Damian, R. Fagerberg, W. L. Keng, J. O'Rourke, A. van Renssen, P. Taslakian, S. Verdonschot, and G. Xia, "New and improved spanning ratios for Yao graphs," *J. Comput. Geom.*, vol. 6, no. 2, pp. 19–53, 2015.

[18] P. Chew, "There are planar graphs almost as good as the complete graph," *J. Comput. Syst. Sci.*, vol. 39, no. 2, pp. 205–219, 1989.

[19] D. P. Dobkin, S. J. Friedman, and K. J. Supowit, "Delaunay graphs are almost as good as complete graphs," *Discret. Comput. Geom.*, vol. 5, pp. 399–407, 1990.

[20] G. Xia, "The stretch factor of the Delaunay triangulation is less than 1.998," *SIAM J. Comput.*, vol. 42, no. 4, pp. 1620–1659, 2013.

[21] G. Xia and L. Zhang, "Toward the tight bound of the stretch factor of Delaunay triangulations," in *Proceedings of the 23rd Annual Canadian Conference on Computational Geometry, Toronto, Ontario, Canada, August 10-12, 2011*, 2011.

[22] N. Bonichon, C. Gavoille, N. Hanusse, and L. Perkovic, "Tight stretch factors for L_1- and L_∞-Delaunay triangulations," *Comput. Geom.*, vol. 48, no. 3, pp. 237–250, 2015.

[23] A. van Renssen, Y. Sha, Y. Sun, and S. Wong, "The tight spanning ratio of the rectangle Delaunay triangulation," *Algorithmica*, vol. 87, no. 7, pp. 1060–1080, 2025.

[24] P. Bose, J.-L. De Carufel, and S. Njoo, "The exact spanning ratio of the parallelogram Delaunay graph," *Theor. Comput. Sci.*, vol. 1037, p. 115 152, 2025.

[25] P. Bose and P. Morin, "Online routing in triangulations," *SIAM J. Comput.*, vol. 33, no. 4, pp. 937–951, 2004.

[26] P. Morin, "Online routing in geometric graphs," Ph.D. dissertation, Carleton University, 2001.

[27] P. Bose, P. Morin, I. Stojmenovic, and J. Urrutia, "Routing with guaranteed delivery in ad hoc wireless networks," *Wirel. Networks*, vol. 7, no. 6, pp. 609–616, 2001.

[28] P. Bose, J.-L. De Carufel, and O. Devillers, "Expected complexity of routing in Θ_6 and half-Θ_6 graphs," *J. Comput. Geom.*, vol. 11, no. 1, pp. 212–234, 2020.

[29] W. M. Z. Kalnay, "Routing ratio of the directed Yao-6 graphs," M.S. thesis, Carleton University, 2023.